



UNIVERSIDADE ESTADUAL DE CAMPINAS - UNICAMP
FACULDADE DE ENGENHARIA DE ALIMENTOS - FEA

FABRÍCIA FARIAS DE MENEZES

**CHARACTERIZATION OF ENZYMATIC HYDROLYSIS RESIDUE FROM
SUGARCANE BAGASSE AND LIGNOBOOST KRAFT LIGNIN FROM
EUCALYPTUS AND OF THEIR PHENOLIC RESINS**

**CARACTERIZAÇÃO DO RESÍDUO DA HIDRÓLISE ENZIMÁTICA DE BAGAÇO
DE CANA-DE-AÇÚCAR E DA LIGNINA KRAFT LIGNOBOOST DE EUCALIPTO E
DE SUAS RESINAS FENÓLICAS**

CAMPINAS

2018

FABRÍCIA FARIAS DE MENEZES

**CHARACTERIZATION OF ENZYMATIC HYDROLYSIS RESIDUE FROM
SUGARCANE BAGASSE AND LIGNOBOOST KRAFT LIGNIN FROM
EUCALYPTUS AND OF THEIR PHENOLIC RESINS**

**CARACTERIZAÇÃO DO RESÍDUO DA HIDRÓLISE ENZIMÁTICA DE BAGAÇO
DE CANA-DE-AÇÚCAR E DA LIGNINA KRAFT LIGNOBOOST DE EUCALIPTO E
DE SUAS RESINAS FENÓLICAS**

Thesis presented to the Faculty of Food Engineering of the University of Campinas in partial fulfilment of the requirements for the degree of Doctor in Science.

Tese apresentada à Faculdade de Engenharia de Alimentos da Universidade Estadual de Campinas como parte dos requisitos exigidos para a obtenção do título de Doutora em Ciências.

Supervisor: PROF. DR. RUBENS MACIEL FILHO

Co-supervisor: PROF. DR. GEORGE JACKSON DE MORAES ROCHA

ESTE EXEMPLAR CORRESPONDE À VERSÃO FINAL
DA TESE DEFENDIDA PELA ALUNA FABRÍCIA
FARIAS DE MENEZES, ORIENTADA PELO PROF. DR.
RUBENS MACIEL FILHO E CORIENTADA PELO PROF.
DR. GEORGE JACKSON DE MORAES ROCHA

CAMPINAS

2018

Agência(s) de fomento e nº(s) de processo(s): FAPEAM, 253/2014

ORCID: <https://orcid.org/0000-0002-9489-3502>

Ficha catalográfica
Universidade Estadual de Campinas
Biblioteca da Faculdade de Engenharia de Alimentos
Claudia Aparecida Romano - CRB 8/5816

M524c Menezes, Fabrícia Farias de, 1990-
Characterization of enzymatic hydrolysis residue from sugarcane bagasse and LignoBoost Kraft lignin from Eucalyptus and of their phenolic resins / Fabrícia Farias de Menezes. – Campinas, SP : [s.n.], 2018.

Orientador: Rubens Maciel Filho.

Coorientador: George Jackson de Moraes Rocha.

Tese (doutorado) – Universidade Estadual de Campinas, Faculdade de Engenharia de Alimentos.

1. Lignina. 2. Biomassa. 3. Etanol - Indústria. 4. Indústria de celulose. 5. Polímeros. I. Maciel Filho, Rubens. II. Rocha, George Jackson de Moraes. III. Universidade Estadual de Campinas. Faculdade de Engenharia de Alimentos. IV. Título.

Informações para Biblioteca Digital

Título em outro idioma: Caracterização do resíduo da hidrólise enzimática de bagaço de cana-de-açúcar e da lignina Kraft LignoBoost de Eucalipto e de suas resinas fenólicas

Palavras-chave em inglês:

Lignin

Biomass

Alcohol fuel - Industry

Cellulose industry

Polymers

Área de concentração: Bioenergia

Titulação: Doutora em Ciências

Banca examinadora:

Rubens Maciel Filho [Orientador]

Sarita Cândida Rabelo

Vinícius Fernandes Nunes da Silva

Lamia Zuniga Linan

Adilson Roberto Gonçalves

Data de defesa: 03-04-2018

Programa de Pós-Graduação: Bioenergia

EXAMINATION COMMITTEE

Dr. Rubens Maciel Filho - Presidente

Universidade Estadual de Campinas

Dr. Sarita Cândida Rabelo - Membro Titular

Centro Nacional de Pesquisa em Energia e Materiais

Dr. Vinícius Fernandes Nunes da Silva - Membro Titular

Suzano Papel e Celulose S/A

Dr. Lamia Zuniga Linan - Membro Titular

Universidade Federal do Maranhão

Dr. Adilson Roberto Gonçalves - Membro Titular

Universidade Estadual Paulista

A ata de defesa com as respectivas assinaturas dos membros consta em seu processo de vida acadêmica.

*How much better it is to get wisdom than gold!
And to get knowledge is more to be desired
than silver. Proverbs 16:16*

*Whatever you do, do it readily, as to the Lord
and not to men; Colossians 3:23*

ACKNOWLEDGMENT

I am grateful to God for the life gift, for renewing my joy every morning, and for encouraging me throughout this doctorate.

I am grateful to my supervisor Professor Rubens Maciel Filho and my co-supervisor Professor George Jackson de Moraes Rocha for sharing their knowledge with me, for contributing a lot in the development of this research and for being part of my training and professional growth.

I thank the 'Fundação de Amparo à Pesquisa do Estado do Amazonas' (FAPEAM) for the financing of my PhD scholarships.

I acknowledge LOPCA/FEQ/UNICAMP and CTBE/CNPEM for institutional support.

I thank the professionals and friends:

Dr. Lamia Zuniga Linan for helping me, in particular, in the rheology analyzes that were essential for this research. Thank you very much.

Renan Henrique da Silva Fernandes who was fundamental in my admission process of this doctorate. I am grateful that you have been present in my walk during the entire my doctorate course.

Ms. Viviane Marcos Nascimento by pyrolysis-gas chromatography-mass spectrometry analyses, besides the daily support in CTBE. Thank you very much.

Ms. Fernanda Miranda Mendes by Thermogravimetric analyses (CTBE).

Dr. Silvana Aparecida Rocco and Dr. Mauricio Luís Sforça by Nuclear Magnetic Resonance Analyses (LNBio).

Disney Ricardo Thomazelli by Dynamic Mechanical Thermal Analysis (LACAM/FEQ). Thank you very much.

Tatiane Tarley Pereira, Daniela Cristina Joaquim Santoro, Edilaine de Melo Ferreira and Gabriela Silva Jorge for assisting me in experimental activities in the facilities from CTBE.

Dr. Marco Antonio Sabino and Liliana Hurtado by molar mass determination of lignin ('Universidad Simón Bolívar').

Dra. Maria Ingrid Rocha Barbosa for helping me in Differential Scanning Calorimetry analyses (LOPCA).

I am very grateful to my family, especially my mother Helenise Farias de Menezes and my father Luiz Gonzaga Amazonas de Menezes (In memoriam), without them I would not get so far. Thank you very much, mom. I also thank my brother Gabriel Farias de Menezes.

I thank my boyfriend Sérgio dos Anjos Silva for his support and for being by my side during the whole period of my doctorate.

I thank my friends, especially, Janaína, Karina, Dayane, Elaine, Maurício, Zélia and Adam. You are part of my trajectory. Thank you very much.

Anyway, I thank all those who contributed directly or indirectly to the development of my doctorate. Thank you very much! It was God who put you on my way.

RESUMO

Atualmente, a indústria de etanol celulósico ainda não gera tanta lignina quanto a indústria de polpa celulósica. No entanto, é esperado que grandes quantidades de lignina sejam geradas pela expansão da indústria de etanol celulósico. Sendo assim, alternativas para usar a lignina para outros propósitos, que não seja para a cogeração de energia, têm sido consideradas. Nesta pesquisa, Resíduo de Hidrólise Enzimática (EHR) de bagaço de cana-de-açúcar e lignina Kraft LignoBoost (LBL) de Eucalipto foram usados na síntese de resinas fenol-formaldeído. O EHR foi gerado em uma planta piloto de etanol celulósico sendo principalmente composto de lignina (47% m/m) e de fibras de celulose bem dispersas (40% m/m). Esta pesquisa objetivou inserir o EHR na produção de resinas sem qualquer prévio processo de purificação a fim de avaliar como as fibras do EHR influenciam nas propriedades destas resinas. Através da técnica de pirólise acoplada à cromatografia gasosa e à espectrometria de massas, foi possível analisar o EHR sendo observadas maiores quantidades de unidades de *p*-hidroxifenilas (H) (22%) do que a LBL (3%). Assim, o EHR parece ser mais promissor para a produção de resinas fenólicas do que a LBL, uma vez que o EHR possui maior quantidade de unidades H, ou seja, o EHR apresenta mais posições *orto* livres para a incorporação do formaldeído. Resinas fenólicas com LBL (5 - 60% m/m) e com EHR (5 - 45% m/m) foram obtidas e comparadas com uma resina padrão fenol-formaldeído (sem lignina). As resinas produzidas foram submetidas a um estudo cinético completo para obter os parâmetros de cura e caracterização físico-químico e termomecânica. Em geral, a inserção de EHR ou de LBL nas resinas fenólicas levaram a um decréscimo no tempo de gelificação (tempo de cura). Os teores de sólido e os valores de perda de massa (antes de 100 °C) indicaram que as resinas fenólicas com EHR exibiram maiores quantidades de água/formaldeído livre do que a resina padrão; isto pode ser devido a hidrofiliabilidade das fibras de celulose. Por outro lado, o estudo reológico indicou que EHR reduziu o tempo de gelificação das resinas. Todas as resinas fenólicas com EHR ou com LBL exibiram maiores módulos de armazenamento de energia mecânica (G') do que a resina padrão (77 MPa), indicando um melhoramento no grau de cura das resinas. As resinas fenólicas com LBL apresentaram módulos de G' de 107 a 159 MPa, enquanto os módulos de G' das resinas com EHR apresentaram uma faixa de 84 a 192 MPa. Portanto, o EHR e a LBL parecem ser adequadas para substituir parcialmente o fenol oriundo de petróleo na produção de resinas fenólicas.

ABSTRACT

The cellulosic ethanol industry does not produce as much lignin as the pulp and paper industry nowadays. However, it is expected that relatively large amounts of lignin will be generated by the cellulosic ethanol industry with its expansion. Hence, alternatives to use that lignin for other purposes than energy co-generation have to be considered. In this research, Enzymatic Hydrolysis Residue (EHR) of sugarcane bagasse and LignoBoost Kraft Lignin (LBL) of Eucalyptus were used for the synthesis of phenol-formaldehyde resins. The EHR was generated at pilot scale and is composed of lignin (47% w/w) and well dispersed cellulose fibers (40% w/w). This research aimed to insert the EHR in resins synthesis without any previous purification in order to assess how these fibers influence the properties of their resins. By means of pyrolysis-gas chromatography-mass spectrometry, EHR showed higher amount of *p*-hydroxyphenyl (H) units (22%) than in the LBL (3%). Thus, the EHR appears to be more promising for phenolic resins production than the LBL, since it has larger H-lignin units, *i.e.*, the EHR has more free *ortho*-positions to formaldehyde incorporation. Phenolic resins using LBL (5 - 60% w/w) and using EHR (5 - 45% w/w) were obtained and compared with the standard resin (without lignin). The produced resins were submitted to a complete kinetic study to obtain the curing parameters and to physicochemical and thermomechanical characterization. In general, EHR or LBL addition on phenolic resins led to decrease on gel time values (curing time). The solids content and the weight loss values (until before 100 °C) showed that the phenolic resins with EHR exhibited more amount of water/free formaldehyde than the standard resin, which can be due to hydrophilicity of cellulose fibers. Conversely, the rheological study indicated that EHR reduces the gel time of the resins. All phenolic resins with EHR or LBL exhibited higher storage modulus (G') than the standard phenolic resin (77 MPa), indicating an improvement on curing degree. Phenolic resins with LBL showed G' modulus between (107-159 MPa), while for resins with EHR ranged from 84 to 192 MPa. Therefore, the EHR and the LBL can be suitable to partially replace based-petroleum phenol in phenolic resins production.

FIGURE LIST

Figure 2.1 - Components of lignocellulosic biomass	19
Figure 2.2 - Aromatic lignin units and their precursor alcohols	20
Figure 2.3 - Arrangement of aromatic lignin units and main interlinkages	21
Figure 2.4 - Scheme of lignocellulosic biomass components in plant secondary wall	22
Figure 2.5 - Conceptual biorefinery	23
Figure 2.6 - Ethanol production from sugarcane bagasse	25
Figure 2.7 - LignoBoost process	26
Figure 2.8 - A full contour map of 2D HSQC NMR of a lignin.	32
Figure 2.9 - Main structures found in oxygenated aliphatic region of lignins HSQC	33
Figure 2.10 - Main structures found in aromatic region of HSQC lignins	33
Figure 2.11 - Regions of the fundamental vibrational spectrum	35
Figure 2.12 - FTIR spectra of cellulose, hemicelluloses and lignin	36
Figure 2.13 - TG curves of cellulose, hemicelluloses and lignin	38
Figure 2.14 - Global phenolic resin demand by end use	41
Figure 2.15 - Phenolic resin applications	41
Figure 2.16 - Schematic representation during a thermosetting curing	43
Figure 2.17 - Classification of the fiber reinforced composites	47
Figure 4.1 - Schematic representation of the main steps of this research.....	50
Figure 4.2 - Obtainment of the EHR at pilot scale	51
Figure 4.3 - LignoBoost lignin process	53
Figure 4.4 - Synthesis system of resole-type phenolic resins.....	63
Figure 4.5 - Curing process to obtain the thermosetting phenolic resins.	67
Figure 5.1 - Mass balance of the EHR obtainment.....	73
Figure 5.2 - Mass balance to the acid-dioxane (a) and alkaline processes (b)	74
Figure 5.3 - Chemical composition of EHR from alkaline and acidic-dioxane processes.	74
Figure 5.4 - FTIR spectra of the EHR and LBL.	75
Figure 5.5 - LBL pyrogram.	77
Figure 5.6 - EHR pyrogram.	78
Figure 5.7 - (a) Alkaline EHR and (b) acidic-dioxane EHR pyrogram.	81
Figure 5.8 - Entire 2D HSQC NMR contour maps of the EHR (a) and the LBL (b)	84

Figure 5.9. Aromatic regions from HSQC spectra of the EHR (a) and LBL (b)	86
Figure 5.10 - TG (a) and DTG (b) curves of the EHR and LBL	90
Figure 5.11 - Photographs of the EHR particles from each sieve.	91
Figure 5.12 - The particle size distributions by laser scattering of the LBL and EHR	92
Figure 5.13 - SEM images of (a) the EHR from bottom of sieve set and (b) milled EHR.	93
Figure 5.14 – Intrinsic viscosity as a function of the LBL concentration	95
Figure 5.15 - Viscoelastic properties curves of the LBL 60% resin at 105 °C.	97
Figure 5.16 - t_{gel} values for all phenolic resins at 90 - 120 °C.....	98
Figure 5.17 - Arrhenius relationship for each phenolic resin.	99
Figure 5.18 - E_a values for each phenolic resin.	100
Figure 5.19 - TG and DTG curves at different heating rates of (a) the LBL 5% and (b) EHR 5% resins.	102
Figure 5.20 - Conversion percent curves for (a) LBL 5% and (b) EHR 5% resins at isotherms from 90 to 120 °C.	103
Figure 5.21 - Flow curves of shear stress (τ) and viscosity (η) as a function of shear rate (γ). (a) LBL 5% resin, (b) EHR 5% resin and (c) standard resin.	107
Figure 5.22 - FTIR spectra of the phenol, formaldehyde and Standard phenolic resin.....	108
Figure 5.23 - FTIR spectra of (a) phenolic resins before curing reaction; and of (b) phenolic resins after curing reaction.	110
Figure 5.24 - 2D HSQC NMR spectra of the standard and the LBL 30% resins.....	113
Figure 5.25 - Diarylmethane structures (methylene bridges).	114
Figure 5.26 - DSC of the phenolic resins without any previous curing process.	115
Figure 5.27 - DSC of the thermosetting phenolic resins	116
Figure 5.28 - G' and G'' curves of the phenolic resins.	118
Figure 5.29 - Tan delta curves of the phenolic resins with (a) LBL and (b) EHR.	119
Figure S1 - Curves of viscoelastic properties as a function of time.	148
Figure S2 - Viscosity curves for determination of zero shear rate viscosity (η_0).	152
Figure S3 - TG and DTG curves for EHR resins.....	153
Figure S4 - TG and DTG curves for LBL resins.	154
Figure S5 - DMTA curves of the standard phenolic resin.	155

TABLE LIST

Table 2.1 - Characterization of lignins from sugarcane bagasse.	27
Table 2.2 - Chemical compositions of different lignocellulosic biomasses.	29
Table 2.3 - Chemical shifts of ^1H and attribution in acetylated lignins	31
Table 2.4 - Main compounds released from S-, G- and H-units of sugarcane bagasse lignins from Py-GC/MS	34
Table 2.5 - Thermoanalytical techniques classification according to properties	37
Table 2.6 - Main product requirements and lignin applicability based on inherent structural features	40
Table 2.7 - Some papers about lignin use in resole-type phenolic resins.	44
Table 2.8 - Advantages and disadvantages of the nature fibers use	47
Table 4.1 - Main acquisition parameters of 2D NMR spectra.	57
Table 4.2 - Factorial design 2^2 of solubility tests and their response	62
Table 4.3 - Factorial design 2^2 of solubility tests.	62
Table 4.4 - pH of the synthesis reactions of the resole-type phenolic resins.	66
Table 5.1 - Determination of components of the EHR and the LBL	71
Table 5.2 - The main FTIR bands assignment	76
Table 5.3 - Aromatic units of the LBL and EHR by Py-GC/MS technique.	79
Table 5.4 - Aromatic units of the alkaline EHR and acidic-dioxane EHR by Py-GC/MS technique.	82
Table 5.5 - ^1H -NMR results.	83
Table 5.6 - Aromatic lignin units by 2D HSQC NMR technique	87
Table 5.7 - Elemental composition, DBE, protein content and HHVs	88
Table 5.8 - Particle size distribution by sieving of the EHR	91
Table 5.9 - Intrinsic viscosity and molar mass of the LBL.	95
Table 5.10 - Curing time for LBL 5% and EHR 5% resins and their E_α values.	104
Table 5.11 - Solid content, viscosity values (η_0) and TG results.	105
Table 5.12 - DMTA data for the phenolic resins.	117

ABBREVIATIONS AND ACRONYMS LIST

CNPEM: Brazilian Center for Research in Energy and Materials

CTBE: Brazilian Bioethanol Laboratory

DMTA Dynamic Mechanical Thermal Analysis

DSC: Differential Scanning Calorimetry

DTG: First derivative thermogravimetry

E_a : Activation Energy

EHR: Enzymatic Hydrolysis Residue

FA: Ferulic acid

FTIR: Fourier Transform InfraRed spectroscopy

G: Guaiacyl unit

G' : Storage modulus

G'' : Loss modulus

H: *p*-Hydroxyphenyl unit

HHV: Higher Heating Value determination

HSQC: Heteronuclear Single-Quantum Correlation Spectroscopy

$^1\text{H-NMR}$: proton Nuclear Magnetic Resonance spectroscopy

LACAM: Laboratório de Caracterização de Materiais

LBL: LignoBoost Lignin

LDPS: 'Laboratório de Desenvolvimento de Processos de Separação'

LNBio: Brazilian Biosciences National Laboratory

LNNano: Brazilian Nanotechnology Laboratory

LOPCA: Laboratory of Optimization, Design, and Advanced Control

LRAC 'Laboratório de Caracterização de Biomassa'

PCA: *p*-coumaric acid

Py-GC/Ms: Pyrolysis-gas chromatography/mass spectrometry

S: Syringyl unit

SEM: Scanning Electron Microscope

TG: ThermoGravimetric analysis

t_{gel} : gel time

η_0 : zero shear rate viscosity

TABLE OF CONTENTS

Chapter 1 INTRODUCTION	16
1.1 Thesis Organization	18
1.2 Main results achieved in this research	18
Chapter 2 REVIEW LITERATURE	19
2.1 Lignocellulosic biomass	19
2.2 Lignin application	22
2.3 Biorefinery	23
2.4 Cellulosic ethanol production	24
2.5 LignoBoost Process in a Kraft Pulp mill	25
2.6 Characterization of lignocellulosic materials	26
2.6.1 Chemical compositional analyses	28
2.6.2 Nuclear Magnetic Resonance (NMR) spectroscopy	30
2.6.3 Py-GC/MS technique	34
2.6.4 Fourier Transform InfraRed (FTIR) spectroscopy	34
2.6.5 Elemental Analysis	36
2.6.6 Thermogravimetric analysis (TG)	37
2.6.7 Scanning Electron Microscope technique (SEM)	38
2.7 Lignin and lignin-based products market	39
2.8 Phenolic resin	41
2.8.1 Synthesis of phenolic resins	42
2.8.2 Cure Kinetics of phenolic resins	43
2.8.3 Lignin as feedstock in phenolic resins	44
2.9 Composites using fibers as reinforcement	46
Chapter 3 OBJECTIVES	49
3.1 General Purpose	49
3.2 Specific Purposes	49
Chapter 4 MATERIALS AND METHODS	50
4.1 Obtainment and characterization of the EHR and LBL	50
4.1.1 Chemical composition	54
4.1.2 NMR Spectroscopy	56

4.1.3 Pyrolysis-gas chromatography-mass spectrometry (Py-GC/MS).....	57
4.1.4 Fourier Transform - InfraRed spectroscopy (FTIR)	57
4.1.5 Elemental Analysis and C9-formulae	58
4.1.6 Molar mass determination by viscosimetry	58
4.1.7 Determination of Higher Heating Value.....	60
4.1.8 Thermogravimetry analyses.....	60
4.1.9 Physical characterization	60
4.1.10 Scanning Electron Microscope (SEM) analysis	61
4.2 Synthesis of phenolic resins with the EHR and LBL	61
4.3 Determination of curing kinetics of phenolic resins with the EHR and LBL.....	67
4.3.1 Rheological study	67
4.3.2 TG Kinetics Analysis.....	68
4.4 Characterization of the phenolic resins with the EHR and LBL	68
4.4.1 Solid content and viscosity determination	68
4.4.2 TG Analyses	69
4.4.3 FTIR spectroscopy	69
4.4.4 HSQC Spectroscopy	69
4.4.5 DSC.....	70
4.4.6 DMTA technique	70
Chapter 5 RESULTS AND DISCUSSION.....	71
5.1 Characterization of the EHR and the LBL.....	71
5.1.1 Chemical composition and mass balance	71
5.1.2 FTIR spectroscopy	75
5.1.3 Py-GC/MS technique.....	77
5.1.4 NMR Spectroscopy	83
5.1.5 Elemental Analysis and HHV determination.....	88
5.1.6 Thermogravimetric analysis	89
5.1.7 Physical characterization	91
5.1.8 Scanning Electron Microscopy (SEM)	93
5.1.9 Molar mass determination	94
5.2 Determination of curing parameters of the phenolic resins with the EHR and LBL.....	96
5.2.1 Rheological study	96

5.2.2 TG analyses.....	101
5.3 Characterization of the obtained phenolic resins	105
5.3.1 Solid content, viscosity determination and TG analyses	105
5.3.2 FTIR spectroscopy	108
5.3.3 2D NMR spectroscopy (HSQC)	111
5.3.4 Differential Scanning Calorimetry (DSC)	114
5.3.5 Dynamic Mechanical Thermal Analysis (DMTA)	117
Chapter 6 CONCLUSIONS AND FUTURE WORK	121
REFERENCES	123
SUPPLEMENTARY MATERIAL	137
Supplementary Material A: Research dissemination.....	138
Supplementary Material B: Gel time determination.....	139
Supplementary Material C: Zero shear rate viscosity (η_0) determination.....	149
Supplementary Material D: TG and DTG curves of the phenolic resins.....	153
Supplementary Material E: DMTA curves of the Standard phenolic resin.....	155

Chapter 1 INTRODUCTION

Polymeric materials, which are most derived from fossil fuels, have been widely used by society and are importance in global economy (Geyer et al., 2017). However, the widespread use of these materials has some consequences, such as environmental impacts caused by their slow degradation and release of toxins (Brandt and Unnasch 2010). Moreover, their prices are unstable as they depend on the international oil price and political decisions (Verbruggen and Marchohi, 2010). Thus, there is an interest and need to develop polymeric materials derived from renewable sources (Chung and Washburn, 2012).

Several products of industrial relevance, including polymeric materials, can be obtained from lignocellulosic biomass, which in turn it is a renewable, abundant and potentially low cost source (Chung and Washburn, 2012; Isikgor and Becer, 2015). Examples of biomasses that have potential to be employed as feedstock to produce polymeric materials are lignins produced by cellulose pulp industry (Rinaldi et al., 2016) and by sugarcane industry (Tye et al., 2016). These biomasses are promising because of their wide availability and relatively low cost (Isikgor and Becer, 2015). The high amount of sugarcane bagasse generated from sugar-alcohol industry in the world (about 540×10^6 tonnes per year - wet basis) makes this industrial by-product an attractive lignocellulosic feedstock (Bezerra and Ragauskas, 2016). One of the major components of lignocellulosic biomass is lignin, a macromolecule containing several functional groups that can be used to obtain various types of polymers (Chung and Washburn 2012), such as polyurethanes, phenol-formaldehyde resins, epoxy-phenol resins, polyesters, polyolefins and others (Calvo-Flores and Dobado, 2010; Chung and Washburn, 2012).

Lignin is a complex aromatic macromolecule that is mainly composed of *p*-hydroxyphenyl (H), guaiacyl (G), and syringyl (S) units, which differ in the degree of methoxylation of the aromatic ring. Grass lignins also contain *p*-hydroxycinnamic acids (*p*-coumaric acid and ferulic acid). The lignin units are cross-linked between them with a variety of different chemical bonds (β -O-4', β -5', β - β ', 5-5' and 5-O-4') (Rinaldi et al., 2016; del Río et al., 2015; Ralph et al., 2007). Lignin is traditionally obtained from processes that use cellulose as feedstock and is generally considered as a by-product, or sometimes, as a waste (Rinaldi et al., 2016). However, there is a growing recognition of the fact that valorization of the lignin fraction is not just imperative for commercial success of future operations of the

cellulose industry, but also necessary for achieving economic and environmental sustainability (Rinaldi et al., 2016).

An important industrial activity that generates lignocellulosic stream is the production of cellulosic ethanol from sugarcane bagasse (Bezerra and Ragauskas, 2016). Production of ethanol from lignocellulosic biomass consists of three major steps: (i) pretreatment; (ii) saccharification of cellulose (hydrolysis) and (iii) fermentation of released sugars (Singh et al., 2014). Among the major steps to produce cellulosic ethanol, the enzymatic hydrolysis of sugarcane bagasse generates a residual stream that is mainly composed of lignin, and thus here called ‘Enzymatic Hydrolysis Residue (EHR)’.

Another important industrial activity that produces large amounts of lignin is the Kraft pulp industry (Hu et al., 2018). Brazil is the world's fourth largest producer of pulp, producing about 19×10^6 tonnes of cellulosic pulp in 2016 (Brazilian Tree Industry (Ibá), 2017). This lignin is mainly burnt to produce energy, which supplies the pulp mill and is sold to the grid. However, modern pulp industries aim to expand the use of lignin to value-added products (Benali et al., 2014; Menon and Rao, 2012; Ragauskas et al., 2014; Rinaldi et al., 2016). Some pulp mills that aim to transform lignin into products of major interest have employed the LignoBoost process (Tomani, 2010). This process allows for obtaining higher quantities of lignin with higher quality (Hu et al., 2018; Tomani, 2010).

It is essential to seek other alternatives to better use the lignin obtained from industrial processes. For example, integrating biomass conversion processes to efficiently produce power, fuels, and value-added products could reduce or even eliminate any waste (Plaza and Wandzich, 2016). The target product of this investigation is phenol-formaldehyde resin, as it is one of the most common polymers and has various applications, such as adhesives, coatings, wood composites and engineering plastics for the aerospace and for electronics industries.

The lignocellulosic materials that were used in this research to produce phenolic resins came from two sources: the residual stream from enzymatic hydrolysis of sugarcane bagasse in a pilot plant of cellulosic ethanol (Brazilian Bioethanol Laboratory - CTBE) and from LignoBoost process of a Kraft pulp mill. This investigation can be mainly divided into four steps: (1) Obtainment and physicochemical characterization of the lignocellulosic materials; (2) Obtainment of the lignin-phenol resins; (3) Determination of curing parameters of lignin-phenol resins; and (4) Physicochemical and thermomechanical characterization of the lignin-

phenol resins. All references of papers produced from the results of this research are showed in **Supplementary Material A**.

1.1 Thesis Organization

This thesis will be divided into seven different chapters based on a traditional layout:

Chapter 1 – Introduction;

Chapter 2 – Review literature: it will approach important issues to this research;

Chapter 3 – Objectives;

Chapter 4 – Materials and methods: it will approach in details how each step (earlier described) was developed during this research;

Chapter 5 – Results and discussion: in this chapter, all data from experimental analyses will be present and it will discuss the results about those steps;

Chapter 6 – Conclusions: It will demonstrate if the proposed objectives in this research were achieved;

Chapter 7 – References.

1.2 Main results achieved in this research

The Enzymatic Hydrolysis Residue (EHR) from sugarcane bagasse was obtained in a pilot plant of cellulosic ethanol. The EHR is composed of lignin (47% w/w) and cellulose fibers (40% w/w), while the LignoBoost Kraft Lignin (LBL) of Eucalyptus is virtually pure. The EHR has smaller amounts of methoxyl groups and higher amounts of *p*-hydroxyphenyl units than the LBL. The rheological study indicated that EHR reduces the curing time of the resins, despite of hydrophilicity of cellulose fibers. All phenolic resins with EHR or LBL exhibited higher storage modulus (G') than the standard phenolic resin, indicating an improvement on curing degree. The EHR 5% resin showed higher G' modulus than the LBL 5% resin. This fact can indicate that the cellulosic fibers at lower amount enhance this mechanical property.

Chapter 2 REVIEW LITERATURE

Some important topics to this research are approached in this chapter, as lignocellulosic biomass, lignin application, biorefinery, cellulosic ethanol production, LignoBoost process in a Kraft Pulp mill, characterization of lignocellulosic materials, market of lignin-based products, phenolic resins and composites using fibers as reinforcement.

2.1 Lignocellulosic biomass

Lignocellulosic biomass is mainly composed by three components of high molecular weight - cellulose, hemicelluloses and lignin, and others in minor amounts of low molecular weight (Figure 2.1).

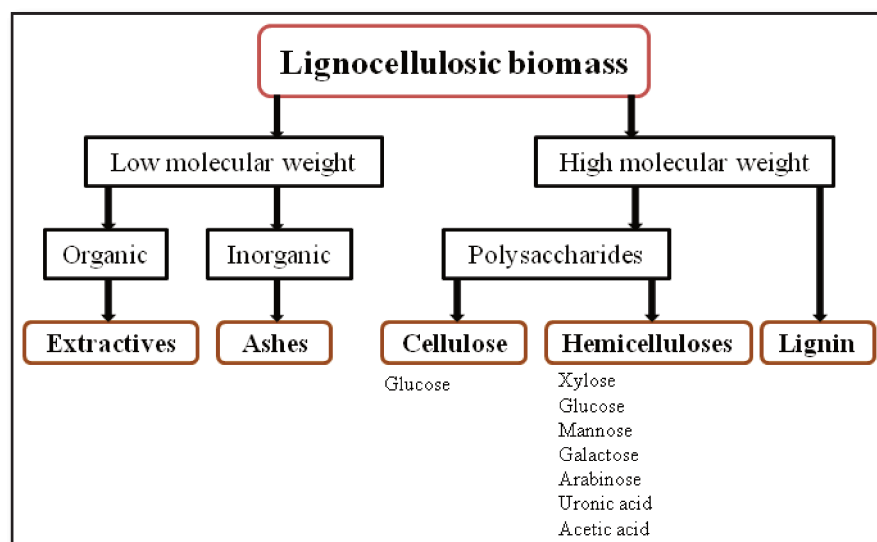


Figure 2.1 - Components of lignocellulosic biomass (adapted from Carvalho, 1999).

Cellulose, main component of cell wall, is a linear homopolysaccharide of the general formula $(C_6H_{10}O_5)_n$ formed by β -D-glucopyranose linked by $\beta(1\rightarrow4)$ bonds, being the cellobiose (glucose-glucose dimers) its repetitive unit (Fengel and Wegener, 1989). Cellulose has a linear and fibrous structure due to the presence of hydroxyl groups. Intramolecular hydrogen bonds are responsible for the chains stiffness that result in the plant fiber, whereas the intermolecular hydrogen bonds are responsible for the formation of supramolecular structures, highly ordered and crystalline regions (Fengel and Wegener, 1989).

Hemicelluloses generally consist of 80 to 200 units of residual sugars, such as pentoses (D-xylose, L-arabinose and L-rhamnose), hexoses (D-glucose, D-mannose and D-galactose) and uronic acids (4-O-methyl-D-glucuronic and D-galacturonic). Hemicelluloses structure can consist in a single monosaccharide (xylans) or in two or more units (xyloglucans, 4-O-methylglucuronoxylan) with several branches. The variation of hemicelluloses structure is related with plant species and tissue type which they belong (Fengel and Wegener, 1989).

Lignin is a complex aromatic macromolecule mainly composed by *p*-hydroxyphenyl (H), guaiacyl (G), and syringyl (S) units, differing in the degree of methoxylation of the aromatic ring (Fengel and Wegener, 1989; Rinaldi et al., 2016). H, G and S units are derived from oxidative polymerization of sinapyl alcohol, coniferyl alcohol and *p*-coumaryl alcohol, respectively (Fengel and Wegener, 1989) (**Figure 2.2**). Grass lignins also contain *p*-hydroxycinnamic acids (*p*-coumaric acid, PCA, and ferulic acid, FA) (del Río et al., 2015; Menezes et al., 2017). The lignin units are cross-linked to each other with a variety of different chemical bonds (β -O-4', β -5', β - β' , 5-5' and 5-O-4') (**Figure 2.3**) (del Río et al., 2015; Rinaldi et al., 2016).

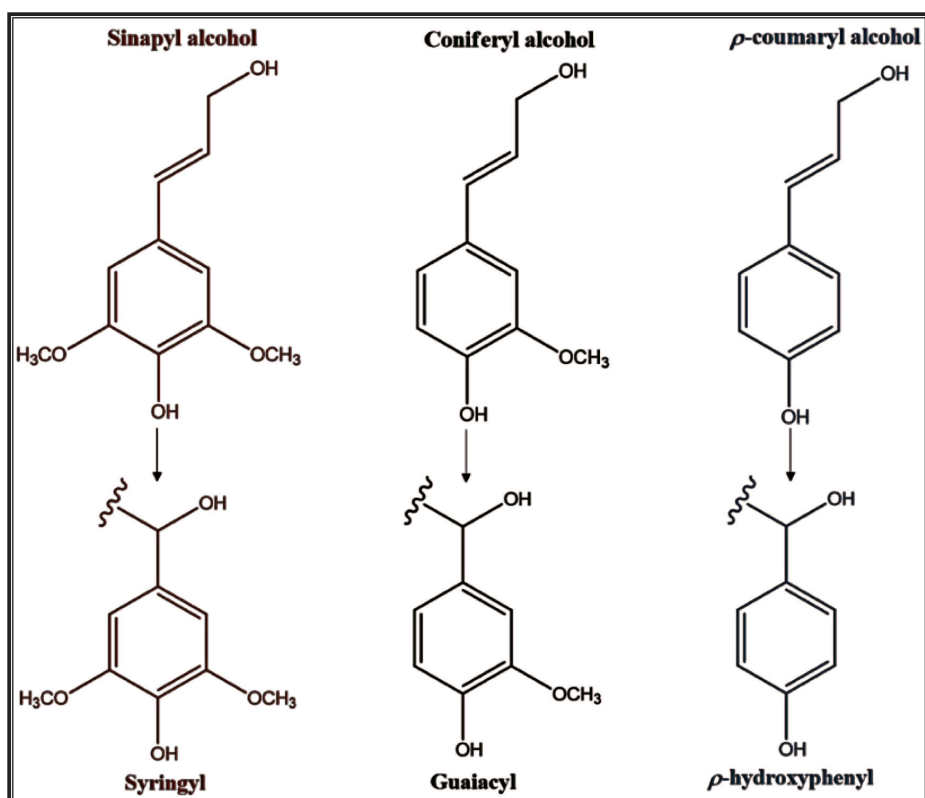


Figure 2.2 - Aromatic lignin units and their precursor alcohols (adapted from Fengel and Wegener, 1989).

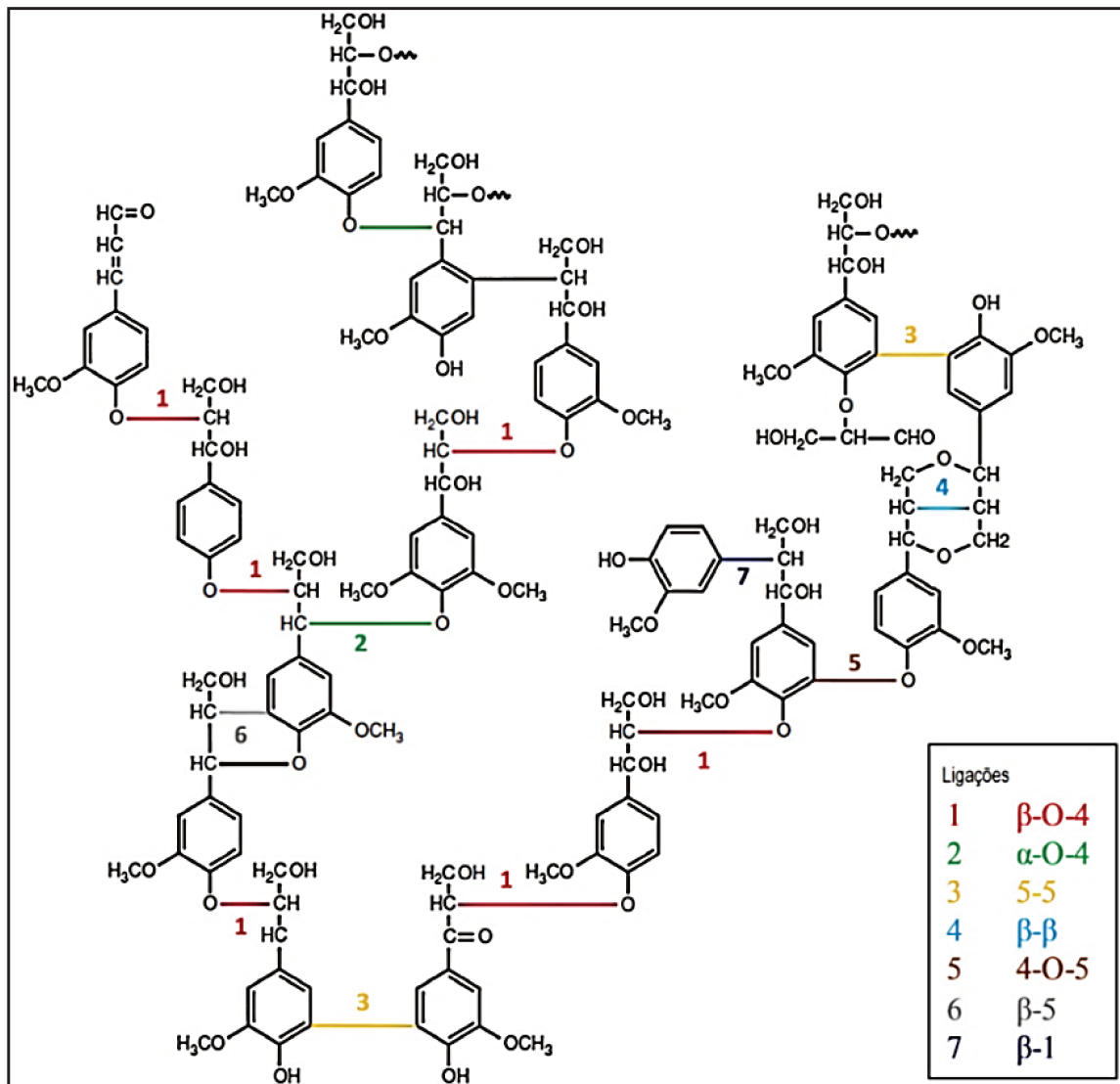


Figure 2.3 - Arrangement of aromatic lignin units and main interlinkages (adapted from Windeisen and Wegener, 2012 and Fernandes, 2015).

Lignin acts on the stiffening within the fiber cell wall (Winandy and Rowell, 2005) because it is an amorphous and hydrophobic material. The adhesion strength between cellulose fibers and lignin is increased by covalent bonds between the hemicelluloses and cellulose constituents and the lignin (Chen, 2014).

Lignin plays an important role in plant development, contributes as a mechanical strength to wood (Winandy and Rowell, 2005) and protects against insect and fungal attack (Freeman and Beattie, 2008). **Figure 2.4** shows a schematic representation of association between the cellulose, hemicelluloses and lignin in second wall of a plant fiber proposed by Salmén and Olsson (1998).

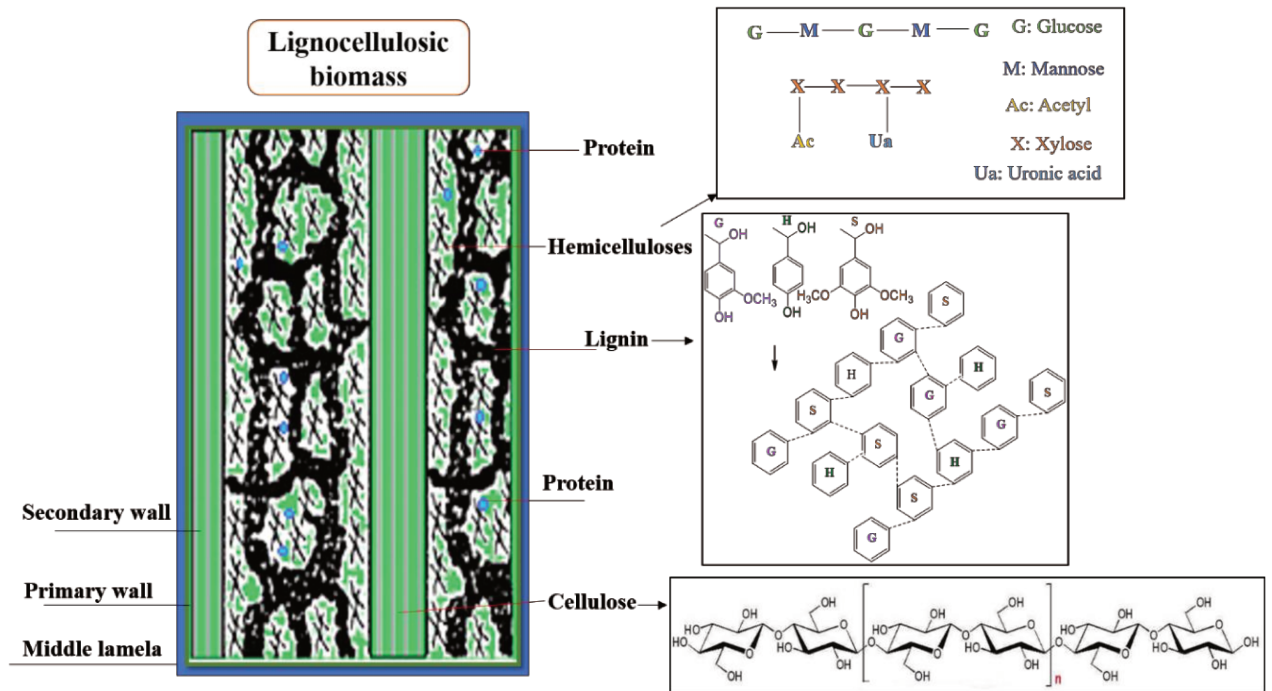


Figure 2.4 - Scheme of lignocellulosic biomass components in plant secondary wall (adapted from Anwar et al., 2014).

2.2 Lignin application

Lignin has potential to replace petroleum-based materials, which are increasingly scarce and expensive, in many industrial applications (Çetin and Özmen, 2002), such as materials for automotive brakes, wood panel products and resins for printed circuit boards and surfactants (Calvo-Flores and Dobado, 2010; Gosselink et al., 2004; Lora and Glasser, 2002; Rinaldi et al., 2016).

Lignin is also a suitable feedstock for the production of low-molecular-mass such as vanillin, aldehydes, aliphatic acids, benzene, toluene, xylene, phenol and many other chemical compounds (Pandey and Kim, 2011). Lignin can be used to obtain many types of polymers, once it contains various functional groups, such as polyurethanes, phenolic resins, epoxy resins, and others (Calvo-Flores et al., 2015; Chung and Washburn, 2012). The application of lignin in phenolic resins is a typical example where it can be used without any previous conversion process. Up to 50% of the phenol content in this material can be replaced by lignin (lignosulfonate, Kraft, or Organosolv) without significantly compromising mechanical properties of phenolic resins (Rinaldi et al., 2016).

2.3 Biorefinery

The biorefinery concept makes reference to both the raw material (biomass) and the bioconversion processes, that are commonly applied in the treatment and processing of raw materials (Fernando et al., 2006). According to the National Renewable Energy Laboratory, a biorefinery is ‘an installation that integrates conversion processes and equipment to produce fuels, power and chemicals from biomass’ (Balagurumurthy et al., 2015). Different technologies from several areas, including polymer chemistry, bioengineering and agriculture, are applied in a biorefinery that aim replace the ‘waste’ term by ‘by-product’ at industrial level. Currently, most petrochemical products are produced in oil refineries, whereas it is expected that many of those products will be produced in biomass refineries (**Figure 2.5**) (Kamm and Kamm, 2004; Ohara, 2003).

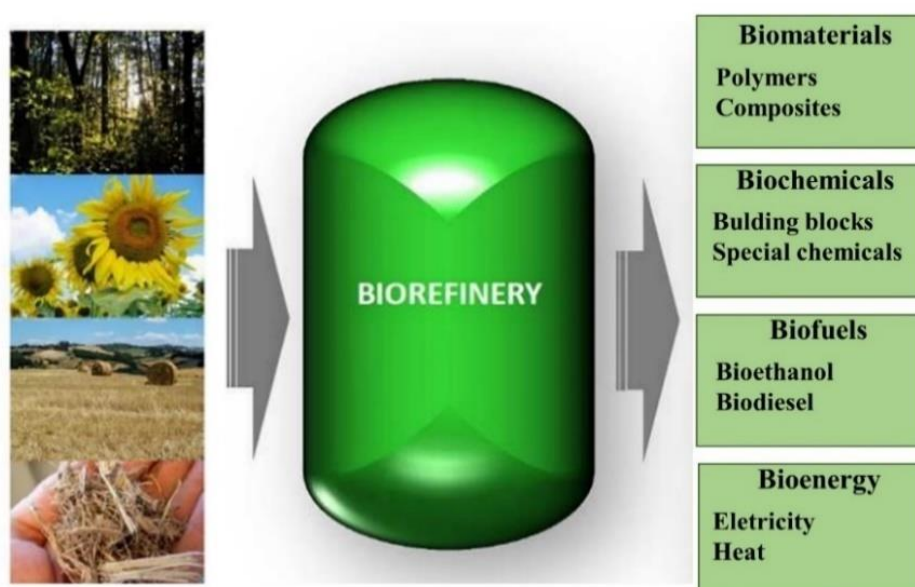


Figure 2.5 - Conceptual biorefinery (adapted from FitzPatrick et al., 2010).

This investigation aimed to extend the application of the biorefinery concept to cellulosic ethanol production turning the residue generated in this process into feedstock to obtain lignin-phenol resins and to use the obtained lignin from Kraft Industry for other purpose than cogeneration. Thus, the residue stream from the enzymatic hydrolysis of sugarcane bagasse, which is mainly composed of lignin, some cellulose fibers, and LignoBoost lignin from the pulp and paper mill, will be used in the synthesis of lignin-

phenol-formaldehyde resins that, in turn, have applications in the construction area and other commercial applications.

The cellulosic ethanol, Kraft and LignoBoost processes are presented below in order to provide an overview of the process and explain where the lignocellulosic materials used in this research to produce phenolic resins were generated.

2.4 Cellulosic ethanol production

Sugarcane bagasse can be used as feedstock to cellulosic ethanol production in some countries, including Brazil, which it could lead to more than a two-fold increase in the current ethanol yield per hectare of sugarcane. Although most of the generated sugarcane bagasse is currently used as solid fuel for cogeneration, it has been demonstrated that the modernisation of the boilers and the rationalisation of the steam usage might permit satisfying the energy requirements of the plants with no more than 50% of the generated sugarcane bagasse, that it would create a surplus of bagasse (Cardona et al., 2010; Galbe and Zacchi, 2010; Mesa et al., 2016).

The main steps in producing bioethanol (**Figure 2.6**) are pretreatment, enzymatic hydrolysis and fermentation (Zhang and Lynd, 2004). The pretreatment step should precede the hydrolysis process in order to activate the cellulose, which is not well-accessible to the enzyme complex (mainly composed of cellulases) in its native state (Cardona et al., 2010). After sugarcane bagasse pretreatment step, it is necessary an enzymatic hydrolysis process to obtain fermentable sugars. The hydrolysis of sugarcane bagasse is a step used to obtain monosaccharides, mainly glucose and xylose, from carbohydrates (cellulose and hemicelluloses) contained in this raw material. Subsequently, the sugar-rich stream is routed to bioreactor, where the fermentation of sugars to ethanol by microorganisms occurs (Galbe and Zacchi, 2010).

The enzymatic hydrolysis of sugarcane bagasse generates, when the pretreatment is hydrothermal or acid, a residual stream that is mainly composed of lignin and some non-hydrolysed cellulose fibers. Besides optimizing the process parameters, fully utilizing the by-products (mainly the residues produced in the enzymatic hydrolysis process) is a feasible method to reduce cost.

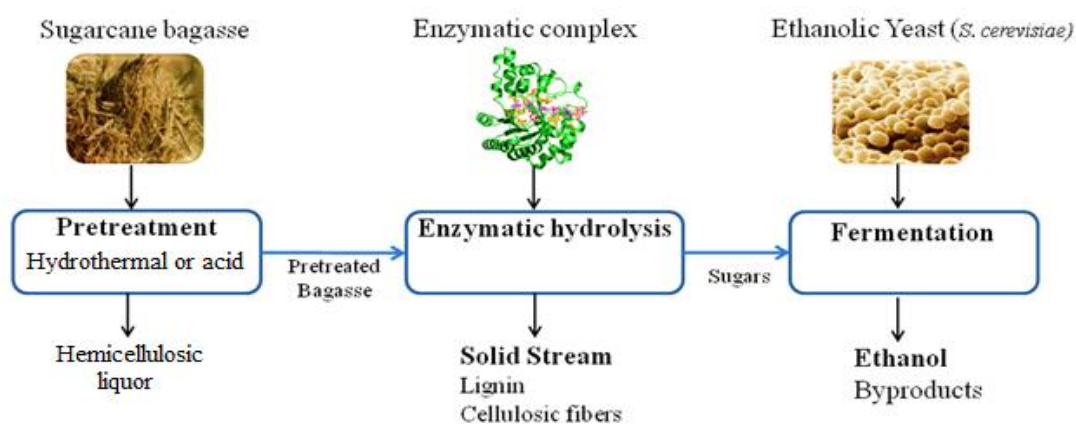


Figure 2.6 - Ethanol production from sugarcane bagasse (adapted from Menezes, 2013).

2.5 LignoBoost Process in a Kraft Pulp mill

The Kraft pulping process, also known as sulphate process, prevails in the pulp and paper industry. Approximately 34×10^6 tonnes of unbleached Kraft pulps were worldwide produced in 2012 (RISI, 2013). This process comprises adding chips and white liquor (NaOH and Na_2S) in a digester with the purpose of removing the maximum possible amount of lignin. The cooking of the chips results in the degradation of lignin. The reaction products are dissolved in the liquor. When the cooking time is over, the liquor (black liquor) is sent to the recovery boiler while the solid part is directed to the decompression zone, leading to the individualization of the fibers (unbleached pulp) (Sjöström, 1993).

The Kraft pulping process produces the largest amount of lignin as a by-product in the paper industry. This lignin is mainly burned as fuel to generate energy to supply the pulp mill. Only about 2% of the lignin available from the pulp and paper industry is commercially used to produce value-added products, like the lignin sulfonate generated by sulphite or bisulphite pulping applied in the construction industry (Gosselink et al., 2004).

One way to deal with the quantity of produced lignin could be using the dry lignin powder as a biofuel lime kiln to replace fossil fuel. Other alternative is using lignin in other burners or boilers where fossil fuel is normally used (Tomani, 2010). A further use of this lignin could be a feedstock in value-added products (Chung and Washburn, 2012; Ragauskas et al., 2014).

Morden pulp and paper industries apply the concept of biorefineries in the recovery of lignin by the means of the LignoBoost process (**Figure 2.7**). This process aims to produce a solid biofuel with high energy density and low ash content from the Kraft lignin precipitated

by the black liquor; *i.e.*, this process consists in concentrating lignin from the black liquor (Tomani, 2010).

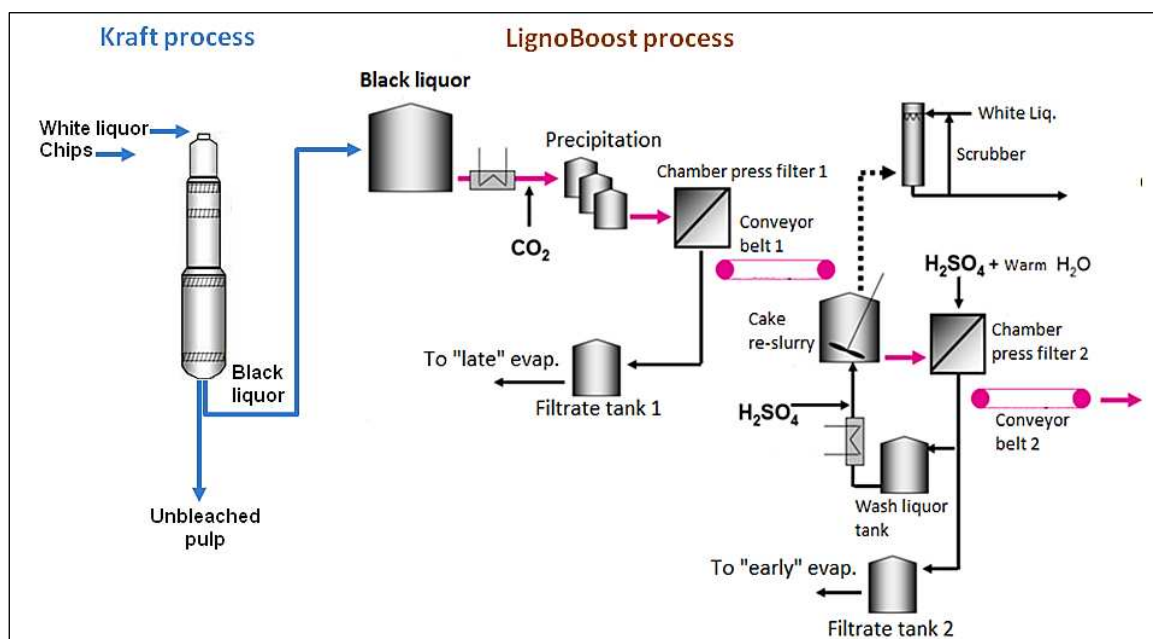


Figure 2.7 - LignoBoost process (adapted from Tomani, 2010).

In the LignoBoost process, a stream of black liquor is taken from the black liquor evaporation plant; then lignin is precipitated by acidification and filtered. The filter cake is re-dispersed and acidified. The resulting slurry is then filtered and washed by means of displacement washing. The major advantages this process when compared to the traditional process are lower investment costs, lower operational costs, higher lignin yield, lower ashes and carbohydrate contents and a higher content of dry solids (Tomani, 2010).

2.6 Characterization of lignocellulosic materials

It is known that the suitability of lignin as feedstock for value-added products can vary widely according to its physicochemical characteristics. The chemical features of lignocellulosic biomass depends on various factors, such as type of biomass, plant species or part of plants, growth processes, growing conditions, age of the plants, fertilizer and pesticide doses used, harvesting time (Vassilev et al., 2010), the process by which lignin was stemmed (Menezes et al., 2016a; Menezes et al., 2016b) processing conditions, severity of the pretreatment (Menezes et al., 2017) and others. **Table 2.1** gathers some papers that characterized lignins obtained from sugarcane bagasse by means of different techniques.

Table 2.1 - Characterization of lignins from sugarcane bagasse.

Authors (year)	Characterization techniques	Lignins from sugarcane bagasse
del Río et al. (2015)	Chemical composition HSQC Py-GC/MS Heteronuclear Multiple Bond Correlation	1. whole-cell-wall 2. 'milled-wood' lignin
Mousavioun and Doherty (2010)	Chemical composition Elemental analysis Functional groups determination Molar mass TG Differential Scanning Calorimetry	1. Alkaline pretreatment 170 °C, 1.5 h, 40 g L ⁻¹ NaOH, 1:10 w/v 2. Organosolv lignin
Moghaddam et al. (2014)	Chemical composition Elemental analysis Molar mass Mannich reactivity FTIR spectroscopy TG 2D HSQC ³¹ P NMR	2. Pretreatment using acidified ethylene glycol with HCl 3. Pretreatment using acidified ethylene glycol with H ₂ SO ₄ 4. Pretreatment process using ionic liquids with HCl 5. Pretreatment process using ionic liquids without HCl 5. Alkaline pretreatment (170 °C, 1.5 h, 40 g L ⁻¹ NaOH and 1:10 w/v
Nakanishi (2016) Menezes et al. (2017)	Chemical composition Elemental analysis HHV determination Molar mass 2D HSQC Py-GC/MS	From alkaline pretreatment (1.5% w/v NaOH, 1:15 solid/liquid for 30 min) L1. At 130 °C L2. At 130 °C with anthraquinone (AQ) L3. At 170 °C L4. At 170 °C with AQ
Tana et al. (2016)	Chemical composition Elemental analysis ¹³ C NMR/ 2D HSQC / ³¹ P NMR FTIR Py-GC/MS Molar mass TG	1. Lignin from pretreatment 2. Lignin from enzymatic hydrolysis, early pretreated 3. Lignin from fermentation step, early submitted to a pretreatment and enzymatic hydrolysis steps

In this investigation, it was performed a physicochemical characterization of the Enzymatic Hydrolysis Residue (EHR) and LignoBoost Lignin (LBL) in order to understand details about their chemical and structural characteristics, enabling future processes and

product designs. Besides the chemical characterization and elemental analysis, these raw materials were characterized by the following methods/analyses: proton nuclear magnetic resonance spectroscopy ($^1\text{H-NMR}$), 2D NMR Heteronuclear Single-Quantum Correlation Spectroscopy (HSQC), Pyrolysis-gas chromatography-mass (Py-GC/Ms) spectrometry and Fourier Transform InfraRed (FTIR) spectroscopy to determine their functional and structural groups; Higher Heating Value (HHV) determination, and thermogravimetric (TG) analysis for thermal analysis and stability; particle size distributions by sieving and by laser scattering and Scanning Electron Microscope (SEM) for their morphological analysis. Some of these techniques are approached in the following.

2.6.1 Chemical compositional analyses

It is essential to determine the chemical composition before or during their use/application because of several factors that can affect the chemical composition of lignocellulosic biomasses. Methods for determination of chemical composition of lignocellulosic materials aim to quantify accurately all components present in biomass, such as extractives amounts, cellulose and hemicelluloses (carbohydrates), lignin and ashes contents (Sluiter et al., 2010).

Extractives can be easily extracted using water or organic solvents that consist in all plant parts that are extracellular or non-structural material from biomass (Hames, 2009). It is necessary to remove the extractives from biomass prior to analysis to prevent interference in later analytical steps (Sluiter et al., 2008). Woody feedstocks tend to contain less non-structural materials than Herbaceous biomasses (Sluiter et al., 2010).

Cellulose comprises 40-50%, hemicelluloses 15-30% and lignin 15-30% of lignocellulosic biomass (Alonso et al., 2012). **Table 2.2** shows chemical composition of different type and species of lignocellulosic biomass.

Ashes (inorganic material) in lignocellulosic biomass can be divided according to its origin and its plant part: (1) inherent vascular ash within the cells, (2) structural ash contained in cell walls, and (3) ashes from soil and sand contamination during all processing of biomass (Kenney et al., 2014; Thyrel, 2014). The ashes content in biomass, either structural or extractable, should be measured as part of the total composition. Structural ash is bound in the physical structure of the biomass, while extractable ash can be removed by washing or extracting the biomass (Sluiter et al., 2008). The ashes in woody biomass are mainly composed

by Ca, Mg and Mn, whereas in herbaceous biomass by K, P, S and Cl (Thyrel, 2014; Vassilev et al., 2010). The major elements in descending order contained in charcoal from sugarcane bagasse are K, Ca, Mg, P, Fe, Na, Al and Ti (García-Pèrez et al., 2002). The ash content in sugarcane bagasse is about 3% (Rocha et al., 2015), whereas in different *Eucalyptus* wood species (Neiva et al., 2015), such as *E. globulus* and *E. grandis*, is about < 1.0%. Some factors influence this ash content, such as the crop and the harvest period.

Table 2.2 - Chemical compositions of different lignocellulosic biomasses.

Lignocellulosic biomass	Lignin	Cellulose	Hemicelluloses	References
Gramineous	10-30	25 – 40	25 – 50	Betts et al. (1991)
Sugarcane bagasse	24	46	30	Rocha et al. (2015)
Sweet Sorghum	22	49	28	Kim and Day (2011)
Corn Stover	23	46	31	Zhu et al. (2005)
Hardwoods	18 - 25	45 – 55	24 – 40	Betts et al. (1991)
<i>Eucalyptus globulus</i>	19 - 30	47 – 50	12 – 22	Carvalho (1999)
<i>E. grandis</i> bark	27	49	23	Lima et al. (2014)
<i>E. grandis x urophylla</i> bark	28	52	20	Lima et al. (2014)
Beech	22	43	34	Demirbaş (2005)
Softwoods	25 - 35	45 – 50	25 – 35	Betts et al. (1991)
Spruce	29	48	23	Demirbaş (2005)
Pine (sapwood)	29	51	20	Waliszewska et al. (2015)
Cedar	35	41	24	Rabemanolontsoa (2015)

All values were normalized to sum 100%. Moisture, ash and extractive free basis.

Chemical characterization methods are applied to compare different lignocellulosic feedstocks; to monitor the compositions of biomass (component balances) at different stages of global process in biorefineries; to determine process yields; analyzing the economic viability, for example, of biomass-to-biofuel processes (Templeton et al., 2016); to estimate the nutritional value of animal feed; to analyze the dietary fiber content of human food (Sluiter et al., 2010); and, to others purposes. In context of this study, it is essential to perform a suitable characterization before applying the lignocellulosic biomass as the feedstock in phenolic resin formulations.

A portfolio of analytical methods (gravimetric or instrumental) is required to account for all the different components present in different lignocellulosic biomasses. The main challenge with these characterization methods is, to separately, isolate and quantify each component individually without any double counting, resulting in a summative mass close to 100% (Hames, 2009; Templeton et al., 2016). Among the analytical methods of chemical characterization, the sulfuric acid hydrolysis of lignocellulosic biomass has been used to measure all its components for more than 100 years (Sluiter et al., 2010).

2.6.2 Nuclear Magnetic Resonance (NMR) spectroscopy

NMR technique, a powerful tool, has been widely employed in elucidating of lignin by means of its detailed structural characterization (Chen and Robert, 1988; Pu et al., 2011; Ralph and Landucci, 2010; Ralph et al., 2004). Important functional groups of lignins can be determined such as methoxyl (Gonçalves et al., 2000) and phenolic hydroxyl (Pu et al., 2011).

Currently, different types of NMR spectroscopy are applied to assess the chemical structural of lignins, among them are ^1H -NMR (more traditional and older) (Chen and Robert, 1988; Gonçalves et al., 2000; Ibrahim et al., 2011; Tejado et al., 2007), ^{13}C -NMR (Balakshin and Capanema, 2015; del Río et al., 2007; Nadji et al., 2009; Samuel et al., 2010; Santos et al., 2011; Yang et al., 2014), 2D ^1H - ^{13}C HSQC NMR (del Río et al., 2012, 2015; Menezes et al., 2017; Menezes et al., 2016(b); Rencoret et al., 2009; Samuel et al., 2011; S. Yang et al., 2014) and ^{31}P -NMR (Balakshin and Capanema, 2015; Granata and Argyropoulos, 1995; Jiang and Argyropoulos, 1998; Pu et al., 2011). In this study, ^1H -NMR and 2D HSQC NMR techniques were used to chemical assessment of the lignocellulosic biomasses. In the following, the both NMR techniques will be addressed.

^1H -NMR spectroscopy

^1H -NMR spectroscopy has been used as an alternative and non-degradative technique for the characterization of lignocellulosic materials. As shown in the literature (Chen and Robert, 1988; Gonçalves et al., 2000), hydrogen signals can be assigned in a ^1H -NMR spectrum of acetylated lignin (**Table 2.3**). From integral of the area of main groups from lignin, relative amounts of important groups such as methoxyl and aromatic and aliphatic hydroxyls can be estimated.

Table 2.3 - Chemical shifts of ^1H and attribution in acetylated lignins (adapted from Chen and Robert, 1988).

Region chemical shift δ (ppm)	Attribution
9.00 - 12.00	Carboxylic acids and aldehydes
6.25 - 7.90	Aromatic region
5.75 - 6.25	Noncyclic benzylic region
5.20 - 5.75	Cyclic benzylic region
3.95 - 5.20 and 2.50 - 3.55	Aliphatic region
3.55 - 3.95	Methoxyl
2.20 - 2.50	^a Aromatic acetyl region
1.60 - 2.20	^a Aliphatic acetyl region
< 1.60	Nonoxygenated aliphatic region

^aFor acetylated lignins.

Heteronuclear Single Quantum Coherence (HSQC) spectroscopy

HSQC NMR spectroscopy, a powerful analytical technique, shows the correlation between ^1H and ^{13}C atoms directly bonded to each other and is now widely employed for the assessment of lignin structure (del Río et al., 2015; Menezes et al., 2017; Ralph and Landucci, 2010; Ralph et al., 2004; Rencoret et al., 2009; Rinaldi et al., 2016). The spectrum from 2D HSQC NMR of lignin can be divided up into three regions (Campos, 2014; Ibarra et al., 2007; Yang et al., 2014): (1) the aliphatic region ($\delta_{\text{C}}/\delta_{\text{H}}$ 5-50/0.5-3.0), the oxygenated aliphatic region C-O ($\delta_{\text{C}}/\delta_{\text{H}}$ 50-95/2.75-6.0), and (3) the aromatic region ($\delta_{\text{C}}/\delta_{\text{H}}$ 95-145/6-8.5). **Figure 2.8** illustrates a full 2D HSQC contour map of a lignin. The main signals in aliphatic region are of acetyl correlation, in both alcoholic and phenolic acetates. Additionally, it can observed signals corresponds to lipids and lignin degradation products (Ibarra et al., 2007).

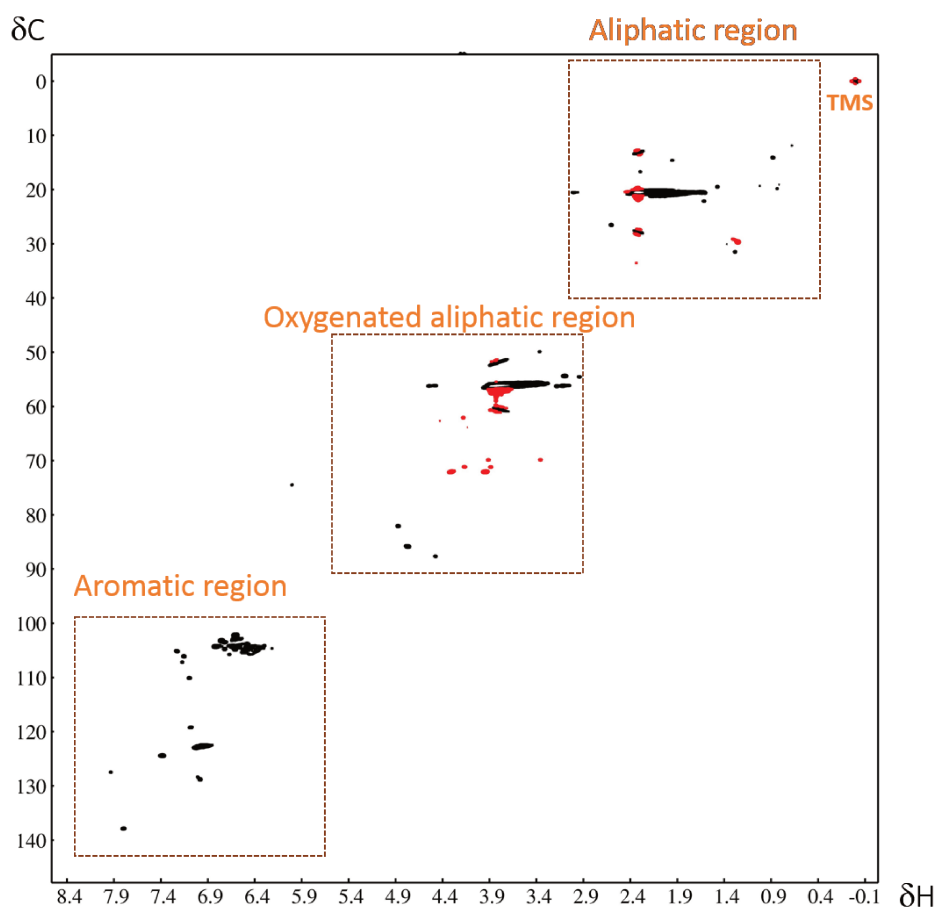


Figure 2.8 - A full contour map of 2D HSQC NMR of a lignin.

The oxygenated aliphatic region is the most important for the assessment of the lignin structure, because the major linkages in lignin (β -O-4, β - β' , β -5, α -O-4) (Rinaldi et al., 2016) can be assigned in this region, thus, the main substructures (β -O-4' alkyl-aryl ethers, phenylcoumaran, tetrahydrofuran, resinol and others) present in lignins can be determined (del Río et al., 2015; Rencoret et al., 2009). It can also be observed methoxyl group and carbohydrates (if it has) (Constant et al., 2016; del Río et al., 2015). Main structures which have been found in lignins in oxygenated aliphatic region are showed in **Figure 2.9**.

The aromatic region is the most important from the view point of the lignin composition, since the correlations of different aromatic units (H, G and S) are showed in this region (Constant et al., 2016). Main structures which have been found in lignins for this region are depicted in **Figure 2.10**.

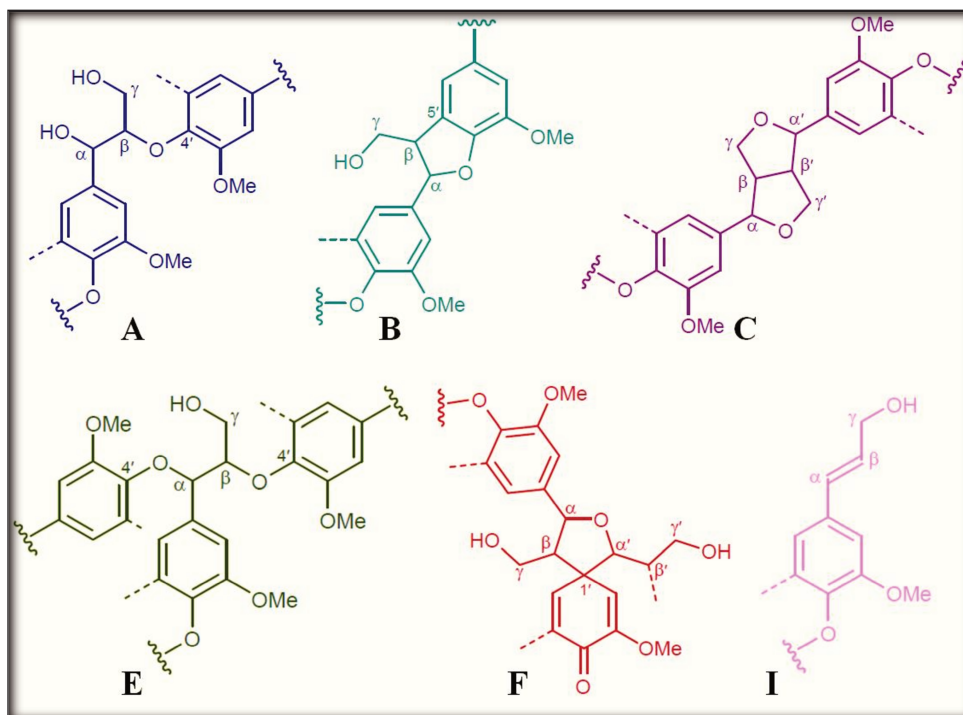


Figure 2.9 - Main structures found in oxygenated aliphatic region of lignins HSQC (adapted from del Río et al., 2015). (A) β -O-4' alkyl-aryl ethers; (B) phenylcoumarans; (C) resinols; (C') β - β tetrahydrofuran structure, (E) α,β -diaryl ethers; (F) spirodienones; (I) cinnamyl alcohol.

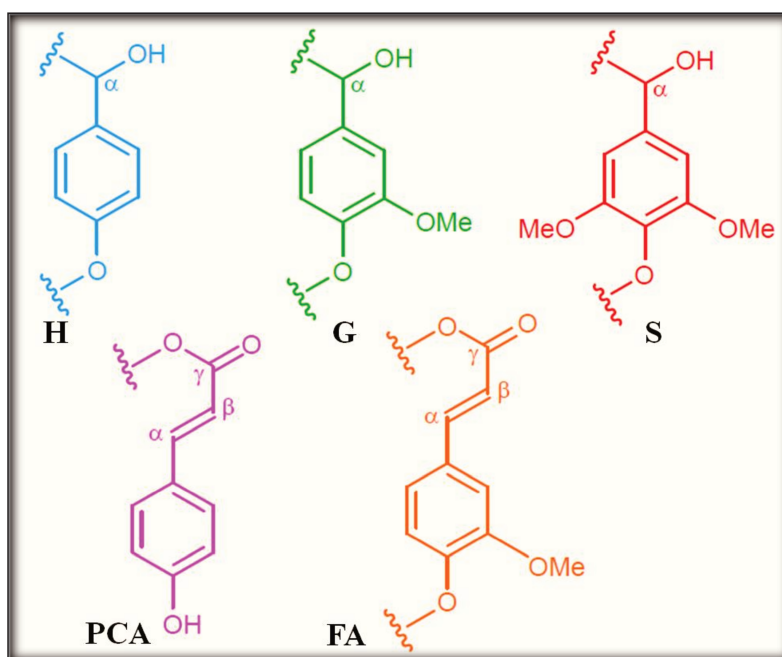


Figure 2.10 - Main structures found in aromatic region of HSQC lignins (adapted from del Río et al., 2015). PCA: *p*-coumaric acid; FA: ferulic acid; H: *p*-hydroxyphenyl unit; G: guaiacyl unit; S: syringyl unit.

2.6.3 Py-GC/MS technique

Py-GC/MS has proven to be a useful tool for lignin structure elucidation (Bezerra and Ragauskas, 2016; del Río et al., 2015; Rencoret et al., 2011; Tana et al., 2016). The Py-GC/MS allows an estimative of the S-, G- and H-lignin units. **Table 2.4** contains the main components released from these lignin aromatic units (S-, G- and H-units).

Table 2.4 - Main compounds released from S-, G- and H-units of sugarcane bagasse lignins from Py-GC/MS (based on Tana et al., 2016).

From S-unit	From G-unit	From H-unit
Syringyl	Guaiacyl	Phenol
4-methylsyringol	4-ethylguaiacol	3-methylphenol
4-ethylsyringol	Eugenol	4-methylphenol
4-allylsyringol	4-propylguaiacol	4-ethyl phenol
4-propylsyringol	<i>cis</i> -isoeugenol	4-allylphenol
<i>cis</i> -propenylsyringol	<i>trans</i> -isoeugenol	<i>cis</i> -4-propenylphenol
<i>trans</i> -propenylsyringol	Vanillin	<i>trans</i> -4-propenylphenol
Syringaldehyde	Homovanillin	4-hydroxybenzaldehyde
Homosyringaldehyde	Vanillic acid methyl ester	
syringic acid methyl ester	Acetovanillone	
Acetosyrigone	Guaiacylacetone	
Syringylacetone	dihydroconiferyl alcohol	
Propiosyringone	<i>trans</i> -coniferyl alcohol	
syringyl vinyl ketone	Coniferaldehyde	
syringic acid		
dihydrosinapyl alcohol		
<i>trans</i> -sinapyl alcohol		
<i>trans</i> -sinapaldehyde		

2.6.4 Fourier Transform InfraRed (FTIR) spectroscopy

Spectroscopy methods are based on the measurement of radiation emitted from a media or the interaction of electromagnetic radiation with a media. Electromagnetic radiation can be described a wave, for example, by its wavelength (μm), or its wavenumber (cm^{-1}) - the number of waves per unit of distance. Infrared radiation covers the wavenumbers of 13,300 - 3.3 cm^{-1} . The infrared radiation can be divided into three regions: near-infrared (13,300 - 4,000 cm^{-1}), middle-infrared (4,000 - 200 cm^{-1}) and far-infrared (200 - 3.3 cm^{-1}) (Bykov, 2008).

Infrared spectroscopy measures transitions between molecular vibrational energy levels as a result of the absorption of mid-infrared radiation (Larkin, 2011). Since the vibrational energy levels are unique to each molecule, infrared spectrum provide a “fingerprint” of a particular molecule (Larkin, 2011). The vibrational spectrum may be divided into typical regions shown in **Figure 2.11**. Infrared spectrometer can be divided into two groups: dispersive and Fourier Transform (Bykov, 2008). However, currently the FTIR spectrometers are the most used because they are more modern and have several performance advantages in relation to dispersive infrared (Thermo Nicolet, 2002).

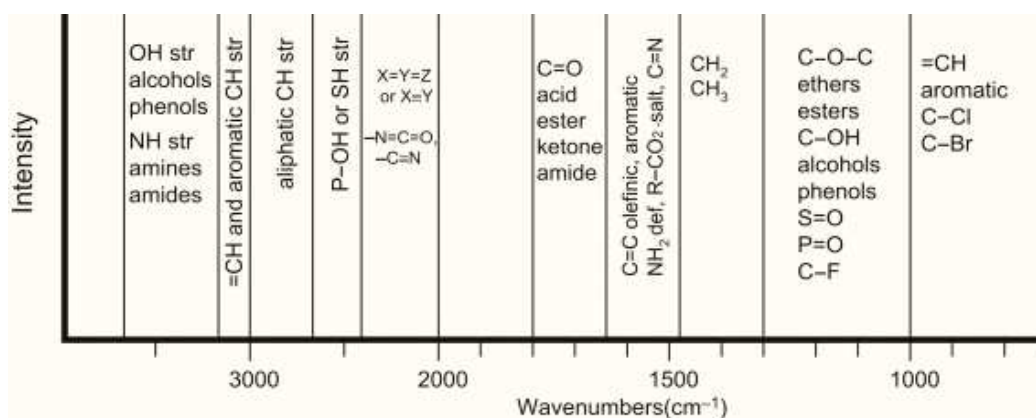


Figure 2.11 - Regions of the fundamental vibrational spectrum (adapted from Larkin, 2011).

FTIR spectroscopy is a rapid, a time-efficient, a nondestructive technique that requires only small quantities of sample material (Traoré et al., 2016; Tucker et al., 2001). FTIR spectroscopy, an useful analytical method, is widely used in qualitative and also quantitative analysis of components in solids in the middle-infrared region (Tucker et al., 2001) because of its ability to provide information about functional groups abundance and other specific structural features (Traoré et al., 2016). The **Figure 2.12** depicts the characteristics spectra of the main biomass components (cellulose, hemicelluloses and lignin).

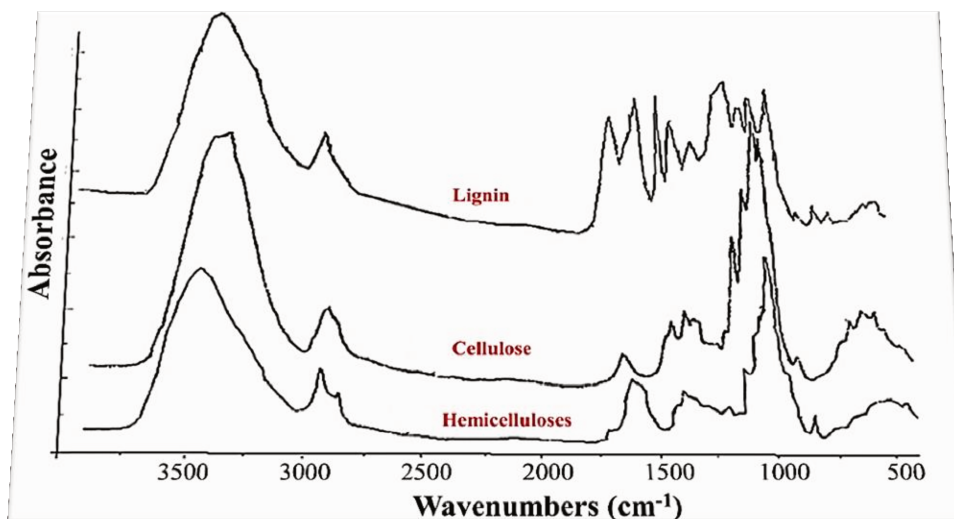


Figure 2.12 - FTIR spectra of cellulose, hemicelluloses and lignin (adapted from Yang et al., 2007).

2.6.5 Elemental Analysis

Elemental composition of the biomass consists in determination of carbon, hydrogen, oxygen, nitrogen and sulfur amounts. This information can be expressed in a dry or ash-free basis. Determination of the elemental composition of biomass is important, for example, in performing balances on biomass conversion processes, such as hydrogenation, pyrolysis, and gasification (Demirbas, 2004; Rennè et al., 2007).

Lignocellulosic biomasses contain higher oxygen content (typically 40-45 wt.%) than fossil fuels (Demirbas, 2010). Cellulose and hemicelluloses can be represented for a generic molecular formula $\text{CH}_{1.7}\text{O}_{0.83}$ and $\text{CH}_{1.6}\text{O}_{0.8}$, respectively, based on one mole of carbon (Rennè et al., 2007). It is a common practice to express the chemical composition of lignins in terms of a C9 unit structure based on elemental analysis and OCH_3 determination. The formula of a typical milled wood from softwood is reported as $\text{C}_9\text{H}_{8.3}\text{O}_{2.7}(\text{OCH}_3)_{0.97}$ and from a typical hardwood such as $\text{C}_9\text{H}_{8.7}\text{O}_{2.9}(\text{OCH}_3)_{1.58}$ (Calvo-Flores et al., 2015). From the elemental analysis data of biomass, higher heating values (HHVs) can also be calculated (Demirbas et al., 1997).

2.6.6 Thermogravimetric analysis (TG)

The fundamental of thermal analysis can be summarized ‘as the measurement of a change in a sample property, which is the result of an imposed temperature alteration’ (Hemminger and Sarge, 1998; White et al., 2011). **Table 2.5** shows a listing of thermoanalytical techniques classified according to their measured physical properties. Among thermos analytical techniques, TG analysis was applied to assess the lignocellulosic materials (EHR and LBL). TG analysis and Differential Scanning Calorimetry (DSC) techniques were used in lignin-phenolic resins produced in this study.

TG analysis is the most commonly applied thermoanalytical technique in solid-phase thermal degradation studies. Yang et al. (2007) performed TG analysis separately for the three major components of biomass (cellulose, hemicelluloses and lignin) (**Figure 2.13**).

It may be observed that the decomposition of hemicelluloses started easier in relation to others biomass components. This fact can be related with random and amorphous structure of hemicelluloses rich in branches which are easier to remove from the main stem. The weight loss of cellulose mainly happens at a higher temperature range (315 - 400 °C) (Yang et al., 2007). Among these three components, lignin is the most difficult one to decompose (Yang et al., 2007).

Table 2.5 - Thermoanalytical techniques classification according to properties (White et al., 2011).

Thermoanalytical techniques	Property
Thermogravimetric analysis (TG)	Mass
First derivative thermogravimetry (DTG)	Mass
Differential thermal analysis (DTA)	Temperature
Differential scanning calorimetry (DSC)	Heat
Thermomanometry	Pressure
Thermodilatometry	Dimensions
Thermomechanical analysis (TMA)	Mechanical properties
Thermoelectrical analysis (TEA)	Electrical properties
Thermomagnetic analysis	Magnetic properties
Thermoacoustic analysis (TAA)	Acoustic properties
Thermooptical analysis (TOA)	Optical properties

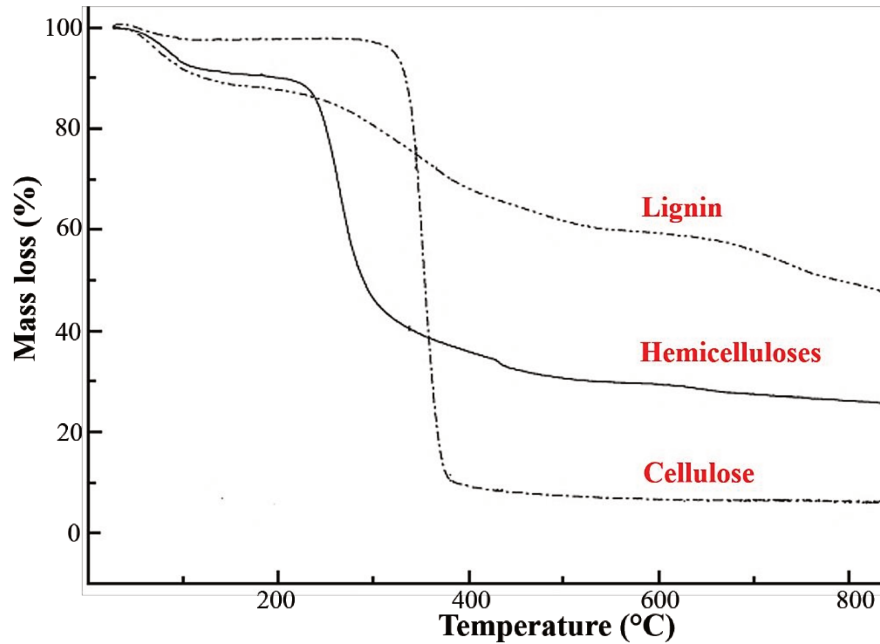


Figure 2.13 - TG curves of cellulose, hemicelluloses and lignin (adapted from Yang et al., 2007).

2.6.7 Scanning Electron Microscope technique (SEM)

SEM technique have been applied for observing lignocellulosic materials, for example, to visualize the morphological changes of their surfaces when submitted to different pretreatments. Nongthombam et al. (2017) analyzed six different biomasses submitted to two different pretreatments (hydrothermal and alkaline), among them, the sugarcane bagasse. The surface of raw sugarcane bagasse and the surface of sugarcane bagasse hydrothermally pretreated did not presented any marked difference except with an appearance of a few droplets like structures (Nongthombam et al., 2017). However, the sugarcane bagasse submitted to alkaline pretreatment, changes in terms of the disappearance of smooth covering accompanied by fragmentation and fibrillation more than raw sugarcane bagasse was evident with higher numbers of droplets like structures (Nongthombam et al., 2017).

Michel et al. (2013) observed by means of SEM of four types of fibers extracted by chemical processing at different alkaline concentrations in a pilot scale. The SEM analysis of these extracted fibers allowed to assess the influence of the extraction conditions on the surface of fibers. In general, the SEM analyses are applied in the morphological characterization of lignocellulosic materials, mainly to observe the cellulose fibers present in them. When the lignocellulosic material consists essentially of lignin, the SEM technique is

not suitable. An alternative to physically analyze lignin would be the small-angle X-ray scattering technique (SAXS). Brenelli et al. (2016) applied the small-angle X-ray scattering technique to provide biophysical parameters from lignin of soluble fractions. SAXS studies (Brenelli et al., 2016; Harton et al., 2012) have been performed to characterize lignin molecular architecture, shape, dimensions and intermolecular interactions.

2.7 Lignin and lignin-based products market

Lignin is the major by-product of chemical pulping and one the major in emerging biorefineries. About 55×10^6 tonnes year⁻¹ of Kraft lignin are produced by chemical pulping (Liitiä and Tamminen, 2016). Lignin is mainly burnt in a chemical recovery process where it is an integral part of the pulp industries. As a result, less than 2% of the available lignin is isolated and sold, primarily in the formulation of dispersants, adhesives and surfactants. However, lignin-based product development is essential to extend the biorefinery concept. Pulp mills need to diversify their products portfolio to maintain their existence; and emerging biofuel/bioenergy technologies need to develop value-added from lignin in order to achieve economic and environmental sustainability (Mordor Intelligence, 2017).

The lignin market can be segment based on product type, on its source and on its application. Based on product type, the lignin market can be divided as lignosulphonates, Kraft lignin, high-purity lignin (LignoBoost) and others. For example, the market for high purity lignin was expected to be valued at USD 8.82 million in 2015. Based on source of lignin, it is classified as Kraft pulping, sulphite pulping, and cellulosic ethanol. For example, the sulphite pulping source type in the global lignin products market was estimated at USD 616 million in 2015. The production of sulphite pulps is much smaller than the production of Kraft pulps. Based on applications of lignin, the market is segment as concrete additives, animal feed, vanillin, dispersants, resins, and others. The vanillin segment in the global lignin products market was estimated at USD 54 million in 2015 (Mordor Intelligence, 2017). **Table 2.6** gathers some lignin-based products and their requirements. Among the lignin-based products, phenolic resins provide high-volume markets for lignin. Global demand of phenolic resins was 6×10^6 tonnes in 2013. In **Figure 2.14**, it can be observed the global phenolic resin demand by end use (Liitiä and Tamminen, 2016).

The major companies that use lignin as raw material include Borregaard LignoTech, Tembec Inc., Domtar Corporation, WestRock Company, Asian Lignin Manufacturing Pvt.

Ltd. and among others (Mordor Intelligence, 2017). In Brazil, the Suzano (a Pulp and Paper Industry) is installing the first industrial plant of lignin and derivatives of Latin America (Limeira Unit - State of São Paulo) (Suzano, 2018).

The objective of this research is to produce a phenol-formaldehyde resin, as this type of thermosetting polymer is quite common and has several applications (Chung and Washburn, 2012). A brief outline of phenolic resins; their synthesis process, characteristics and applications, cure kinetics of phenolic resins and lignin as feedstock in phenolic resins will be presented next.

Table 2.6 - Main product requirements and lignin applicability based on inherent structural features (based on Liitiä and Tamminen, 2016).

Lignin-based products	Main product requirements
Phenol-formaldehyde resins	Reactivity: high phenol and low methoxyl content Alkali solubility
Polyurethanes	Reactivity: aliphatic hydroxyl functionalities Dispersion stability Low molar mass
Thermoplastic composites	Thermally mouldable Strength Thermal stability
Surface active agents	Water solubility Hydrophilic/hydrophobic balance Molar mass
Carbonised materials	Less sensitive for purity or chemical structure High quality demands for carbon fibers
Fuels and chemicals	Native structure (high β -O-4 linkages) Sulphur free

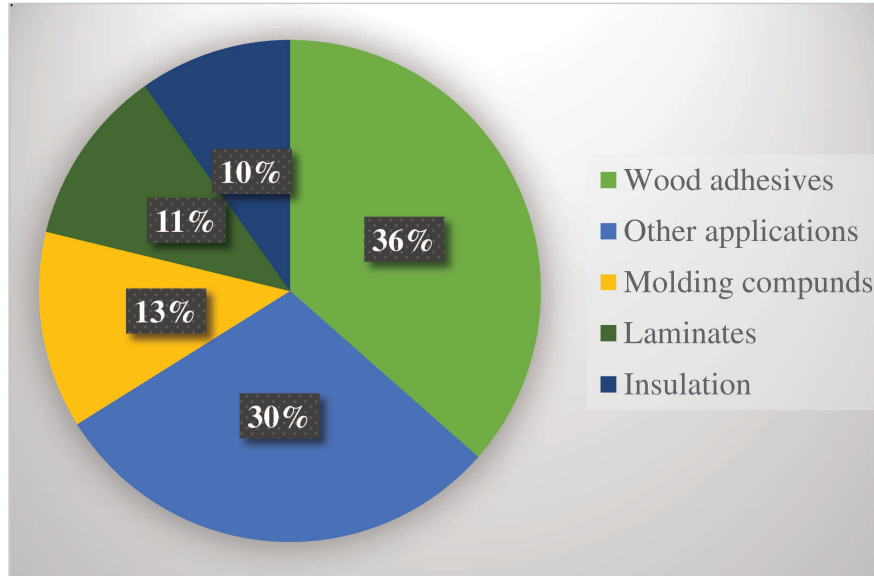


Figure 2.14 - Global phenolic resin demand by end use (adapted from Liitiä and Tamminen, 2016).

2.8 Phenolic resin

Phenol-formaldehyde resins were first commercially available in 1907 (American Chemical Society National, n.d.) and have been of vital importance to the polymer industry. They are today among of the most widely produced resins (Showa Denko Group, 2017). The phenolic resins are used in a wide variety of applications and industries (**Figure 2.15**).



Figure 2.15 - Phenolic resin applications (adapted from Showa Denko Group, 2017).

The main types of the phenolic resins, novolac and resole, can be used in different ways and applications. Concerning phenolic novolac resins, they are applied in wood coatings. They are used to formulate high-performance varnishes and oil-based vehicles and as curing agents for epoxy resins in applications such as moulding materials, laminates, coatings and adhesives. Moreover, novolac resins are used as coatings in the oil and gas industries and for saturating substrates in applications such as oil and air filters and cooling water media (Georgia-Pacific Chemicals, 2017). The resole-type phenolic resins are used in the automotive and aerospace industries, fiber-reinforced polymers, public transport and car rails. They are also used in the manufacture of wood and plywood products, oriented strand boards, laminated veneer lumber and composite panels (Chemicals, 2017; Ibeh, 1998; Showa Denko Group, 2017). Resole-type phenol-formaldehyde resin is the most common type of adhesive among the various adhesives that are required in many wood processing industries (particleboard, wood panels, fiber boards and plywood) (Chemicals, 2017).

2.8.1 Synthesis of phenolic resins

Phenolic resins are commonly produced by reacting phenol (C_6H_5OH) with formaldehyde ($HCOH$). Phenol is reactive towards formaldehyde at the *ortho* and *para* sites (sites 2, 4 and 6) allowing up to three units of formaldehyde to attach to the ring. Under acidic catalysis and an excess of phenol, novolac-type phenolic resins are formed; whereas resole-type phenolic resins are formed under basic catalysts and an excess of formaldehyde, after heat and/or pressure application.

Various parameters, such as formaldehyde/phenol (F/P) molar ratio, catalyst concentration, pH, reaction temperature and reaction time, could affect the characteristics of these resins (Pasch and Schrod, 2004). Depending on the formaldehyde to phenol molar ratio and the catalysts that are used, two different classes of resins can be formed: novolacs or resoles. Novolacs are thermoplastic polymers that require an 'additive' to enable further curing and the formation of insoluble and infusible products. On the other hand, resoles are capable of forming a network structure when submitted to heat and pressure during the moulding process (Ibeh, 1998).

The cure of a thermosetting reactive prepolymer usually involves transformation of low-molecular weight monomers from the liquid to the solid state as a result of the formation of a

polymer network by the chemical reaction of the reactive groups of the system. The formation of a thermosetting crosslinked network is depicted schematically in **Figure 2.16**.

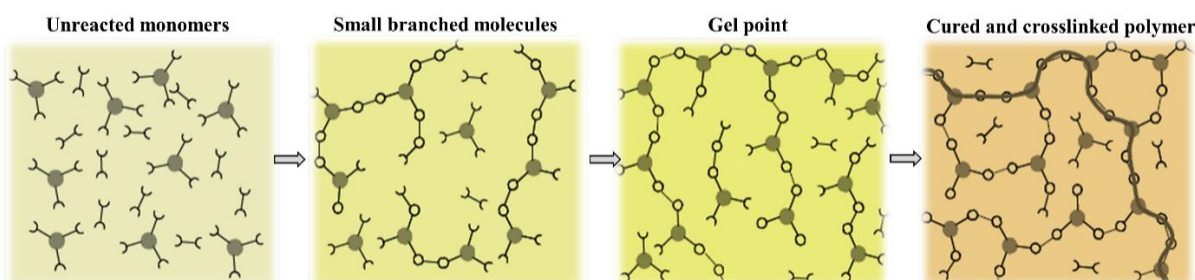


Figure 2.16 - Schematic representation during a thermosetting curing (adapted from TA Instruments, 2004).

Two stages, which are divided by the gel point (t_{gel}), are usually distinguished in this process (Laza et al., 2002):

- (1) Growth and branching of the polymer chains that occur in the liquid state, where the reactive system is soluble and fusible (thermoplastic resin).
- (2) An infinite network of polymer chains that appears and develops only after the gel time (t_{gel}). Then, the reactive system loses its solubility and fusibility, which leads to the final reactions, which take place in the solid state (thermosetting resin).

Since lignin is rich in phenolic groups and is from a renewable source - and is more readily available, less toxic and less expensive than phenol - it can be a good option to produce these resins (Mansouri and Salvadó, 2006).

2.8.2 Cure Kinetics of phenolic resins

The cure step is the most critical element in thermoset processing (TA Instruments, 2004). Understanding of the formation of a thermoset crosslinked network process (**Figure 2.16**) has been advanced substantially (TA Instruments, 2004). From curing kinetics study, important kinetics parameters can be reached, as gel point, curing time, activation of energy and conversion values (TA Instruments, 2003). Kinetics study of curing process for phenolic resins can be performed by means of main three techniques: DSC, TG and rheology. These techniques can provide valuable information about the kinetics of curing reaction.

The curing condensation reaction of the phenolic resin occurs, generally, up to 100 °C. In DSC curve, the endothermic evaporation of the water byproduct distorts the curing exotherm which must be analyzed in its entirety to obtain a valid kinetic model. As indicated

in literature (Alonso et al., 2006, 2004; Hitachi, 1981), this type of system must be run in a pressure DSC which can suppress the volatilization of the water. Thus, in this research it was chosen to perform the kinetic study by means of rheology, in particular, and thermogravimetry. Rheology technique allows measurement of the curing and rheological characteristics of phenolic resins and gives information about the changes in rheological properties (viscoelastic behavior) with time (isothermal) or temperature (dynamic)(Laza et al., 2002).

2.8.3 Lignin as feedstock in phenolic resins

No further depolymerisation is required and processing is thus simpler to use lignin from industrial processes as feedstock in phenol-formaldehyde resins. Up to 50% of the phenol content in this material can be replaced, for example, by lignosulfonate, Kraft, or Organosolv lignin without significantly compromising properties of the resin (Rinaldi et al., 2016).

Numerous reports have been published on the preparation of resole-type phenolic resins from woody or agricultural lignin. **Table 2.7** depicts some researches that used various type of lignin to partially replacing the petroleum-based phenol in synthesis of phenol-formaldehyde resin.

Table 2.7 - Some papers about lignin use in resole-type phenolic resins.

Lignin type	% phenol by lignin	Authors (year)
Enzymatic hydrolysis lignin from bioethanol production using cornstalk	10 - 70%	Qiao et al. (2015)
Lignocellulosic ethanol residue from corn and wheat straws	10 - 70%	Zhang et al. (2013)
Enzymatic hydrolysis lignin from cornstalk residues obtained in bioethanol production	5 - 25%	Jin et al. (2010)
Organosolv lignin from white pine sawdust	25 - 75%	Wang et al. (2009)
Methylolated softwood ammonium lignosulfonate	35%	Alonso et al. (2004)
Alkaline lignin from sugarcane bagasse	10 - 60%	Khan et al. (2004)
Acetosolv lignin from sugarcane bagasse	40%	Piccolo et al. (1997)
Organosolv lignin	5 - 40%	Çetin and Özmen (2002)
Lignin obtained by acetosolv delignification of Eucalyptus globulus wood.	20 - 40%	Vázquez et al. (1995)

Çetin and Özmen (2002) studied the potential for partially replacing phenol (5-40%) with organosolv lignin (Commercial Alcell™ lignin) in resole-type phenolic resin used as an adhesive in particleboard production. The physicochemical characteristics analysed were free phenol and formaldehyde contents, hardening time and specific gravity. The greater the lignin amount in resins, higher values of free phenol and formaldehyde content. When compared with a commercial resole resin, it is noted that the hardening times were similar in resins with until 20% of lignin indicated that these resins had good curing properties. With respect to the specific gravity values, they were practically the same in all obtained resins.

Alonso et al. (2004) assessed the potential of the partial phenol replacement (35%) by a methylolated softwood ammonium liginosulfonate in resole phenolic resins. The kinetic parameters of these resins were determined and the effect of liginosulfonate lignin on the curing process was analyzed by DSC technique. The authors observed that the cure process was slower in liginosulfonate resins than in commercial phenolic resins. However, the obtained values for the activation energy and the reaction order in the curing process were similar in both resins.

Khan et al. (2004) partially replaced the oil-based phenol (10-60%) by alkaline lignin from sugarcane bagasse in synthesis of resole-type lignin-phenol resins. Thermal stability of these resins was found to be lower as compared to phenolic resin without lignin. By DSC studies, they observed a lower curing temperature for lignin-phenolic adhesive in comparison to phenolic adhesive.

Zhang et al. (2013) used the lignocellulosic ethanol residue from corn and wheat straw in synthesis of resole-type phenolic adhesives. The better conditions for preparation of these adhesives were substitution rate at 50%. Higher levels of phenol replacement were limited by the decrease of the bonding strength. Phenolic resins without lignin had better heat resistance.

Jin et al. (2010) assessed the potential for 5 - 25 wt% phenol replacement for enzymatic hydrolysis lignin in phenolic adhesives to use in high performance plywood production. This lignin was extracted with sodium hydroxide solution from cornstalk residues in bioethanol production. When the replacement percentage of phenol by lignin was in the range of 5-20 wt%, the properties of glued plywoods with the adhesive are almost same of standard resin for first grade plywood. The wet bond strength was much higher than the standard resin when the maximum lignin replacement content was of 20 wt%.

Qiao et al. (2015) used the enzymatic hydrolysis lignin to partially replace phenol for preparing phenolic resin. The main results found by them were: the limit of replacement

phenol without decreasing the adhesive strength was until 50 wt%. Wang et al. (2009) used the organosolv lignin as replacement of petroleum-based phenol at various ratios of substitution (25 - 75 wt%) in the synthesis of phenolic resole resins. This organosolv lignin was extracted from white pine sawdust with hot-compressed ethanol-water co-solvents. The curing process was retarded for phenol replacement higher than 50 wt%. It was noted that the introduction of lignin in the resin formula decreased the thermal stability of the resin, leading to a lowered decomposition temperature and a reduced amount of carbon residue at elevated temperatures. They concluded that in practical applications the replacement ratio of phenol with lignin be less than 50 wt%.

Piccolo et al. (1997) used organosolv lignin for replacement 40 wt% of phenol in phenolic resin to use in thermosetting composite. This lignin was extracted from sugarcane bagasse by organosolv process (acetic acid/HCl/water). The use of lignin as a partial substitute of phenol in phenolic resins for applications different from those traditionally considered (as for instance adhesives) is viable as demonstrated by the results obtained for lignophenolic matrix composites, including those obtained by TG and DSC, which showed a similar thermal stability for phenolic.

Vázquez et al. (1995) assessed the potential of lignin obtained by acetosolv delignification of *Eucalyptus globulus* wood in resole adhesives for plywood production. The reactivity of lignin-phenol-formaldehyde resins prepared with the eucalyptus lignin, as measured by their gel time, increased with formaldehyde/phenol (1.5 - 2.5) and soda/phenol (0.4-0.6) and decreased with increasing percentage of substitution of phenol by lignin.

2.9 Composites using fibers as reinforcement

Composite term is applied to heterogeneous or multiphase materials in which one of the components is discontinuous (reinforcement), and the other is a continuous component (matrix). The reinforcement is the main responsible for the material resistance, while the matrix is responsible to transfer and distribute the load to the reinforcement (Oliveira, 2008). Different types of composites present different characteristics, and their uses in different applications depend on factors such as structural performance, price and availability of raw materials, among other parameters (Pardini and Levy Neto, 2006).

The use of lignocellulosic materials (renewable) has been growing in recent years with the growing need to protect the environment and minimize dependence on non-renewable

resources, and thus effectively promote sustainable development (Pardini and Levy Neto, 2006). Natural fibers exhibit many advantageous properties, for example, they have low-density producing composites with high specific properties. In addition, natural fibers have relatively lower costs and ease of processing (Loh et al., 2013; Verma et al., 2012). Briefly, **Table 2.8** brings the main advantages and disadvantages of using nature fibers as reinforcement in composites. **Figure 2.17** shows the classification of fiber reinforced compounds.

Table 2.8 - Advantages and disadvantages of the nature fibers use (Pardini and Levy Neto, 2006).

ADVANTAGES	DISADVANTAGES
Low specific mass	Do not withstand high processing temperatures
Softness and reduced abrasiveness	High variability in mechanical properties
Recyclable, non-toxic and biodegradable	high sensitivity to environmental effects
stimulate jobs in rural areas	complex and non-uniform geometry
Low power consumption in production	modest mechanical properties
Low specific mass	Do not withstand high processing temperatures

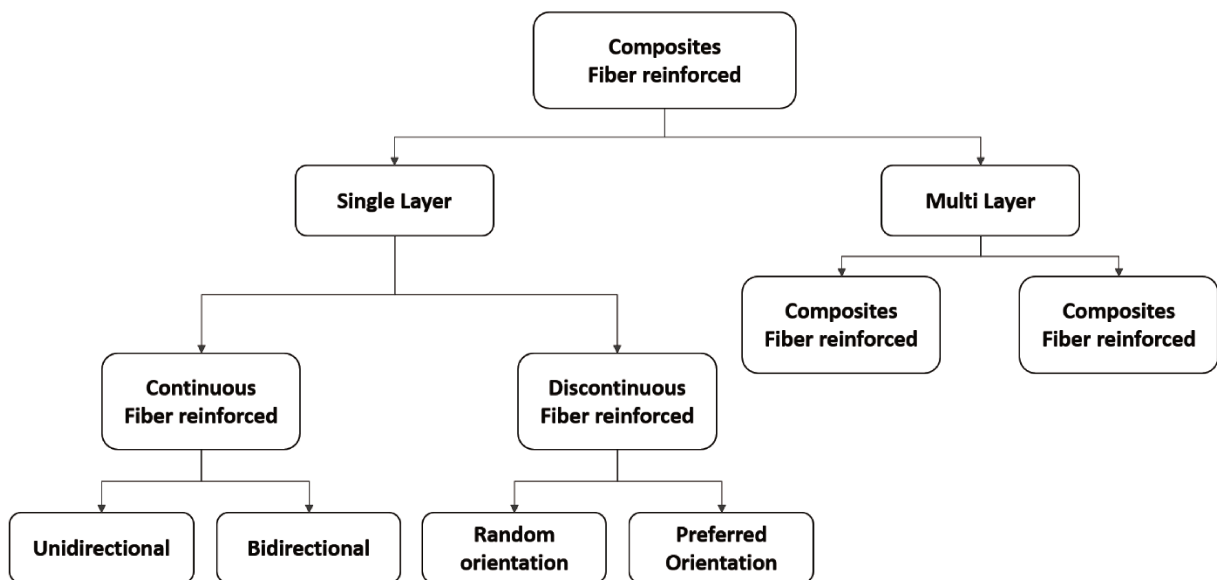


Figure 2.17 - Classification of the fiber reinforced composites (adapted from Pardini and Levy Neto, 2006).

Natural fibers, when used as reinforcement, provide good results compared to the technical fibers, such as glass fiber. Several natural fiber composites achieve the mechanical properties of composites with glass fibers and they are already applied, for example, in automobile and furniture industries. Some important natural fibers are jute, flax, bagasse and coir. Bagasse fiber composites appears to be promisor because they are cheaper, lighter and environmentally less aggressive to, in general, composites with glass fiber or other synthetic fiber (Verma et al., 2012).

As earlier mentioned, this research aimed to insert the EHR (Enzymatic Hydrolysis Residue) in resins synthesis without any previous purification. Taking into account the concept of composite presented in this section, it was preferred to call the phenolic system with EHR (mainly lignin and cellulose fibers) as a resin. However, the idea of this research was to evaluate if these cellulose fibers present in the EHR acts as reinforcement in the phenolic resin.

Chapter 3 OBJECTIVES

3.1 General Purpose

This research aimed to explore the potential of two lignocellulosic materials (sugarcane bagasse and Kraft lignin) that are abundant in Brazil to produce phenolic resins formulations. The Enzymatic Hydrolysis Residue (EHR) from sugarcane bagasse and the LignoBoost Kraft lignin (LBL) from Eucalyptus were applied on the phenolic resins production.

3.2 Specific Purposes

- To perform a full characterization of the EHR and the LBL;
- To synthesize phenolic resins by partially replacing petroleum-based phenol with LignoBoost lignin (LBL) in fractions of 5, 15, 30, 45 and 60 wt%;
- To synthesize phenolic resins by partially replacing petroleum-based phenol with the EHR lignin in fractions of 5, 15, 30 and 45 wt%;
- To determine the curing parameters of the phenolic resins with the EHR and LBL;
- To perform a physicochemical and thermomechanical characterization of the phenolic resins with the EHR and LBL.

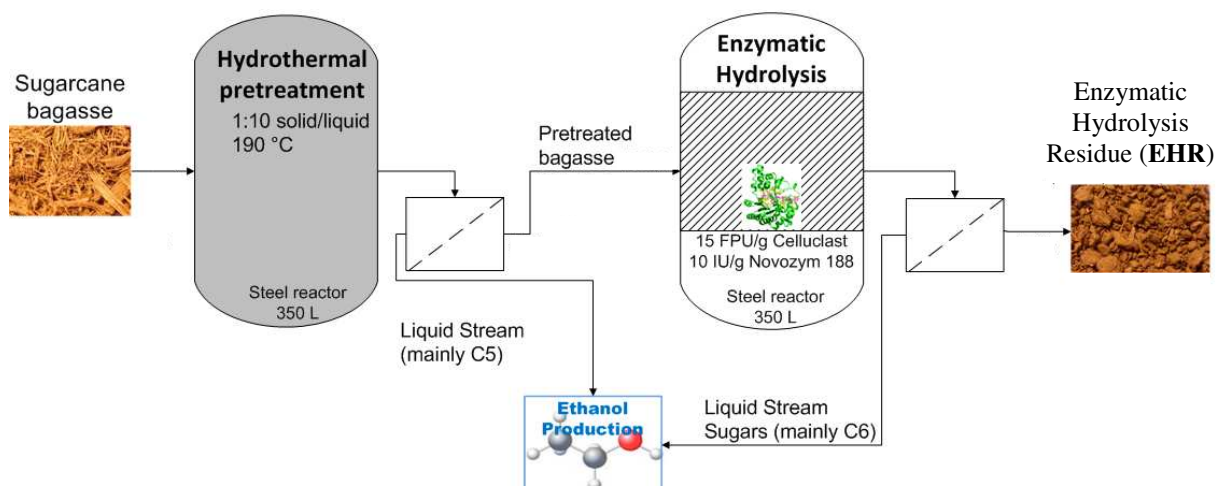


Figure 4.2 - Obtainment of the EHR at pilot scale (adapted from Menezes et al., 2016b).

It was obtained from a process where sugarcane bagasse was pretreated in a 350 L steel reactor (Hastelloy C276) built by Pope Scientific. The hydrothermal pretreatment occurred at 190 °C for 15 min with constant temperature and a solid/liquid ratio of 1:10. The purpose of this process was to hydrolyze the hemicelluloses, decreasing the recalcitrance of the biomass. Then, the enzymatic hydrolysis process was undertaken at 50 °C using the 15 FPU/g of dry biomass of cellulolytic complex (CelluclastTM 1.5 L) and 10 IU/g dry lignocellulose of β -glucosidase (NovozymeTM 188).

The enzymatic hydrolysis process was carried out in the same reactor used to the pretreatment process, a 350 L Hastelloy C276 (Pope ScientificTM) steel reactor. After the filtration step in a Nutshe filter (100 L capacity, Hastelloy C-276, Pope Scientific), a liquid stream enriched in glucose and a solid stream enriched in lignin were obtained. The former was conducted to the fermentation step and the latter was washed with water and dried at room temperature, obtaining the EHR. Mass yield values of each step were estimated for each step. Mass yield was determined divided the total final mass by total initial mass on each process and multiplied by 100 (%).

In order to better characterize the EHR, it was submitted to two different extraction processes: the alkaline and the acidic-dioxane. These extracted lignins were used only for analytical and comparative purposes. The alkaline EHR and the acidic-dioxane EHR were analyzed by pyrolysis-gas chromatography-mass spectrometry (Py-GC-MS) in order to determine the H, G and S-units amounts present in these lignins. The alkaline EHR and acidic-dioxane EHR were not used to phenolic resins production. The EHR was inserted in

resins synthesis without any previous purification in order to assess how its fibers influence on the properties of their resins.

The alkaline process for extraction of the EHR was performed as follow. Alkaline delignification process of the EHR using a NaOH solution (1.5%) was performed in a Parr Stirred Vertical Reactor (2 L). The solid/liquid ratio was 1:10. The reaction conditions were the following: 100 °C for 1 hour with stirring at 300 rpm. Next, the material was filtrated to precipitate the lignin; sulfuric acid (98%) was added slowly to the liquid part until pH 2 was reached. After storing it overnight in a refrigerator, the vacuum filtration was conducted. The extracted lignin from the EHR (alkaline EHR) was washed until pH 5 was reached. Lastly, it was dried overnight using a Thermo Scientific™ SpeedVac centrifuge.

The acidic-dioxane method can be suitable for extracting lignin from EHR, because it uses mild conditions as organic solvents, minimizing the reactions of degradation and/or condensation (Fukushima and Hatfield, 2001). The acidic-dioxane extraction process based on Pepper et al. (1959) was performed in a system with a flask connected to a reflux condenser in a heating mantle. EHR and dioxane/HCl 2N (9:1) at ratio of 1:10 w/v were added to the flask. The extraction process occurred at 90 °C for 4 h. Then, it was submitted to filtration and wash processes. The liquid part was concentrated in a rotaevaporator to a small volume. Water was added to this concentrated and then, it was subjected to centrifugation process. The solids decanted consisted the extracted lignin, called here as acidic-dioxane EHR (Fukushima and Hatfield, 2001; Mobley, 1994; Pepper et al., 1959).

Another material used in this research was a Eucalyptus Kraft Lignin from LignoBost process (LBL). This was provided by the Fibria Industry (a Brazilian pulp and paper company) for this research. It was obtained in a pilot plant of the LignoBoost process in the Fibria Industry. The LBL was originated from a Kraft pulping of Eucalyptus and obtained through the LignoBoost process (Hu et al., 2018; Tomani, 2010) (**Figure 4.3**).

**PULP INDUSTRY
FIBRIA (JACAREI)**

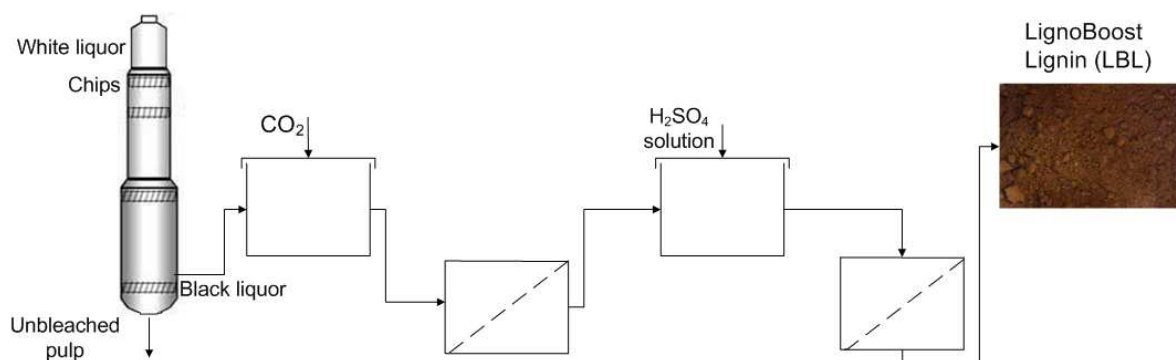


Figure 4.3 - LignoBoost lignin process (Based on Tomani, 2010).

The following analyses were carried out in order to obtain a detailed characterization of the EHR and the LBL:

- Chemical composition: lignin, cellulose, hemicelluloses and ashes contents;
- Elemental analysis: C, H, N, S, O%;
- Fourier-transform Infrared (FTIR) spectroscopy: main functional groups;
- ¹H-Nuclear Magnetic Resonance (NMR) spectroscopy: methoxyl and hydroxyl groups;
- 2D Nuclear Magnetic Resonance (NMR) spectroscopy (Heteronuclear Single Quantum Coherence - HSQC): H-, G-, S-lignin unit amounts;
- Pyrolysis - gas chromatograph/mass spectrometry technique: H-, G-, S-lignin unit amounts;
- Molar mass determination (only for LBL);
- Calorific power: Higher Heat Value (HHV);
- Thermogravimetric analysis (TG);
- Particle size distribution by sieving and by laser diffraction;
- Scanning Electron Microscopy (SEM).

All characterization analyses of the LBL and EHR were carried out in facilities from the Brazilian Center for Research in Energy and Materials (CNPEM), with exception the molar mass determination that was performed in the Universidad Simón Bolívar (Venezuela).

4.1.1 Chemical composition

The EHR and the LBL were chemically characterized according to the methodology developed by Rocha et al. (1997) and validated by Gouveia et al. (2009). The lignocellulosic materials were analyzed in order to determinate carbohydrates, acid-insoluble and soluble lignin and ash contents. The first step consists in acid hydrolysis of the samples. Two grams of dried and milled sample (≤ 20 mesh) were weighed into a 100-mL beaker. They were placed in a thermostated bath at 45 °C for 10 min. Then, H₂SO₄ 72% solution (15 mL) was mixed vigorously with them for 7 min. They were removed from the bath and distilled water (50 mL) was added. Then, the solution was transferred to a flask (500 mL) and it was added distilled water (225 mL). The flask was capped and autoclaved at 121 °C for 30 min. Lastly, the hydrolysed solution was filtered and washed until complete 500 mL in a volumetric flask.

Determination of acid-insoluble lignin content

The filtrated was washed with 1.5 L of distilled water and placed in a weighing crucible. Later, it was put in drying oven at 105 °C until constant weight. After cooling the material, the mass was recorded. It was placed in a muffle furnace, adjusted to the following conditions: (1) 200 °C for 1 h, (2) 400 °C for 1 h, and (3) 800 °C for 2 h. After cooling, the mass was recorded again. By difference of the masses, the acid-insoluble lignin content was determined.

Determination of acid-soluble lignin content

The filtered solution was diluted (1:10) and the pH was adjusted to 12-12.5. The absorbance was measured at 280 nm in the Evolution 300 UV-Vis Thermo Scientific™ spectrophotometer. The content of soluble lignin was estimated applied the **Equation (1)**.

$$C_{\text{lignin}} = (4.187 * 10^{-2} (A_T - A_{\text{pd}}) - 3.279 * 10^{-4}) \quad (1)$$

C_{lig} : Concentration of acid-soluble lignin (g/L);

A_T : Absorbance of the lignin and degradation products solution (280 nm);

A_{pd} : Absorbance at 280 nm of the decomposition products from sugars ($c_1 \varepsilon_1 + c_2 \varepsilon_2$) where the c_1 and c_2 concentrations were previously determined by High Performance Liquid Chromatography and ε_1 and ε_2 are the absorptivity values that correspond, respectively, 146.85 e 114.00 L g⁻¹ cm⁻¹.

Equation (2) (Ehrman, 1996) would be more adequate to estimate the amount of acid-soluble lignin in the LBL since the absorptivity of $110 \text{ L g}^{-1} \text{ cm}^{-1}$ is the usual value for wood. However, once the LBL has a relatively low content of acid-soluble lignin, it was preferred to use **Equation (1)** in order to better compare with the EHR.

$$C_{\text{lignin}} = \frac{A}{b \times a} \times \text{df} \quad (2)$$

C_{lig} : Concentration of acid-soluble lignin (g/L);

A: Absorbance of the wood lignin at 205 nm;

df: dilution factor;

b: cell path length (1 cm)

a: absorptivity.

The total lignin content was resulting of the sum of the acid-insoluble lignin and acid-soluble lignin.

Determination of carbohydrates contents

Sugars, organic acids, furfural and hydroxymethylfurfural (HMF) contents of the hydrolysed solution were quantified using High Performance Liquid Chromatography technique. Glucose, cellobiose, formic acid and HMF concentration values were inserted in **Equation (3)** to determine the cellulose content and xylose, arabinose, methyl glucuronic acid (MGA), acetic acid (AA) and furfural concentration values were inserted in **Equation (4)** to determine the hemicelluloses content.

$$\text{Cellulose} = \frac{0.90 \text{ Glucose} + 0.95 \text{ Cellobiose} + 1.29 \text{ HMF} + 3.5 \text{ Formic acid}}{\text{Dry lignocellulosic material (g)}} \times 100 \quad (3)$$

$$\text{Hemi} = \frac{0.88 \text{ Xylose} + 0.88 \text{ Arabinose} + 0.72 \text{ AA} + 1.0 \text{ MGA} + 1.37 \text{ Furfural}}{\text{Dry lignocellulosic material (g)}} \times 100 \quad (4)$$

Determination of ash content

Samples of 2.0 g were placed in a crucible (previously dried and weighed) and placed into a muffle furnace adjusted as the following conditions: 200 °C (1 h); 400 °C (1 h); 800 °C (2 h). After cooling, the crucible with ash was weighed. The total ash content is determined by discounting the weight of the dried crucible.

4.1.2 NMR Spectroscopy

The EHR and the LBL were submitted to acetylation reaction with anhydrous pyridine (10:1 V/w of sample) and acetic anhydride (10:1 v/w of sample) for 12 h with stirring at room temperature (Lu and Ralph, 1997). Acetylated and dried samples were submitted to analysis of solution $^1\text{H-NMR}$ and 2D HSQC NMR. Samples with concentration of 25 mg/mL of deuterated chloroform (Aldrich, 99.8 atom% D, containing 0.03% v/v TMS) were placed in a 5 mm NMR tube into the NMR equipment (AgilentTM DD2 500 MHz with inverse z-gradient triple resonance probe). NMR analyses were carried out in a facility from Brazilian Biosciences National Laboratory (LNBio - CNPEM).

$^1\text{H-NMR}$ spectroscopy

$^1\text{H-NMR}$ spectra of acetylated lignins were obtained with following conditions: acquisition time of 2.0 s, relaxation delay of 1.0 s, spectral width of 8000 Hz and 256 scans (Chen and Robert, 1988). The software Mnova NMR was used for visualization, processing and reporting of the 1D NMR spectra.

2D HSQC NMR spectroscopy

Pulse programme HSQC adiabatic (gHSQCad) was selected with spectral widths of 8000 Hz (0 - 16 ppm) and 25000 Hz (0 - 200 ppm) for ^1H - and ^{13}C - dimensions, respectively. The main acquisition parameters of HSQC contour maps are displayed in **Table 4.1**. The free NMRPipe software was used for processing, analysing and exploiting the 2D HSQC data. Prior to Fourier transformation, two-dimensional data were zero-filled to obtain a matrix size of 4K x 1K points. Additionally, a Gaussian and a shifted sine-bell window were applied in f_2 (^1H) and f_1 (^{13}C), respectively. Finally, a polynomial baseline correction was performed. HSQC cross-signals were assigned by comparison with literature data (Ralph et al., 2004; del Río et al., 2015).

Table 4.1 - Main acquisition parameters of 2D NMR spectra.

Parameters		
Pulse sequence	gHSQCad	
Number of Scans	32	
Recycle delay (s)	1.0	
Nucleus	¹ H	¹³ C
Spectrometer frequency (MHz)	500	125
Spectral Width (Hz)	8,000	25,000
Spectral Size	2,048	2,048

4.1.3 Pyrolysis-gas chromatography-mass spectrometry (Py-GC/MS)

Pyrolysis of the LBL, EHR, alkaline EHR and acidic-dioxane EHR (approximately 100 µg) was performed with an EGA/PY-3030S micro-furnace pyrolyzer (Frontier Laboratories Ltd.) connected to a Shimadzu CG2010Plus gas chromatograph using an Ultra alloy fused-silica capillary column (30 m x 0.25 mm i.d., 0.25 µm film thickness) and a Shimadzu QP-2010 Ultra mass selective detector. The pyrolysis was performed at 500 °C. The oven temperature was programmed from 45 °C (4 min) to 300 °C (20 min) at 2 °C min⁻¹. Helium was the carrier gas (1 mL min⁻¹). The compounds were identified by comparing their mass spectra with those of the Wiley and NIST libraries and those reported in the literature (Ralph and Hatfield, 1991; Tana et al., 2016). Peak molar areas were calculated for the lignin-degradation products, the summed areas were normalized, and expressed as percentages. Two analyses were performed for each sample.

4.1.4 Fourier Transform - InfraRed spectroscopy (FTIR)

Dried previously samples of the EHR and LBL were used in the preparation of KBr pellets (1 mg of sample to 100 mg of KBr at 10 - 12 kgf cm⁻²). FTIR spectra were obtained in the range of wavenumber from 4000 to 650 cm⁻¹ using a Perkin ElmerTM 400 spectrophotometer. The FTIR bands of lignocellulosic samples spectra were assigned by comparison with literature data assignment (Singh et al., 2005).

4.1.5 Elemental Analysis and C9-formulae

Carbon, hydrogen, nitrogen and sulfur contents from the EHR and LBL were determined by using in the PerkinElmer™ 2400 Series II CHNS/O Elemental Analyzer. The oxygen content was calculated by difference. The Double Bonds Equivalent (DBE) was calculated based on the elemental compositional ($C_aH_bO_cS_d$) (**Equation 5**) and the protein content was calculated according to **Equation (6)** (Hussein et al., 2011).

$$DBE = \frac{(2a + 2) - b}{2} \quad (5)$$

$$\text{Protein content (\%)} = 6.25 * N(\%) \quad (6)$$

The C9-formulae of the EHR and the LBL were estimated (Gonçalves et al., 2000). C9-formula is an empirical formula of the lignin macromolecule based on its phenylpropane unit. It is composed by six carbon atoms at the benzene ring plus three carbon atoms of the propane side-chain (Gonçalves et al., 2000). The C9-formula of LBL was based on the data from the elemental analysis and 1H -NMR. The C9-formula of the EHR was also estimated. However, it is known that the high cellulose content in the EHR contributes to its C9-formula.

4.1.6 Molar mass determination by viscosimetry

The EHR and the LBL were sent to Universidad Simón Bolívar (Venezuela) in order to determine their molar mass by viscosimetry technique performed by group of the Professor Dr. Marcos A. Sabino.

The solubility of the samples is a predominant factor in order to perform the measurement of the molar mass by viscosimetric methods. Thence, a previous test of solubility was carried out. Methanol, ethanol, tetrahydrofuran and a 0.5 M NaOH solution were used as solvent for this solubility study.

100 mg of each sample was dissolved in 10 mL of the solvent. It was left during overnight at room temperature. Subsequently, it was filtered under vacuum, using a porosity paper. After filtration, it was dried in the oven at 60 °C. This procedure was repeated for each solvent. Through this solubilization study, it was found that the highest solubility reported for

the LBL was in a NaOH solution (0.5 M). The EHR was discarded from the viscosimetry analysis because it presented many problems to achieve its solubility. The gel formed was very difficult to handle, and it was not possible to dissolve or under conditions of temperature, ultrasound, etc.

The molar mass determination of the LBL was performed as described in the following. A stock solution of approximately 1% w/v in 0.5 M NaOH was prepared and placed in the ultrasound for two hours to obtain the highest possible solubility. After 24 h, it was filtered. Five diluted solutions (0.8, 0.6, 0.5, 0.4, 0.2% w/v) were prepared from the stock solution at 1% w/v. The decay time through the capillary tube (Ubbelohde viscometer) of the pure solvent and of the each solution were annotated at 30 °C. Ten measures were taken for each solution, and the average value was determined. Then, the viscosities were calculated according to the Mark-Houwink-Sakarada theory.

Capillary viscometry is an easy-to-run experimental method that provides information on the size and conformation of macromolecules in infinitely dilute solutions (Delpech et al., 2007; Mello et al., 2006). This information is provided by the interactions between the polymer and the solvent (Costa et al., 2015). A parameter obtained by this method is the intrinsic viscosity $[\eta]$ (Mello et al., 2006), which is considered a measure of the volume of a single molecule of polymer in ideal condition (Costa et al., 2015). The way to obtain this parameter is by the graphic extrapolation and the application of mathematical equations, such as those proposed by Huggins (H) Kraemer (k) and Schulz-Blaschke (SB) (Costa et al., 2015; Huggins, 1942; Kraemer, 1938). The relationship between the intrinsic viscosity (η) and the average viscometric molar mass (M_v) is that described by the Mark-Houwink-Sakurada (MHS) **Equation (7)**.

$$[\eta] = k(M_v)^a \quad (7)$$

In this equation, k and a are viscosimetric constants that vary according to the type of solvent, temperature and chemical structure of the polymer (Costa et al., 2015; Kasaai, 2007; Shen et al., 2004). In the determination of the molar mass using the capillary viscometry method, it is required to know the two constants of **Equation (7)**. These values are reported in the literature for a temperature of 30 °C in a 0.5 M NaOH solution. The values of the constants are $k = 0.4165$ and $a = 0.23$ (Dong and Fricke, 1995).

4.1.7 Determination of Higher Heating Value

Experimental HHVs of the EHR and LBL were measured using a calorimeter system (IKATM C-200). In addition, theoretical HHVs were estimated as a function of the contents of C, H, O, and N according to **Equation (8)** proposed by Demirbas et al. (1997) for lignocellulosic materials (on dry and ash-free basis). Rocha et al. (2015) estimated the HHVs from elemental composition of 60 sugarcane bagasse samples also using the **Equation (8)**. Theoretical HHV to the EHR and LBL were obtained using **Equation (8)**:

$$\text{HHV} = (33.5 [\%C] + 142.3 [\%H] - 15.4 [\%O] - 14.5 [\%N]) \quad (8)$$

4.1.8 Thermogravimetry analyses

The TG analyses were performed to study the thermal degradation behavior of the EHR and LBL. The equipment was a simultaneous TG/DSC analyzer (TATM Instruments SDT-Q600) with burning method. The samples (6.0 - 6.5 mg) were put in platinum pans and heated from 25 to 700 °C at 10 °C min⁻¹ under nitrogen atmosphere (100 mL min⁻¹).

4.1.9 Physical characterization

The particle size distribution of the EHR was determined by sieving and by Laser Scattering. The particle size distribution of the LBL was only determined by Laser Scattering due to its small particle size. The particle size distribution of the EHR by sieving was performed as following. Initially the EHR were well mixed and the agglomerates contained in it were manually undone. Sampling was performed by quartering to obtain samples with better representativeness. Four EHR samples (\approx 60 g) were forwarded to particle size distribution analysis. A vibratory sieve shaker (Analysette 3, FritschTM) with a sieve stack (sieve opening sizes from 4.75 mm to 0.15 mm) was used in this analysis. The sieving time was set to 15 min and the selected amplitude of the sieve stack vibration was 3.0 mm.

Particle size distributions were evaluated by Laser Scattering to: the LBL, the EHR from bottom of sieve set (< 0.15 mm), and the milled EHR. The milling process of EHR was done in a variable-speed-rotor-mill at 11000 rpm using a 0.08 mm sieve (Pulverisette 14, FritschTM). In the Laser Scattering analysis, the samples were previously suspended in water.

Then, the laser diffraction particle size analyser used was the Beckman Coulter LS 13 320 instrument with the Liquid Universal module. The instrument was operated with 780 nm light source, 8% obscuration, and a Fraunhofer light-scattering model. The applied mathematical treatment considers that the particles are spherical (Driemeier et al., 2011).

4.1.10 Scanning Electron Microscope (SEM) analysis

SEM images of the EHR from bottom of sieve set (< 0.15 mm) and the milled EHR were taken. SEM images were acquired with a Scanning Electron Microscope (FEI™ Quanta 650 FEG) with secondary electron detector - Everhart Thornley Detector (high vacuum). The beam conditions were 5.0 - 15.0 kV with a spot size of 3.0 and a working distance of 8.0-10.0 mm. The samples were mounted on stubs and sputter coated with gold using a BAL-TEC SCD 050 sputter coater (40 μ A, 60 s). SEM analyses were carried out at Brazilian Nanotechnology Laboratory (LNNano - CNPEM).

4.2 Synthesis of phenolic resins with the EHR and LBL

The milling process of EHR was done before the synthesis reactions using a Pulverisette at 11000 rpm with a 0.08 mm. Solubility tests of the EHR and LBL samples were performed prior to start the synthesis of lignin-phenol-formaldehyde resins in order to define which initial conditions provide a more homogeneous reaction medium. The amounts of solubilized EHR and LBL (%) were determined by gravimetric analyses as described in the following. 1 g (dry basis) of lignin from the EHR or the LBL samples was added in a 100 mL flask containing KOH solution (pH 12, solid:liquid 1:10). In a glycerine bath, the system under stirring was warmed until experimental temperature for 1 h. In assays with catalyst addition, about 1 g of 85% KOH pellets (PA ACS. 85% - Dinâmica) was added at the beginning. The material was then filtered through a porous crucible by vacuum filtration. By mass difference, the solubilized lignocellulosic material was quantified. For the tests using EHR, it was considered that there was no loss of cellulose and hemicelluloses under these conditions. A factorial design 2^2 was performed (**Table 4.2**) in order to evaluate the effect of temperature and catalyst (KOH) on lignin solubilization.

Table 4.2 - Factorial design 2² of solubility tests and their response (solubilized lignin).

Samples	T (°C)	Catalyst	Solubilized lignin (%)
LBL	70	Without	9.0 (0.06)
	90		9.3 (0.87)
	70	With	98.6 (0.54)
	90		99.5 (0.06)
EHR	70	Without	12.5 (0.95)
	90		15.0 (1.10)
	70	With	59.5 (0.74)
	90		65.9 (1.52)

In parentheses, standard deviation values are shown.

Using the Statistic software, the principal effects and interaction effect, the *p* values and the confidence interval were obtained (**Table 4.3**).

Table 4.3 - Factorial design 2² of solubility tests.

	Factor	Effects	<i>p</i> -value	95% confidence interval
LBL	Temperature	0.7	0.28	-0.4 - 1.0
	Catalyst	89.9	0.00	44.2 - 45.6
	Temp. x Catalyst	0.3	0.55	-0.5 - 0.8
EHR	Temperature	4.7	0.01	1.8 - 7.7
	Catalyst	49.2	0.00	46.3 - 52.2
	Temp. x Catalyst	1.6	0.20	-1.3 - 4.6

The effects values that are underlined were significant at the 95% confidence level. The others were neglected because include the zero value in the confidence intervals. Another way to evaluate the effect significance is by the *p* value test. If *p*-value > 0.05 (95% confidence level), the effect is not significant. It is noted in **Table 4.3** that only the principal effect of catalyst has a positive and significant influence on the lignin solubility from the LBL. With respect to the EHR, both the temperature and the catalyst presence have positive and significant influence on its lignin solubility, but the catalyst factor shows a higher positive influence. From this solubility study, it was chosen to add the catalyst in the first reaction step and to carry out the synthesis reaction of resole-type lignin-phenol resins at 70 °C.

The following phenolic resins with LBL and EHR were assessed in this research: LBL 5%, LBL 15%, LBL 30%, LBL 45%, LBL 60%, EHR 5%, EHR 15%, EHR 30% and EHR 45%. If not specified, all the percentages are expressed by weight. In order to compare, a standard resin (phenol-formaldehyde resin without lignin) also was produced.

This research aimed also to insert the EHR in resins synthesis without any previous purification and to assess how these fibers influence the properties of their resins. The synthesis reactions were based on Paiva and Frollini (2001). The mass ratio of formaldehyde, phenol and KOH was 1.41:1.00:0.06. This corresponds to a molar ratio of phenol:formaldehyde of 1.0:1.5. The reactions occurred in alkaline medium with excess formaldehyde in order to favour resole-type phenolic resins. The reaction system is shown in **Figure 4.4**.

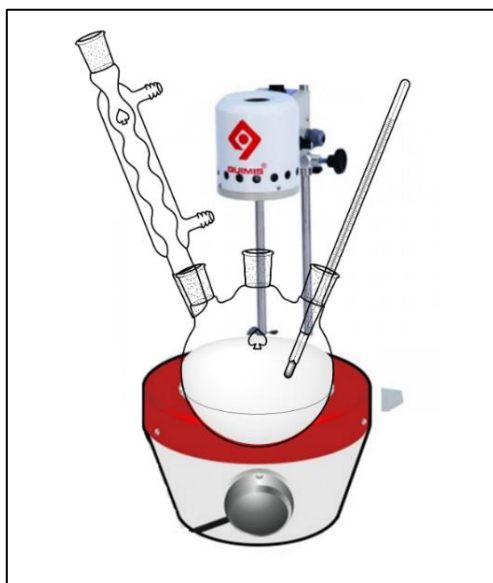
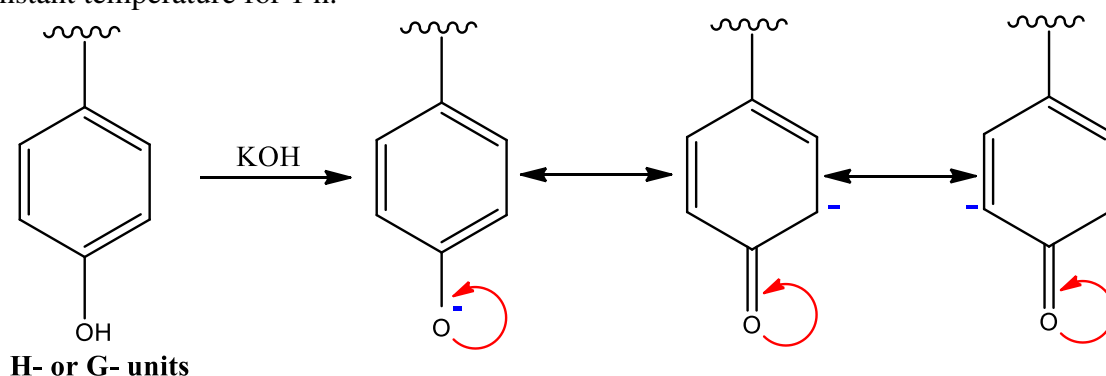


Figure 4.4 - Synthesis system of resole-type phenolic resins.

The reactions were performed in the following steps (method adapted from Paiva and Frollini, 2001):

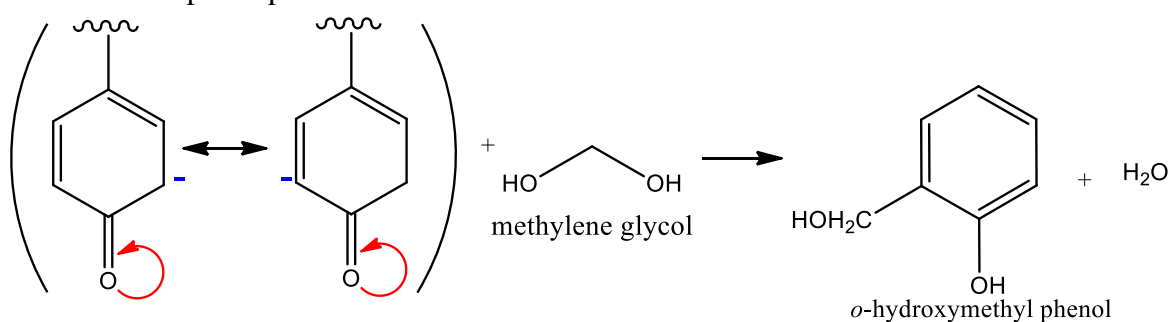
- Lignin Solubilization/Formation of the phenolate anion and stabilization of the formed negative charge.

In a 3-necked flask (500 mL), KOH solution pH 12 (1:10 w/v lignin:alkaline solution) and 50% from total mass of 85% KOH tablets (PA ACS. 85% - Dinâmica) were added. Under mechanical stirring at 200 rpm and heating until 70 °C. Upon reaching this temperature, the LBL or EHR was added to system in order to solubilise it. This solubilization process was at constant temperature for 1 h.

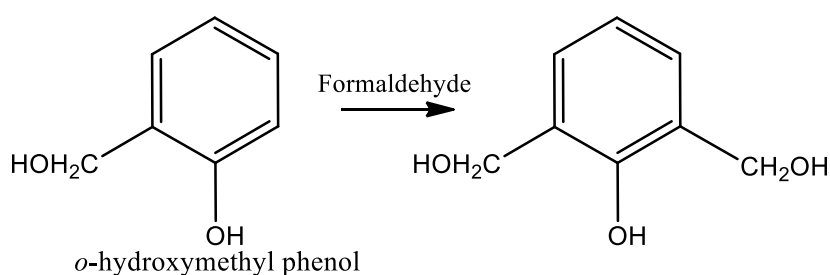


- Hydroxymethylation reaction of the lignin (formaldehyde addition)

After the solubilization of the EHR or the LBL in alkaline solution, formaldehyde solution (Synth, 37 wt.% in H₂O) was added to the system in order to the lignin was hydroxymethylated, since the hydroxymethylated lignin is more reactive than the phenol reactant. This step was performed in 30 min.

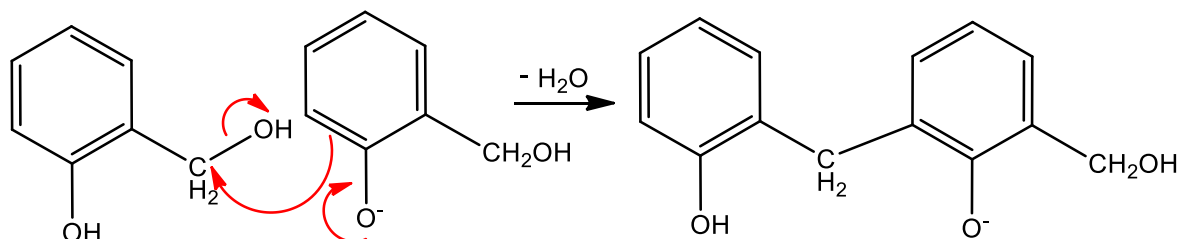


Dihydroxymethylation for H-unit

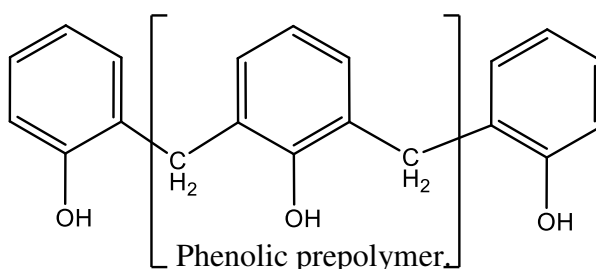


- Self-condensation reaction (remaining phenol and KOH (+3%) addition)

After the hydroxymethylation reaction of lignin, crystal phenol reactant (P.A ACS Dinâmica) and the remaining 50% from total mass of KOH tablets were added to the system. This reaction occurred for 2 h at 70 °C. However, there were variations in temperature because it is an exothermic reaction. At the end of the reaction, the flask was ice-cooled and the reaction medium was neutralized with HCl solution to pH 7.0-7.7.

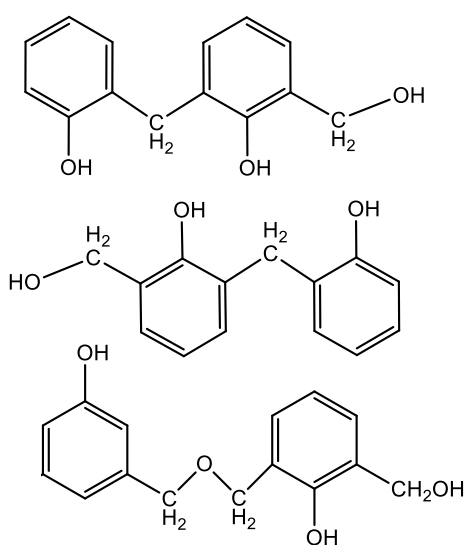


Self-condensation reaction between (hydroxymethyl).



- Solvent removal

The solvent was removed using a rotoevaporator under reduced pressure (30 to 150 mbar), 60 rpm, 55 - 60 °C for about 2 h, resulting in a viscous and brown resin. Aliquots were removed at the end of the reaction for FTIR analysis.



Phenolic resin

The obtained resole-type phenolic resins were removed from the rotary flask still heated so that the resin did not harden within the flask. The well-sealed jars with the resins were put into the freezer at 10 °C for further analysis.

During the synthesis reactions, pH values were measured (**Table 4.4**), since having basic pH is a determinant factor so that the product generated is resole-type phenolic resin.

Table 4.4 - pH of the synthesis reactions of the resole-type phenolic resins.

Phenolic resins	pH_i	pH_f
Standard	7.6	7.6
LBL 5%	8.7	8.6
LBL 15%	9.2	8.9
LBL 30%	9.3	8.9
LBL 45%	9.2	8.8
LBL 60%	8.9	8.4
EHR 5%	9.3	9.1
EHR 15%	9.1	8.8
EHR 30%	9.2	8.8
EHR 45%	9.1	8.5

The curing process of resole-type phenolic resins to obtain thermosetting resins (**Figure 4.5**) was performed in a hydraulic press (Labtech). The curing parameters (temperature and time) were based on the rheological study. The curing cycle used had the following conditions: (i) 70 °C, 30 min; (ii) 90 °C, 30 min and, (iii) 105 °C, 2 h. The pressure applied in entire cycle curing was of 50 Bar. After the curing cycle was completed, thermosetting resins obtained were demoulded from the moulds. The thermosetting phenolic resins for the mechanical tests were prepared in this hydraulic press machine.

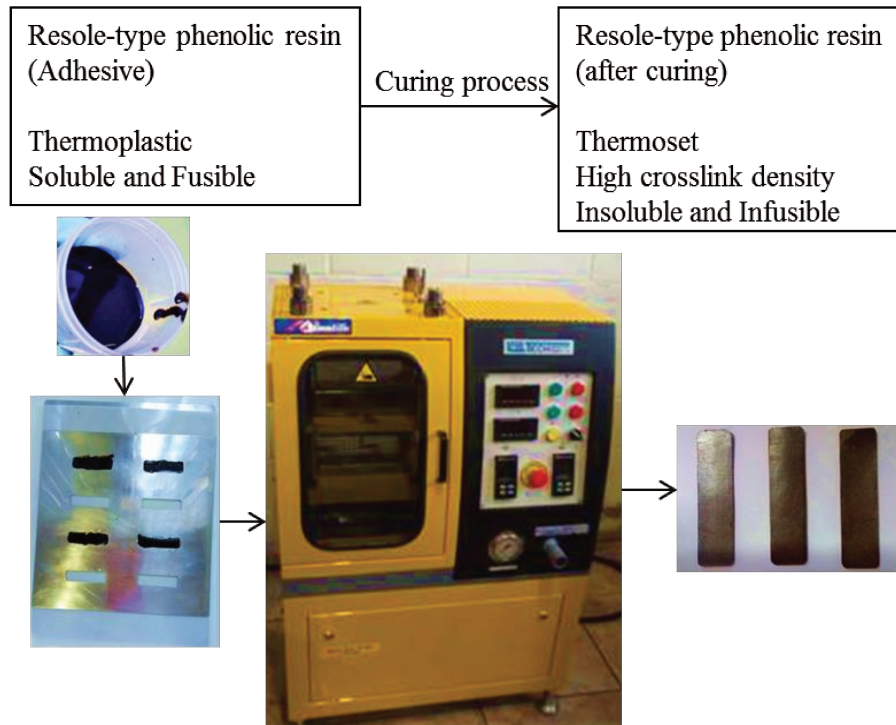


Figure 4.5 - Curing process to obtain the thermosetting phenolic resins.

4.3 Determination of curing kinetics of phenolic resins with the EHR and LBL

Curing kinetic study of the resins was performed from rheological study and from TG analysis.

4.3.1 Rheological study

The rheology technique applied in this study aimed to analyze the curing process of the resole-type phenolic resins under different isothermal conditions (TA Instruments, 2004; Laza et al., 2002). Resins with LBL and EHR were submitted to rheologic analysis at five different temperatures (90, 97.5, 105, 112.5 and 120 °C) at 2.0 Hz (f) and 5.0 Pa (τ).

Rheological tests were performed in a plate–plate PP35 with air bearing support sensor system (HAAKE RheoStress 6000-UTC rheometer). All the measuring sequences were defined and controlled using RheoWin 3 Job Manager software. The sensor is composed of a movable and a stationary plate with a gap of 1 mm from each other. More technical details can be found in Zuniga Linan et al. (2015). The following viscoelastic properties were measured as a function of time by using this technique: storage modulus - G' (elastic

component) and loss modulus – G'' (viscous component) (Bröckel et al., 2013). Gel time (t_{gel}) values for each resin were estimated by the crossover point ($G' = G''$) criteria (Laza et al., 2002). These analyses were performed in the "Laboratório de Desenvolvimento de Processos de Separação (LDPS)" - FEQ - UNICAMP.

4.3.2 TG Kinetics Analysis

The curing parameters of the LBL 5% and EHR 5% resins were also assessed by TG kinetics analysis. The TA Instruments TG Kinetics Analysis program was used to analyze data from the Thermogravimetric Analyzer instrument. This program utilizes data gathered by running a sample at various heating rates (at least three TG data files). This software operates in accordance with the ASTM Standard E1641 "Decomposition Kinetics by TG" (TA Instruments, 2003). TG curves were obtained from 30 to 700 °C at different heating rates (5, 10 and 20 °C min⁻¹) under a N₂ flow of 100 mL min⁻¹ in a SDT Q600 thermogravimetric analyzer (TA instruments).

4.4 Characterization of the phenolic resins with the EHR and LBL

The obtained phenolic resins with LBL and with EHR were submitted to physicochemical and thermomechanical characterization. The following techniques were applied to perform this characterization:

- Solid content determination;
- Zero shear-rate viscosity (η_0) determination;
- Thermogravimetric analyses (TG);
- FTIR spectroscopy;
- 2D HSQC NMR spectroscopy;
- Differential Scanning Calorimetry (DSC);
- Dynamic Mechanical Thermal Analysis (DMTA).

4.4.1 Solid content and viscosity determination

The solid content of the obtained phenolic resins was determined by gravimetric analysis (Dias, 2014). Samples of 1.0 g were placed in a crucible (previously dried and

weighed) and placed in a heating oven (Thermo Scientific™ Vacutherm) at 105 °C (3 h). Then, the crucibles systems were placed in a desiccator for 15 min. After cooling, the crucible systems were weighed. The solid content was determined by discounting the crucible weight (Dias, 2014).

The viscosity profiles of the resole-type resins were determined in the same rheometer used to perform the curing kinetic study. The zero-shear rate viscosity (η_0) of the resole-type resins at 25 °C were determined from the viscosity profiles as a function of shear rate. The shear rate ranged of 0 - 2 s⁻¹ in 50 steps. The η_0 values were determined by linear regression through the Carreau-Yasuda model (Zuniga Linan et al., 2015).

4.4.2 TG Analyses

TG analyses of the obtained phenolic resins were performed in order to evaluate their curing step and thermal resistance. The equipment used was a Shimadzu (50 M) thermogravimetric analyzer. About 10 mg of each resin was put in a pan and heated from 25 °C to 500 °C at 10 °C min⁻¹ under nitrogen atmosphere (100 mL min⁻¹). These analyses were performed on the “Laboratório de Caracterização de Biomassa - LRAC”, FEQ/UNICAMP.

4.4.3 FTIR spectroscopy

Samples of the obtained resins before (adhesives) and after (thermosetting) the curing process performed on the hydraulic press were submitted to FTIR technique. These analyses were performed in order to confirm if reaction product was really phenolic resins (Poljanšek and Krajnc, 2005). FTIR spectra were obtained in the range of wavenumber from 1,750 to 750 cm⁻¹ with spectral resolution of 4 cm⁻¹, 32 scans using a Perkin Elmer™ 400 spectrophotometer. These analyses were performed in a facility from CTBE - CNPEM.

4.4.4 HSQC Spectroscopy

These analyses were performed using a similar method described in **4.1.2 section**, with some differences. Samples of the Standard and LBL 30% resins were previously dried in a high vacuum system for three days at room temperature. The resins were solubilized in a

deuterated dimethyl sulfoxide (DMSO-d6) (Aldrich containing 0.03% v/v TMS) with concentration of 50 mg mL⁻¹. Lignin structure leads much more time to define its signals in the HSQC spectrum than the standard phenolic resin. For this reason, the chosen analysis time was of 3 h for the standard phenolic resin, whereas it was 6 h for the LBL 30% resin. These analyses were carried out in a facility from Brazilian Biosciences National Laboratory (LNBio) - CNPEM. The phenolic resin with EHR was not submitted to this technique, because it was not possible solubilize this sample on DMSO-d6.

4.4.5 DSC

The samples (± 5 mg) were put in a standard Aluminum crucible (Mettler Toledo, 40 μ L, with pin and lid) and heated from 0 to 500 °C at 20 °C min⁻¹ under nitrogen atmosphere (20 mL min⁻¹). These analyses were carried out in Differential Scanning Calorimeter (Mettler Toledo) located on the "Laboratório de Desenvolvimento de Processos de Separação (LDPS)" – FEQ - UNICAMP.

4.4.6 DMTA technique

Samples of the thermosetting phenolic resins of 24x12x1 mm were obtained to DMTA from the curing process in hydraulic press with the following conditions: (i) 70 °C, 30 min; (ii) 90 °C, 30 min and, and (iii) 105 °C, 2 h. The pressure applied in entire cycle curing was of 50 Bar.

DMTA was performed in a dynamic mechanical analyzer (model 2980, TA Instruments) operating in the single cantilever mode. The experimental conditions were frequency of 1 Hz, amplitude of 17.5 μ m, torque of 15 cN, temperature range of 35 - 300 °C, and heating rate of 5 °C min⁻¹. In the beginning of each analysis, an isotherm at 35 °C for 5 min was applied.

The measurement properties in DMTA were G' , G'' and $\tan \delta$ (G''/G'). The same properties that were assessed in rheological study, but in DMTA, the samples analyzed were the thermosetting phenolic resins, *i.e.*, the resins obtained after the curing process in the hydraulic press. For each type-resin, at least two analyses were performed. These analyses were carried out in "Laboratório de Caracterização de Materiais (LACAM)" – FEQ – UNICAMP.

Chapter 5 RESULTS AND DISCUSSION

5.1 Characterization of the EHR and the LBL

5.1.1 Chemical composition and mass balance

Table 5.1 shows the results of moisture, total lignin, cellulose, hemicelluloses, and ash content in the EHR and LBL.

Table 5.1 - Determination of components (% w/w on dry matter) of the EHR and the LBL (Menezes et al., 2016b).

	EHR	LBL
COMPONENTS		
Moisture	6.8	5.9
Acid Soluble Lignin	10.4 (0.15)	11.8 (0.13)
Acid Insoluble Lignin	36.9 (0.07)	87.2 (0.53)
Total Lignin	47.3 (0.08)	99.0 (0.39)
Cellulose	39.8 (1.34)	^a --
Hemicelluloses	4.5 (0.13)	^a --
Total Ash	8.4 (0.06)	0.7 (0.04)

In parentheses, the standard deviation of the samples is shown.

^aThe small amounts of glucose and xylose are probably in lignin-carbohydrate complex, thus, the cellulose and hemicelluloses equivalent values are not shown in this table.

The EHR still remains with about 40% of cellulose content and the LBL has a total lignin content (99%) much higher than in the EHR (47%). This is expected, since the LignoBoost process aims to obtain a high-purity lignin. The EHR also has hemicelluloses (4.5%), but it is still a low amount compared to the cellulose content therein. Its total ash content (8.4%) is even greater than its hemicelluloses content. Further studies should be conducted to evaluate the effect of the ashes contained in the EHR on the mechanical properties of the resins. It must be emphasized that the EHR process provides potentially a high amount of cellulose fibers that could be applied as reinforcement in phenolic resins.

In order to perform the mass balance of the EHR, chemical compositions of the raw sugarcane bagasse and the pretreated sugarcane were also determined. The mass yields of the

hydrothermal pretreatment and enzymatic hydrolysis steps were 63.5% and 53.5%, respectively.

Figure 5.1 represents the mass balance to hydrothermal pretreatment and the hydrolysis enzymatic process. About 92% of the hemicelluloses content from raw sugarcane bagasse was solubilized after the hydrothermal pretreatment step. The cellulose conversion by enzymatic hydrolysis was about 65% using a commercial enzyme cocktails from Novozyme: Celluclast 1.5 L (15 FPU/g) and Novozyme 188 (β -glucosidase -10 IU/g). From 20 kg of the raw sugarcane bagasse was produced 6.8 kg of the EHR. It represents about 34 wt% of the raw sugarcane bagasse. About 70% of the lignin content and 30% of the cellulose content from the raw sugarcane bagasse remained in the EHR after the enzymatic hydrolysis steps.

In order to know better the lignin present in the EHR, two different processes of lignin extraction were performed: the alkaline and the acidic-dioxane lignin, as described in the **4.1 section**. **Figure 5.2** represents the mass balance to the alkaline **(a)** and the acid-dioxane processes **(b)**. Chemical composition values of these lignin-rich streams are reported on the **Figure 5.3**.

Total lignin amount was higher in the acid-dioxane EHR than in the alkaline EHR. Carbohydrates were more preserved in lignin-rich stream produced by alkaline process (8.3%) than in that generated by acidic-dioxane process (6.0%). According to Fukushima and Hatfield (2001), acidic-dioxane extraction process obtains lignin with low carbohydrates contents.

Both lignin-rich streams (alkaline EHR and acidic-dioxane EHR) were obtained in order to better characterize the lignin contained in the EHR. The alkaline EHR and acidic-dioxane EHR were submitted to Py-GC/MS analyses in order to assess their amounts of H-, G-, and S-units (**5.1.4 section**).

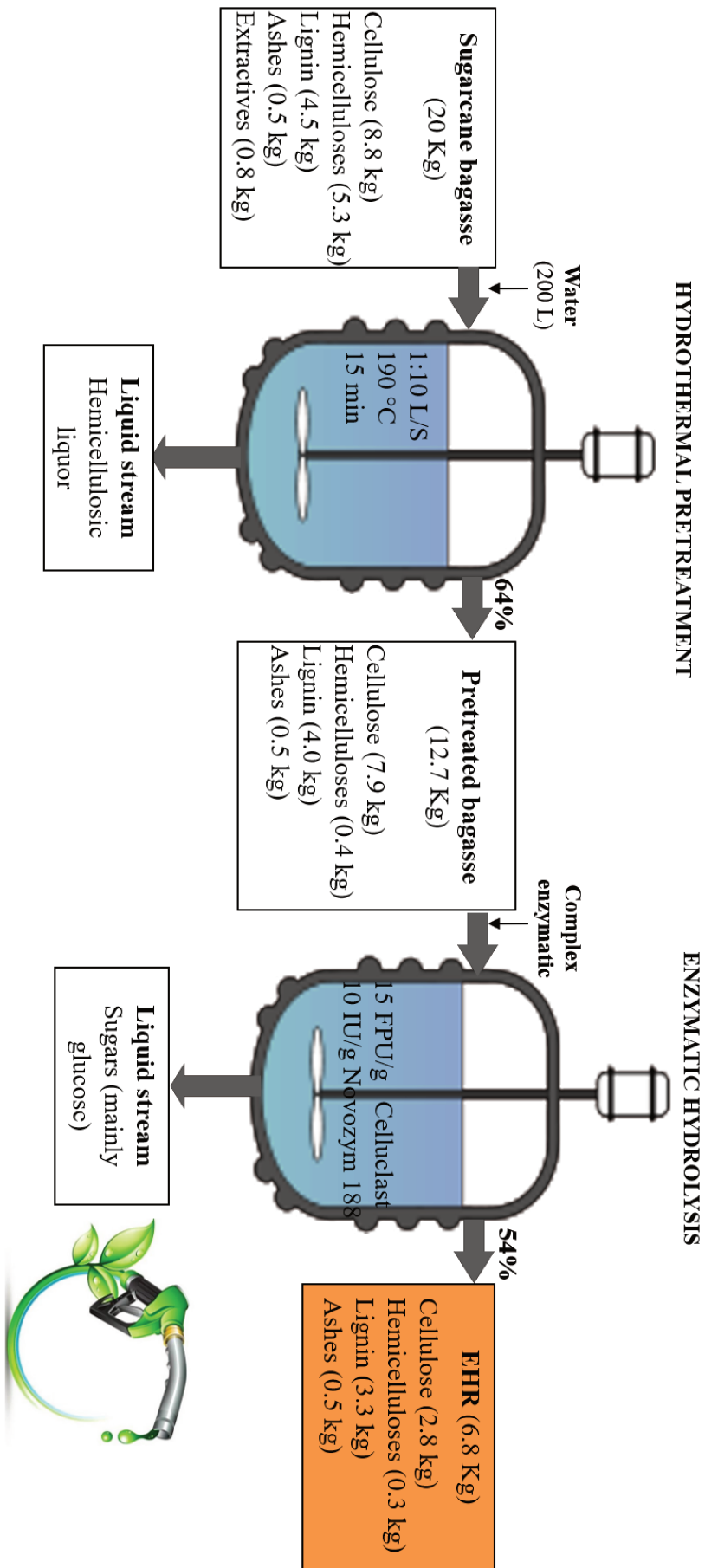


Figure 5.1 - Mass balance of the EHR obtainment.

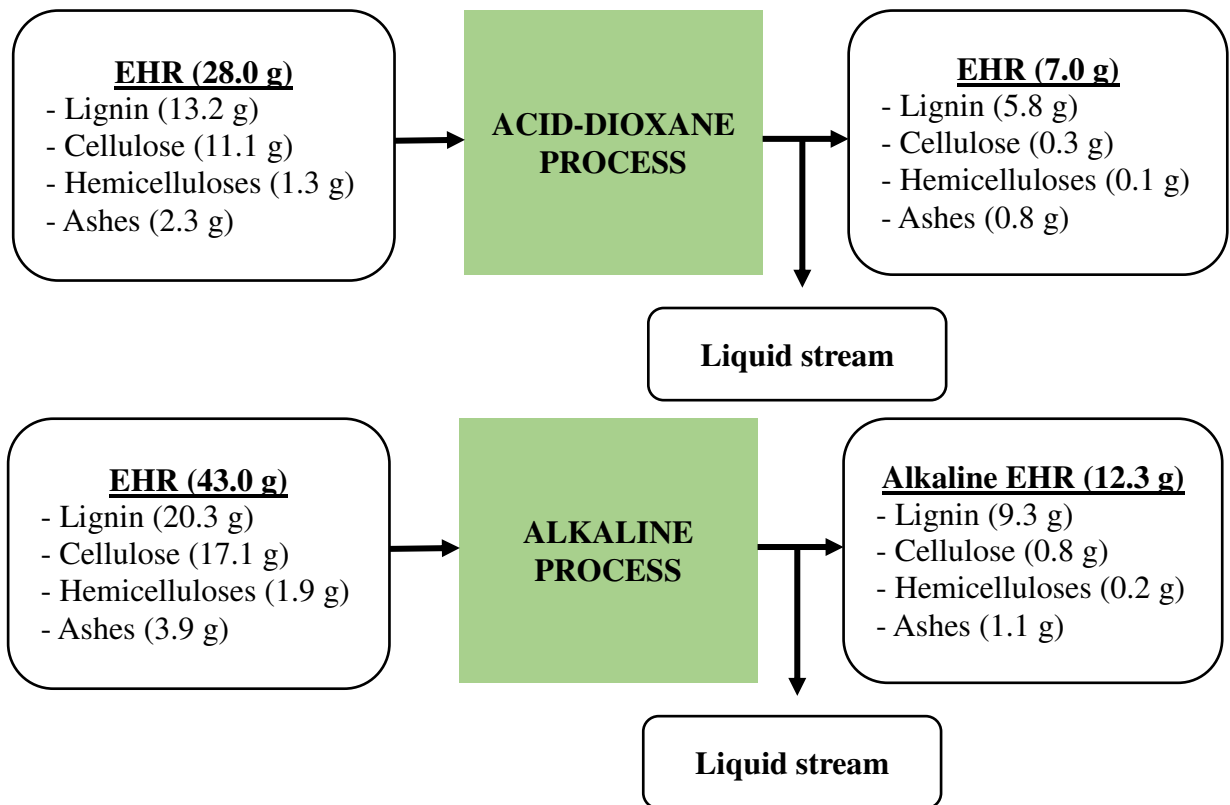


Figure 5.2 – Mass balance (on dry weight) to the acid-dioxane (a) and the alkaline processes (b).

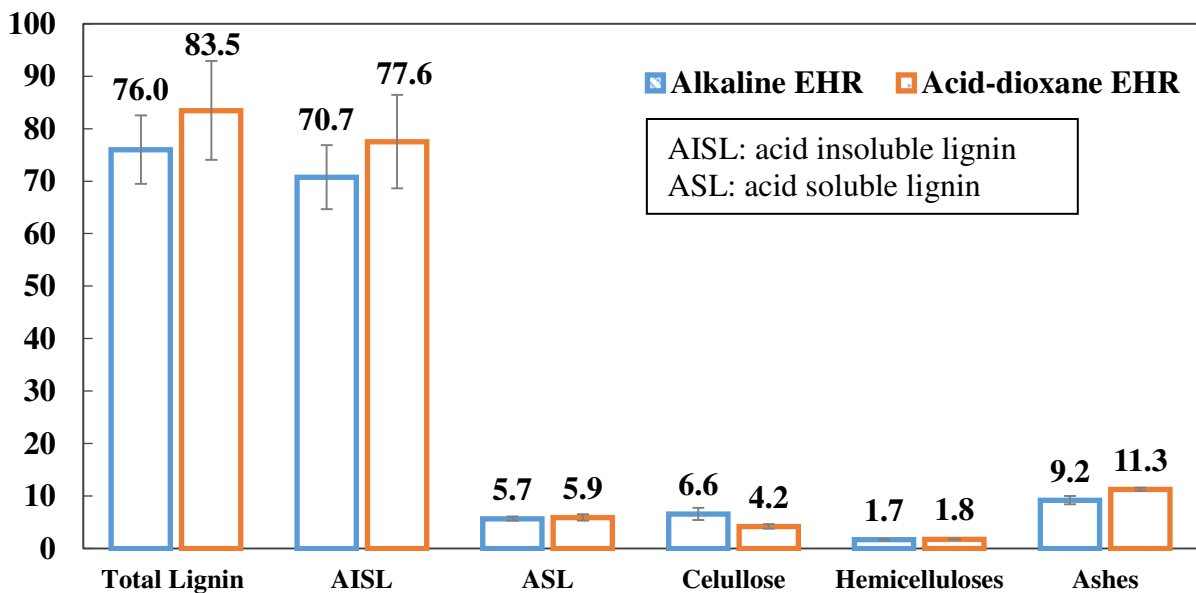


Figure 5.3 - Chemical composition (on dry weight) of EHR from alkaline and acidic-dioxane processes.

5.1.2 FTIR spectroscopy

Figure 5.4 shows FTIR spectra of the EHR and LBL. The Savitzky-Golay method (second-order polynomial with fifteen points of window) was applied in the FTIR spectra in order to enhance the apparent resolution and amplify small differences. **Table 5.2** depicts the main FTIR bands assignment observed in the LBL and EHR spectra.

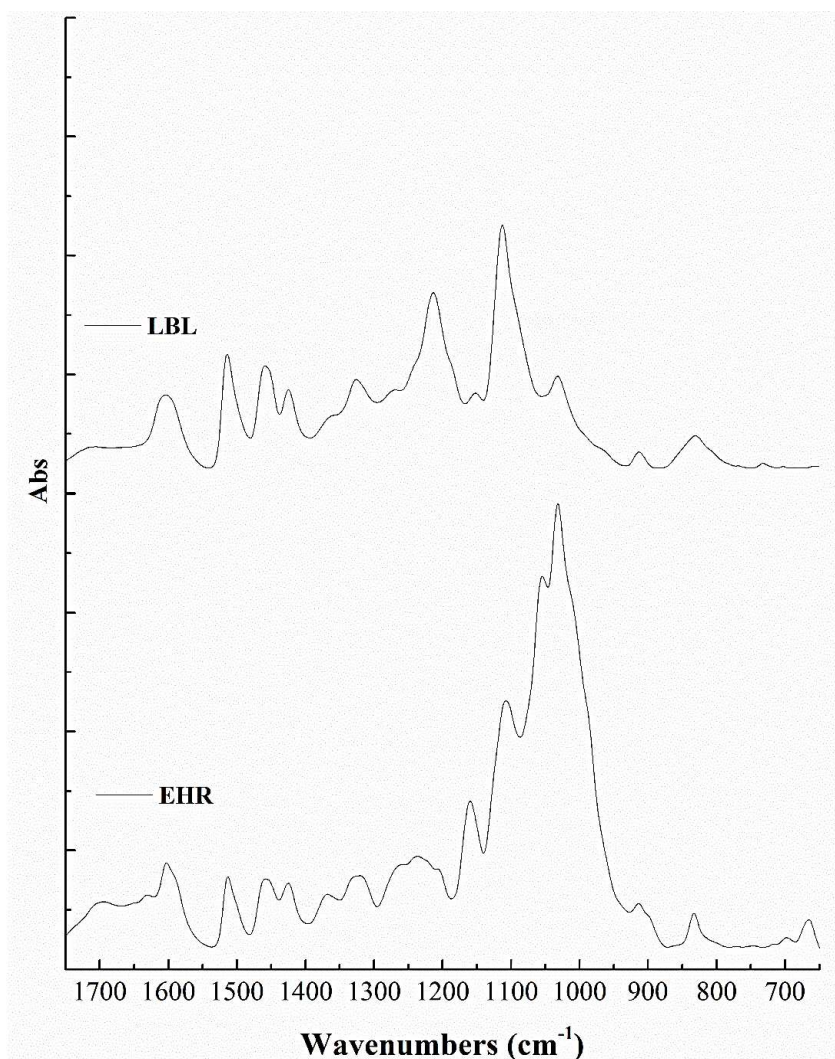


Figure 5.4 - FTIR spectra of the EHR and LBL.

By comparing the spectra of the EHR, strong signal can be observed in the bands 1030 cm^{-1} (C-O stretching in cellulose) and 1160 cm^{-1} (C-O-C asymmetric stretching in cellulose). In the LBL spectra the highest band is observed in 1110 cm^{-1} that refers to aromatic C-H in plane deformation (typical for S-unit), confirming the prevalence of S-unit in it (Popescu et al., 2007).

Table 5.2 - The main FTIR bands assignment (based on Singh et al., 2005).

Band (cm⁻¹)	Vibration	Assignment
1710-1690	C=O stretching	Unconjugated C=O
1600	C=C stretching (S)	Aromatic skeleton
1520	C=C stretching (G)	Aromatic skeleton
1460	C-H asymmetric deformation	CH ₃ + CH ₂
1420	C-H asymmetric deformation	Methoxyl group
1370 (EHR)	CH bending	Cellulose
1320	C-O stretching	S-unit
1270	C-O stretching	G-unit
1210 (LBL)	st C-O(H) + C-O(Ar)	Phenolic OH + ether
1205 (EHR)	OH in-plane bending	Cellulose
1160	C-O-C asymmetric stretching	Cellulose
1110	C-H in-plane deformation and C=O stretch	S-unit
1030	st C-O(H) + C-O(C)	Aliphatic OH and ether
830	Out-plane deformation vibration Ar C-H	S-unit

5.1.3 Py-GC/MS technique

For LBL and EHR

Py-GC/MS gave information about the composition of the LBL (**Figure 5.5**) and EHR (**Figure 5.6**). Pyrolysis released compounds derived from the H-, G- and S-lignin units. In the LBL pyrogram (**Figure 5.5**), the main compounds from H-lignin units: phenol (1), *o*-cresol (2), *p*-cresol (3), 2,4-dimethylphenol (5), 4-vinylphenol (7) and isopropyl-phenol (8). From G-lignin units: guaiacyl (4), 4-methylguaiacol (6), 4-ethyl-guaiacol (11), 4-vinylguaiacol (12), 4-propyl-guaiacol (15 and 21), vanillin (17), *cis*-isoeugenol (18), *trans*-isoeugenol (19), guaiacylacetone (22), *trans*-methyl isoeugenol (23) and acetovanillone (25). From S-lignin units: syringyl (13 and 14), 4-methylsyringol (20), 2,6-dimethoxy-4-(2-propenyl)-phenol (26 and 27), syringaldehyde (28), 4-allylsyringol (29) and acetosyringone (30). The peaks 9, 10, 16 and 24 are polyphenolic structure (non-specific lignin).

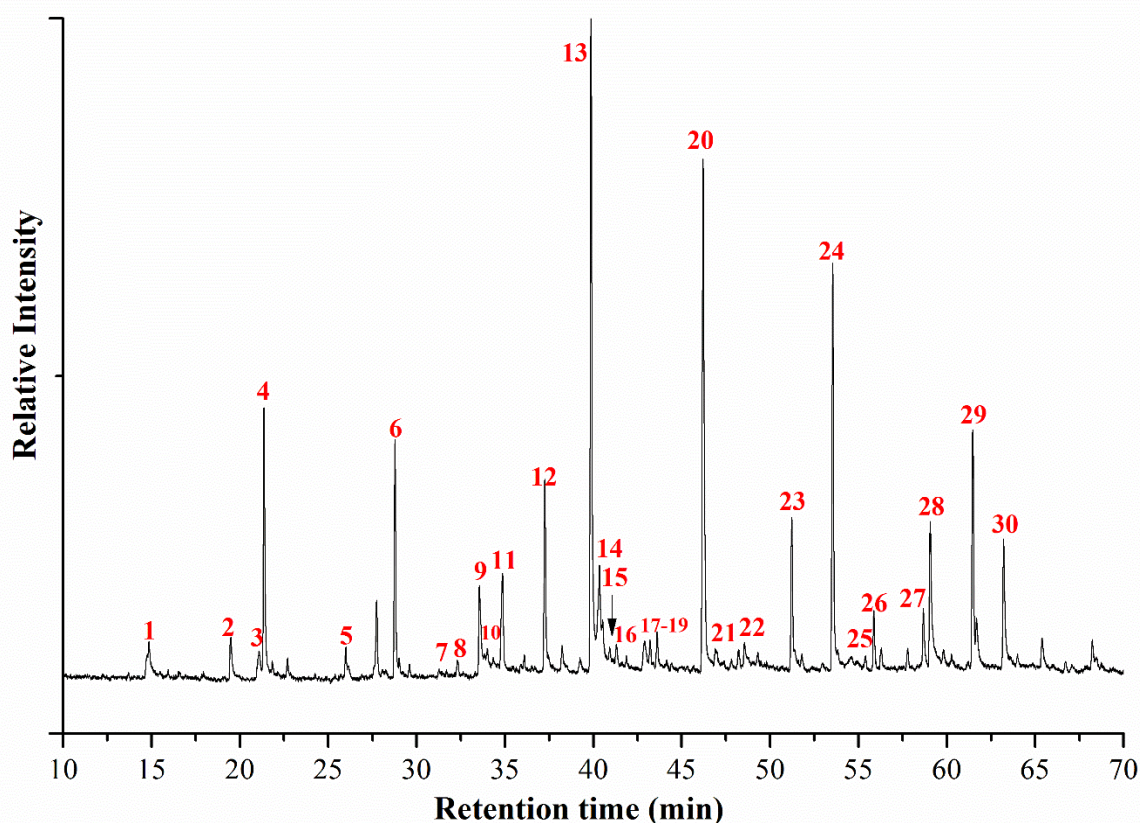


Figure 5.5 - LBL pyrogram.

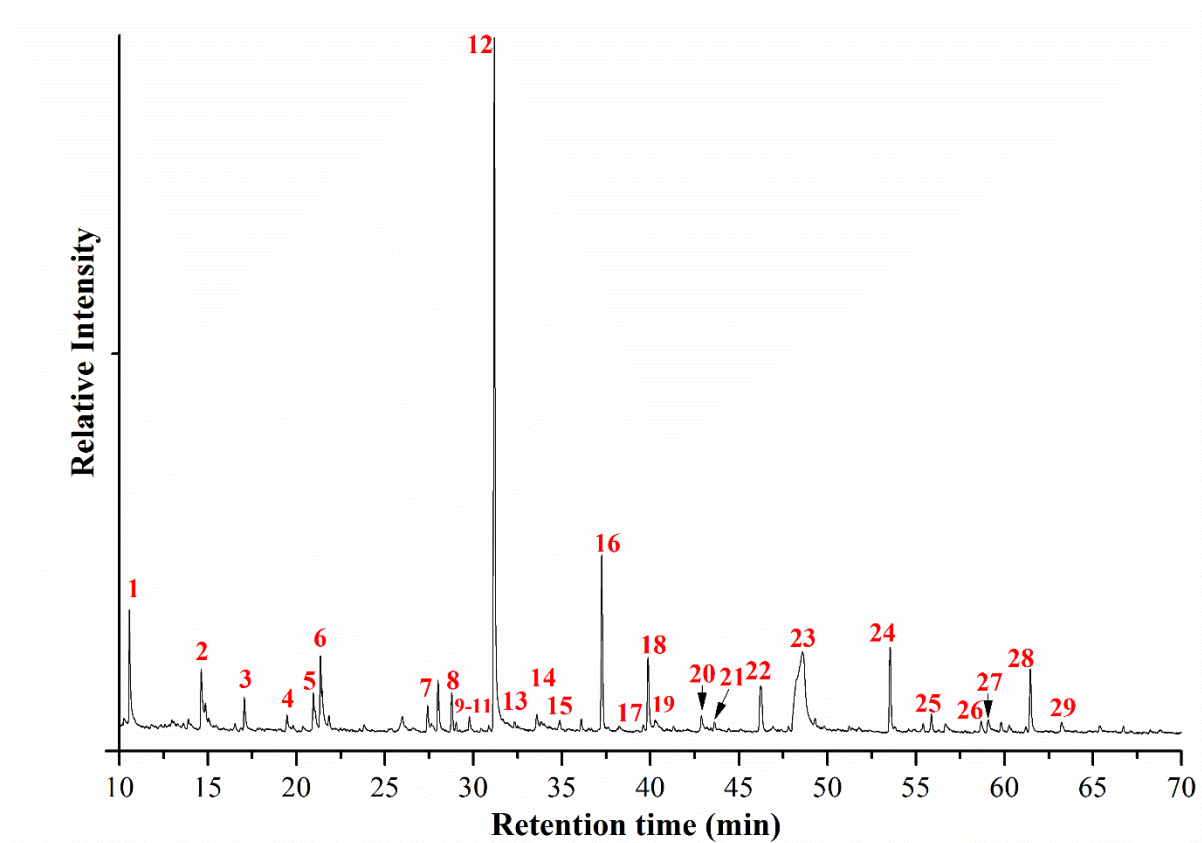


Figure 5.6 - EHR pyrogram.

In **Figure 5.6** (EHR pyrogram), the compounds corresponding to the peaks 1, 3, 9-11 and 23 were released from carbohydrates. The main compounds accounted on H-lignin units estimative were phenol (2), *o*-cresol (4), *p*-cresol (5), 4-ethyl-phenol (7), isopropyl-phenol (13) and 4-allylphenol (17). Guaiacyl (6), 4-methylguaiacol (8), 4-ethyl-guaiacol (15), vanillin (20) and *trans*-isoeugenol (21) were accounted on G-lignin units. The main compounds derived from S-lignin units were syringyl (18), 4-methylsyringol (22), 2,6-dimethoxy-4-(2-propenyl)-phenol (25 and 26), syringaldehyde (27), 4-allylsyringol (28) and acetosyringone (29). The peaks 14 (methoxy-cathecol), 19 (biphenyl), and 24 (dimethoxy acetophenone) are polyphenolic structure (non-specific lignin).

The highest peaks of the EHR pyrogram (**Figure 5.6**) are peak 12 and peak 16. The high amounts of 4-vinylphenol (12) and 4-vinylguaiacol (16) released from the EHR upon pyrolysis is mostly due to the occurrence of *p*-coumarates (PCA) and ferulates (FA) from sugarcane (a *Gramineous* plant), respectively (Menezes et al., 2017; del Río et al., 2015). Therefore, 4-vinylphenol (12) and 4-vinylguaiacol (16) were not inserted on estimative of H- and G-lignin units of the EHR, respectively.

The main lignin structural characteristics obtained from the Py-GC/MS data (H-, G-, and S-lignin units) of the LBL and EHR are shown in the **Table 5.3**.

Table 5.3 - Aromatic units of the LBL and EHR by Py-GC/MS technique.

Lignin aromatic units (%)	LBL	EHR
H	3	22
G	30	22
S	67	56
(H+G+S=100)		

The data from **Table 5.3** indicates that despite the EHR and LBL presented similar amounts of S-lignin units, the EHR has much more amount of H-lignin unit than in the LBL. Therefore, the EHR appears to be more promising for phenolic resins production than the LBL, since it has larger H-lignin units, *i.e.*, the EHR has more free *ortho*-positions to formaldehyde incorporation.

For alkaline EHR and acidic-dioxane EHR

Apparently, the carbohydrates contained in the EHR could be interfering in the resolution of the peaks from lignin pyrolysis in the EHR pyrogram (**Figure 5.6**). The EHR was submitted to the alkaline and the acidic-dioxane processes in order to better characterize the lignin contained on EHR. The alkaline EHR and acidic-dioxane EHR were analyzed by Py-GC-MS in order to determine the H, G and S-lignin amounts. Pyrograms of the alkaline EHR and acidic-dioxane EHR are shown in the **Figure 5.7**. As can be seen in **Figure 5.7**, the alkaline EHR and acidic-dioxane EHR pyrograms presented a better resolution than the EHR pyrogram (**Figure 5.6**).

In **Figure 5.7a** (alkaline EHR pyrogram), the main compounds accounted on H-lignin units estimative were phenol (1), *o*-cresol (2), *p*-cresol (3), 2,4-dimethyl-phenol (5), 4-ethyl-phenol (6), isopropyl-phenol (10) and 4-allylphenol (14). Guaiacyl (4), 6-methylguaiacol (7), 4-methylguaiacol (8), 4-ethyl-guaiacol (12), *cis*-isoeugenol (18), *trans*-isoeugenol (19), acetoguaiacone (22), guaiacyl acetone (23) and methyl ester vanillin acid (28) were accounted on G-lignin units. The main compounds derived from S-lignin units were syringyl (15), 2,6-dimethoxy (16), 4-methylsyringol (20), 2,6-dimethoxy-4-(2-propenyl)-phenol (25 and 26), syringaldehyde (27), 4-allylsyringol (29) and acetosyringone (30). The peaks 9 and 13 are 4-vinylphenol and 4-vinylguaiacol, respectively. The compound corresponding to the peak 21 was released from carbohydrates.

In **Figure 5.7b** (Acidic-dioxane EHR pyrogram), the main compounds accounted on H-lignin units estimative were phenol (1), *o*-cresol (2), *p*-cresol (3), 2,4-dimethyl phenol (5), 4-ethyl-phenol (6), isopropyl-phenol (9) and 4-allylphenol (13). Guaiacyl (4), 4-methylguaiacol (7), 4-ethyl-guaiacol (10), 4-hydroxy-3-methoxy-benzaldehyde (15), *trans*-isoeugenol (16), guaiacylacetone (18) and methyl ester vanillin acid (24) were accounted on G-lignin units. The main compounds derived from S-lignin units were syringyl (14), 4-methylsyringol (17), 2,6-dimethoxy-4-(2-propenyl)-phenol (21 and 22), syringaldehyde (23), 4-allylsyringol (19 and 28) and acetosyringone (26). The peaks not specified or not numbered can be polyphenolic structures (non-specific lignin) and aliphatics. It was not possible to observe peaks derived from carbohydrates. This fact corroborates with the chemical composition results (**section 5.1.1**), where acidic-dioxane process generated a lignin-rich stream with lower carbohydrates amount than the alkaline process.

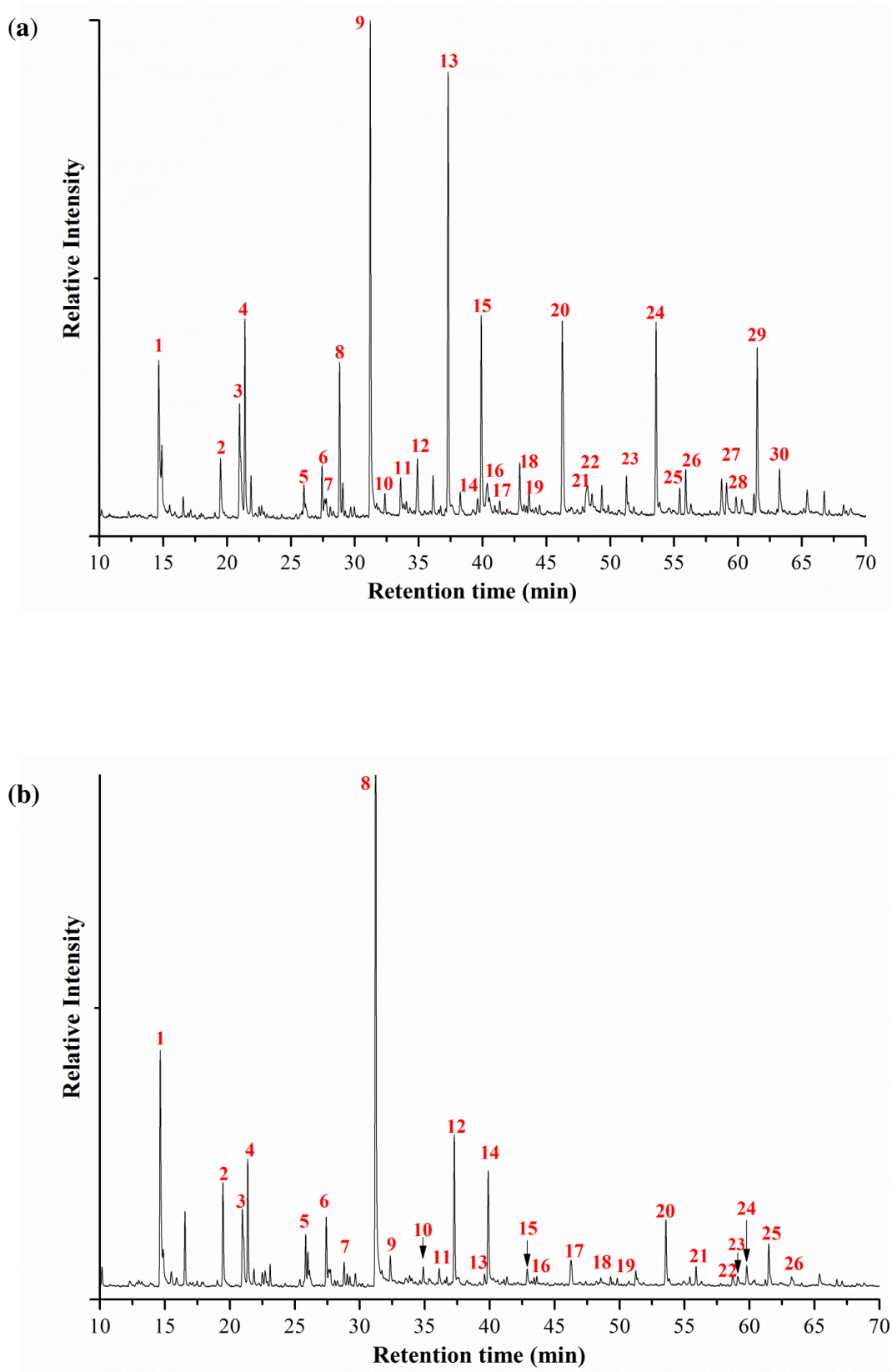


Figure 5.7 - (a) Alkaline EHR and (b) acidic-dioxane EHR pyrogram.

The main lignin structural characteristics obtained from the Py-GC/MS data (H-, G-, and S-lignin units) of the alkaline EHR and acidic-dioxane EHR are shown in the **Table 5.4**.

Table 5.4 - Aromatic units of the alkaline EHR and acidic-dioxane EHR by Py-GC/MS technique.

Lignin aromatic units (%)	Alkaline EHR	Acidic-dioxane EHR	^a L1	^a L3
H	28	38	13	30
G	24	25	36	33
S	48	37	51	37

^aResults for sugarcane bagasse lignins from alkaline pretreatment at 130 °C (**L1**) or 170 °C (**L3**) obtained by Nakanishi (2016). These results were also reported by Menezes et al. (2017).

The EHR lignins submitted to the extraction processes (alkaline e acidic-dioxane) showed higher amounts of H-lignin units and lower amounts of S-lignin units, according to **Table 5.4**, when compared to with the EHR (**Table 5.3**). The G-lignin units remained almost intact. Furthermore, when acidic-dioxane process was applied, there was an enrichment of H units and a depletion of S-lignin units in relation to the alkaline EHR.

Nakanishi (2016) obtained lignins from sugarcane bagasse submitted to an alkaline pretreatment (1.5% w/v NaOH, 1:15 solid/liquid for 30 min) at 130 °C (**L1**) or 170 °C (**L3**). Menezes et al. (2017) reported the H, G and S lignin units for these lignins (**L1** and **L3**) by Py-GC/MS. They noted that the lignins are comparatively depleted in S-lignin units (51% → 37%) and enriched in H-lignin units (13% → 30%) with increasing the severity of the pretreatment (130 °C → 170 °C), as a consequence of the preferential removal of S-lignin during alkaline delignification (Menezes et al., 2017).

del Río et al. (2015) and Murciano Martínez et al. (2016) have reported that sugarcane bagasse contains considerable amount of PCA and FA. The use of tetramethylammonium hydroxide (TMAH) additive in Py-GC/MS allows the discrimination between 4-vinyl phenol/4-vinylguaiacol present as such from being Py-GC/MS products of decarboxylated PCA and FA, respectively (del Río et al., 2007). As these compounds have *ortho* positions free in their phenolic rings, they could participate in the formaldehyde reaction. Therefore, it is suggested the addition of TMAH in the EHR in order to estimate the PCA and FA amounts.

5.1.4 NMR Spectroscopy

¹H-NMR Spectroscopy

The major functional groups of lignin affecting its reactivity for the synthesis of phenolic resins are phenolic hydroxyl and methoxyl. The acetylated EHR and LBL were analyzed by ¹H-NMR specifically to determine these important functional groups. The results of the semi-quantitative analysis of the ¹H-NMR spectra from these samples are depicted in **Table 5.5**. It contains the chemical shift ranges of hydrogen and their corresponding regions (Chen and Robert, 1988).

Table 5.5 - ¹H-NMR results.

δ (ppm)	Group	EHR (%)	LBL (%)
0.7 - 1.6	Nonoxygenated aliphatic region	30.7	10.3
1.6 - 2.2	^a Aliphatic hydroxyl region	9.0	4.0
2.2 - 2.5	^a Phenolic hydroxyl region	3.9	5.3
2.5 - 3.5	Major aliphatic region	4.8	10.5
3.5 - 4.0	Methoxyl	18.8	27.3
4.0 - 5.2	Major aliphatic region	13.3	11.7
5.2 - 5.7	Cyclic benzylic region	2.5	3.6
5.7 - 6.2	Noncyclic benzylic region	1.8	4.3
6.2 - 8.0	Aromatic region	15.2	21.1
8.0 - 10.0	Aldehydes groups	0.1	1.9

^aIt was divided by three because the acyl group has three atoms of hydrogen.

The aliphatic hydroxyl content in the EHR is more than double in comparison to that in the LBL. The $\text{OH}_{\text{phenolic}}/\text{OH}_{\text{aliphatic}}$ ratios of the EHR and the LBL are 0.4 and 1.3, respectively. It can be also observed in the **Table 5.5** that the methoxyl group content is lower in EHR than in the LBL. This lower methoxyl content can indicate that the EHR probably has more *ortho* positions of their phenyl rings unblocked by methoxyl groups and therefore this is an advantage for manufacturing lignin phenol-formaldehyde resins. An intense peak ($\delta\text{H} = 1.25$ ppm) appeared in the non-oxygenated aliphatic region of the EHR spectrum. This indicates the presence of substructures containing non-oxygenated and saturated aliphatic carbons (CH_2 and CH_3 - hydrocarbons) in the side chains of the EHR.

2D HSQC NMR Spectroscopy

The main regions that could be observed in the 2D HSQC contour maps are the aliphatic, oxygenated aliphatic, and aromatic regions (**Figure 5.8**) (del Río et al., 2015).

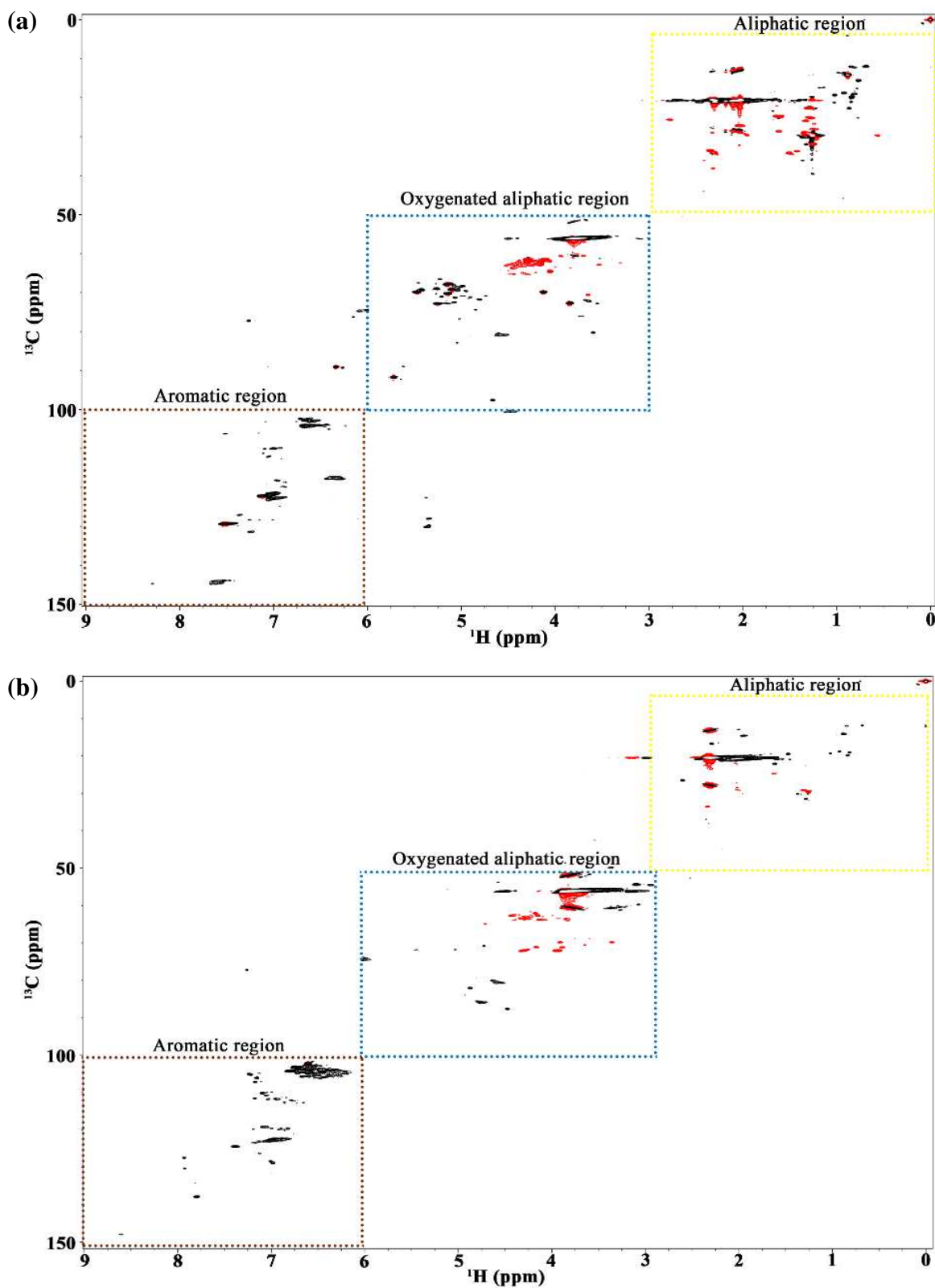


Figure 5.8 - Entire 2D HSQC NMR contour maps of the EHR (a) and the LBL (b).

The main signals in the aliphatic region from the 2D HSQC contour maps are of acetyl correlations, in both alcoholic and phenolic acetates (Ibarra et al., 2007). The oxygenated aliphatic region is important from the viewpoint of the structural study of lignin (β -O-4 structures, phenylcoumaran, resinol, tetrahydrofuran, dibenzodioxocin, α,β -diaryl ether, and spirodienone structures).

The aromatic region of the 2D HSQC contour map is the most relevant to evaluate the potential of the EHR and the LBL for phenolic resin synthesis, since the signals corresponding to the aromatic rings of the S-, G-, and H-unit can be observed. The 2D HSQC NMR contour map of the aromatic region (δ_C : 100-150 ppm/ δ_H : 6.0-9.0 ppm) of the EHR and the LBL are expanded (**Figure 5.9**).

As displayed in **Figure 5.9**, *p*-coumarates (PCA) and ferulates (FA) are present in the EHR. PCA and FA are widely found in the *Gramineae* family, especially in sugarcane (del Río et al., 2015; Menezes et al., 2017). PCA is predominantly attached to the lignin, and FA can be attached to both a carbohydrate-carbohydrate and lignin-carbohydrate complex (del Río et al., 2015).

A semi-quantitative analysis of the volume integrals of the signals corresponding to S-, G-, and H-unit was performed (**Table 5.6**). 2D HSQC NMR cross-signals were assigned by comparison with literature data from Ibarra et al. (2007) and del Río et al. (2015).

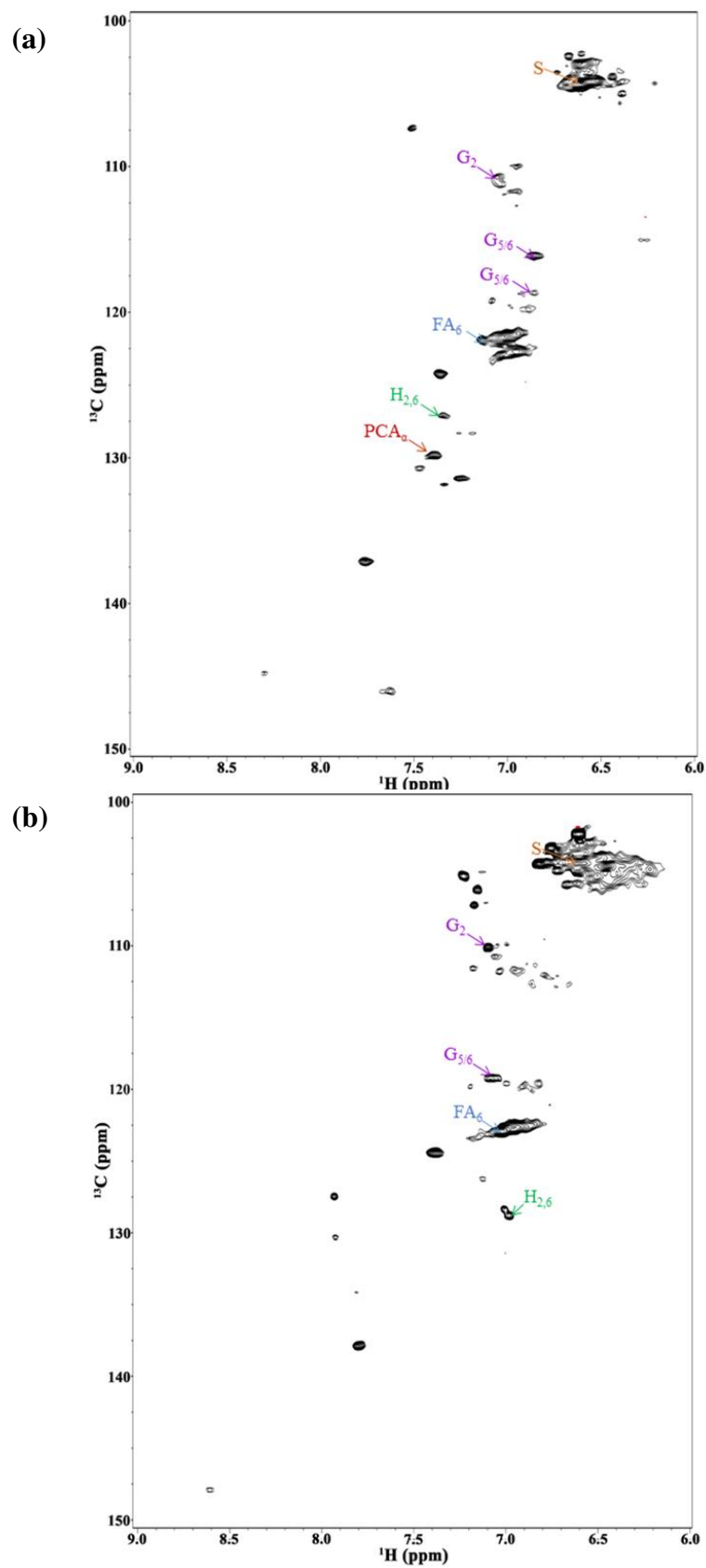


Figure 5.9. Aromatic regions from HSQC spectra of the EHR (a) and LBL (b) (Menezes et al., 2016b). S: syringyl unit; G: guaiacyl unit; H: *p*-hydroxyphenyl unit; Fa: ferulic acid unit; PCA: *p*-coumarate unit.

Table 5.6 - Aromatic lignin units by 2D HSQC NMR technique (Menezes et al., 2016b).

Lignin aromatic units	EHR	LBL
H (%)	11	6
G (%)	31	16
S (%)	58	78
S/G ratio	1.8	4.8

The S/G ratio for the EHR (1.8) are similar to the S/G ratio determined for sugarcane bagasse (1.6) by del R  o et al. (2015). The LBL showed the highest S/G (4.8). These results corroborate with the high amount of the methoxyl group in the LBL (27.3%) determined by the ¹H-NMR analysis. However, it is likely that the S-unit (δ_{H} : 6.62 ppm/ δ_{C} : 104.3 ppm) in the LBL is overestimated because there are overlapping peaks.

Comparing the S-, G- and H-lignin units results from the HSQC and Py-GC/MS analyses, it can be observed that a higher S-lignin amount and a lower H-lignin amount when estimated by HSQC technique. Menezes et al. (2017) observed the same trend for alkaline lignins from sugarcane bagasse (L1 and L3). For example, S-lignin amount of L3 estimated from the HSQC technique was 44%, while by means of the Py-GC/MS technique, S-lignin was 37%.

However, by both the HSQC and the Py-GC/MS techniques, the EHR appears to be more promising for phenolic resin production when compared to the LBL, since the EHR has a lower S-lignin amount among the lignin aromatic units and a higher number of H-lignin units.

5.1.5 Elemental Analysis and HHV determination

Table 5.7 depicts the elemental analysis results, Double Bonds Equivalent (DBE) values, protein (%) amounts, and experimental and theoretical HHVs of the EHR and LBL.

Table 5.7 - Elemental composition, DBE, protein content and HHVs (Menezes et al., 2016b).

	LBL	EHR
%C	61.24 (0.08)	47.46 (0.09)
%H	6.33 (0.13)	6.28 (0.01)
%N	0.07 (0.03)	0.57 (0.04)
%S	2.55 (0.06)	0.59 (0.01)
%O	29.82 (0.13)	45.11 (0.13)
DBE	4.5	1.7
Protein (%)	0.4	3.6
HHV _{theoretical} (kJ kg ⁻¹)	24913	17806
HHV _{experimental} (kJ kg ⁻¹)	25560	19347

Standard deviation values of the samples are shown in parentheses.

The EHR has about 23% less of carbon content and 50% more of oxygen content in relation to these elements in the LBL. The sulfur content of the LBL (2.55%) can be from the Kraft process, a precedent step of the whole process. The protein amount in the EHR (3.6%) was much higher than in the technical lignin LBL (0.4%). The EHR protein value may be arising from the enzymatic complex used in the enzymatic hydrolysis step in cellulosic ethanol production.

The C9-formula for the EHR (**Equation 9**) and the LBL (**Equation 10**) are extended below:



As expected, it turns out that the C9-formula of the EHR showed the highest OH_{aliphatic} value. With regard to the methoxyl coefficient in the C9-formula of these lignins, the EHR

has a lower methoxyl value in each C9 than in the LBL. This is consistent with the results presented in the discussion of 2D HSQC NMR technique where the syringyl unit amount was larger in the LBL.

The DBE number of lignin is directly correlated to both its aromaticity and its degree of condensation (Kim et al., 2014). The DBE value of the LBL was the largest (4.5). It is worth remembering that the LBL was earlier submitted to high temperature on the Kraft process. Kim et al. (2014) noted that heat application on lignin could lead it to become more condensed in relation to the native lignin structure, leading to an increase in its DBE value. It also is noted that the EHR showed the smallest DBE value (1.7). This is due to the high amount of cellulose fibers fully dispersed in the EHR. The lower DBE value may be related to a higher amount of free phenolic hydroxyl groups, which is an advantage for the synthesis of lignin-phenol resins (Mansouri and Salvadó, 2006).

The experimental and estimated HHVs can be considered close. The highest HHV value was found in the LBL. This fact can be explained because higher carbon and lower oxygen contents lead to a higher HHV value (Demirbas, 2004).

5.1.6 Thermogravimetric analysis

The thermogravimetric (TG) curve shows the weight loss (%) with the temperature increase, while the first derivative of TG curve (DTG) shows a corresponding rate of weight loss ($\% \text{ min}^{-1}$) of the lignocellulosic materials. **Figure 5.10** depicts the TG and DTG curves of the EHR and LBL. As for the EHR, two high peaks of the degradation rate appear in the DTG curve. The first is comprised in the range of temperatures between 250 and 350 °C. This is the highest peak due to the high carbohydrate content present in the EHR. The second appears in a temperature range of 350 to 500 °C, referring to the remaining lignin degradation. To the LBL sample, the highest rate of degradation ($16 \text{ wt.}\% \text{ min}^{-1}$ at 490 °C) occurs between 410 and 510 °C. This happens because lignin in the LBL is the major component. It is interesting to note that the peak of remaining lignin degradation in the EHR has appeared at a lower temperature compared to this peak on the LBL spectrum, indicating that the presence of carbohydrates directly influences on weight loss of the EHR.

The weight loss in both samples is practically constant above 500 °C. The residue observed up to 500 °C was around 0.7% and 6.9% for LBL and EHR, respectively. These residues correspond to the ashes present in the samples, since the ash contents are

approximate (0.7% and 8.4% in LBL and EHR, respectively). The thermal characteristics of the EHR and LBL influence directly on the thermal resistance of the phenolic resins.

The TG analysis revealed the thermal limitations of the EHR and LBL before their application in phenolic formulations. The temperature ranges usually applied in the synthesis and the cure processes of the phenolic resins are below 200 °C. Thus, the EHR and LBL are thermally suitable to be processed in lignin-phenol resins.

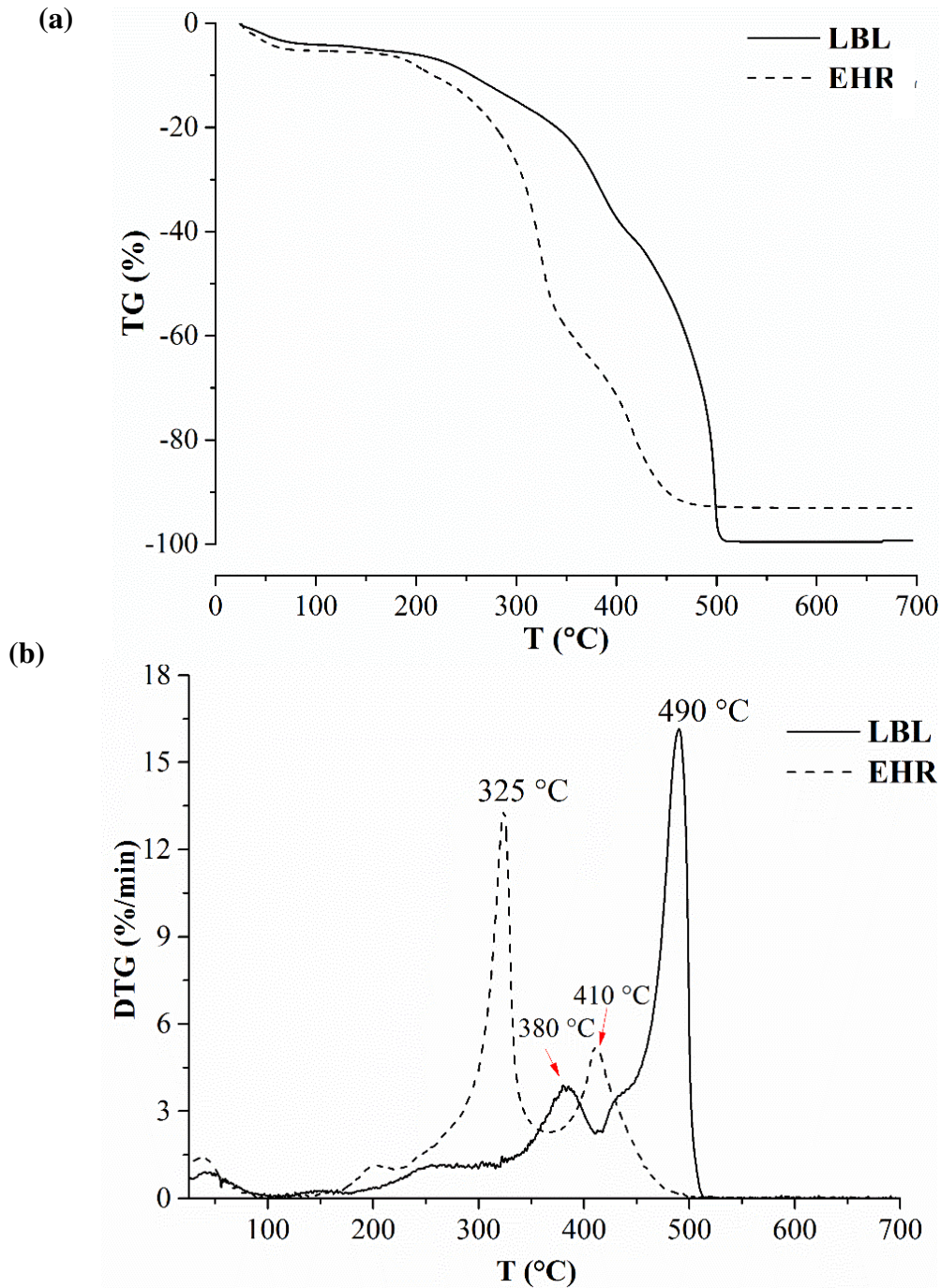


Figure 5.10 - TG (a) and DTG (b) curves of the EHR and LBL (Menezes et al., 2016b).

5.1.7 Physical characterization

A set of ten sieves with opening size ranging from 4.75 to 0.15 mm was used in the particle size distribution by sieving (Menezes et al., 2016a). **Table 5.8** depicts the opening diameter of each sieve, the average diameter and the retained mass fraction in each sieve. **Figure 5.11** shows the pictures of the EHR retained in each sieve with its corresponding average diameter.

Table 5.8 - Particle size distribution by sieving of the EHR (Menezes et al., 2016a).

Opening diameter (mm)	Average diameter (mm)	Retained mass fraction (%)
Bottom	< 0.15	4.0 (0.8)
0.15	0.20	5.7 (0.5)
0.25	0.34	11.6 (0.3)
0.43	0.52	7.4 (0.3)
0.60	0.73	8.1 (0.4)
0.85	1.02	9.6 (0.5)
1.18	1.44	10.8 (0.6)
1.70	2.03	10.8 (0.4)
2.36	2.86	14.4 (0.6)
3.35	4.05	11.8 (1.0)
4.75	> 4.75	5.7 (0.6)

The standard deviation is shown in parentheses.

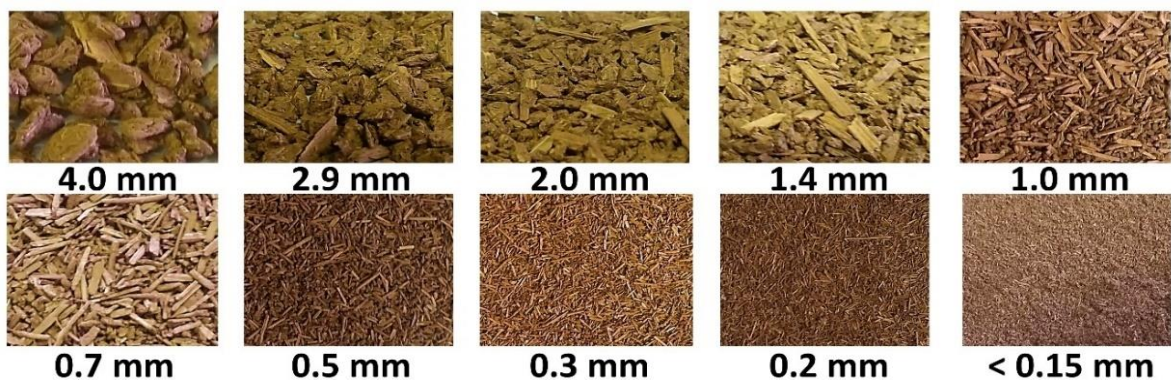


Figure 5.11 - Photographs of the EHR particles from each sieve.

The particle size distribution of the EHR presented profile of polydispersity material since it had two regions with a higher retained mass fraction. About 46% of the EHR was comprised in the set of sieves with average diameter of ≤ 1.0 mm. Size and morphology of fibers influence directly in determining the mechanical properties of resins. It was seen mainly fiber clusters in the sieves with opening diameter of 4.57 and 4.05 mm. In other sieves, it was visibly observed that the fibers of the EHR were released.

Figure 5.12 depicts the particle sizing distributions by laser scattering of the EHR from bottom of sieve set (<0.15 mm), the milled EHR and the LBL.

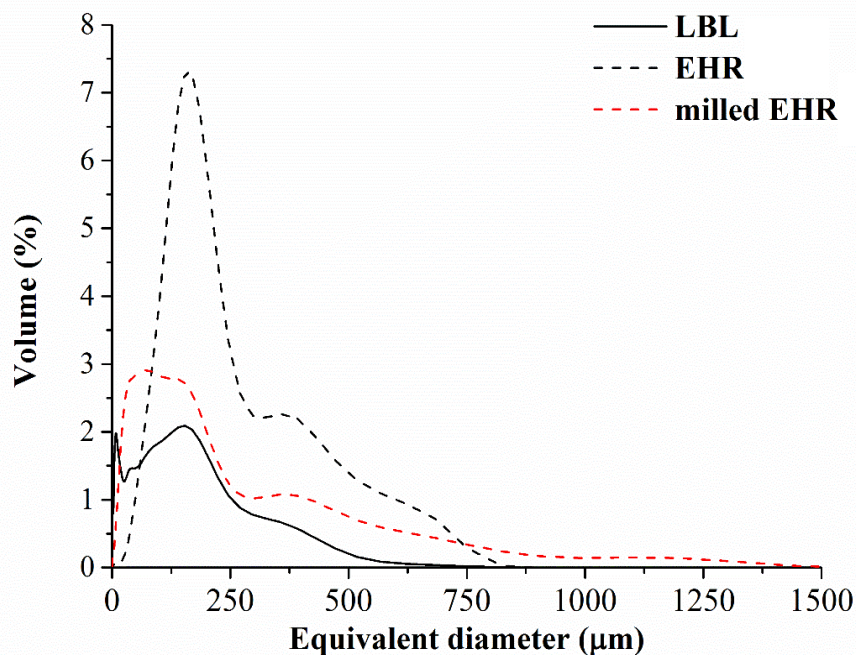


Figure 5.12 - The particle size distributions by laser scattering of the LBL, EHR and milled EHR (Menezes et al., 2016b).

As it can be observed in the **Figure 5.12**, the EHR from the bottom ranged from 0.4 to 820 μm . About 5% of this sample is between 0.4 - 50 μm and 50% is ≤ 170 μm . Only 44% of the EHR from the bottom is ≤ 0.15 mm. This can be explained by the fact that the diameter of each fiber is much smaller than its length, so it is possible that longer fibers can pass through sieves with smaller diameter openings. The milled EHR ranged between approximately 0.4-990 μm . About 5% of the milled EHR is 6.5 - 0.4 μm and 50% it is ≤ 70 μm . The LBL particles ranged from 0.4-1090 μm and 64% of the LBL particles are between 0.4-50 μm , while only 5% of the EHR particles are in this range. More than 75% of the LBL particles are ≤ 100 μm .

5.1.8 Scanning Electron Microscopy (SEM)

The **Figure 5.13** depicts the SEM images of the EHR from the bottom of the sieve set and of the milled EHR.

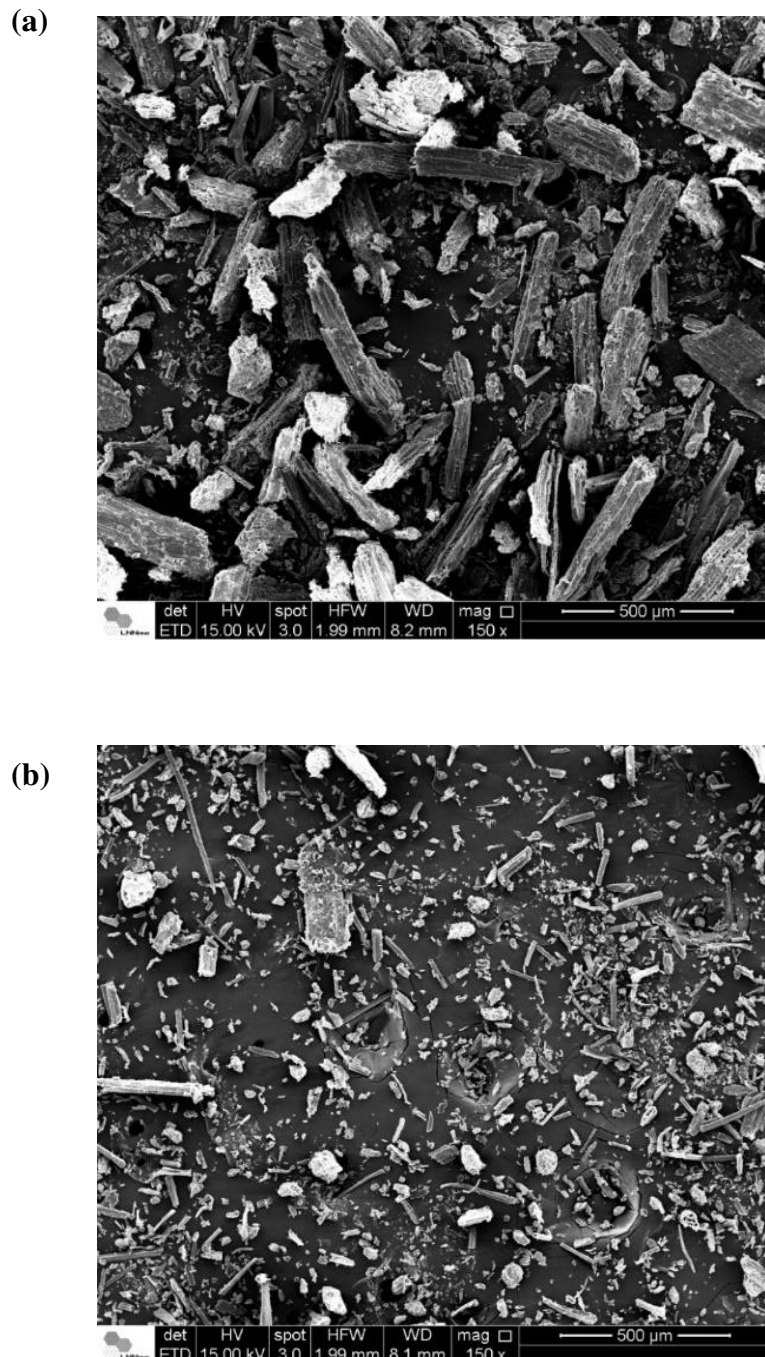


Figure 5.13 - SEM images of (a) the EHR from bottom of sieve set and (b) milled EHR.

SEM images of the EHR from the bottom of the sieve set and of the milled EHR show that the cellulose fibers are well distributed. In addition, some lignin particles appear to be deposited on the cellulose fibers in the EHR. If it really is lignin, it probably will provide an easier reaction between lignin and formaldehyde since it is more susceptible to interact with formaldehyde. Morphological studies of the fibers of both samples (the EHR from bottom and the milled EHR) showed different sizes and arrangement from them, since fibers are not spherical and dispersively arranged.

Regarding the LBL micrographs, it was not possible to visualize anything relevant because the LBL was degraded due to the high intensity of the electron beam equipment. It is suggested to perform some tests with a lower intensity of electron beam or with LBL not coated with gold in order to not burn it.

Small Angle X-ray Scattering (SAXS) technique is suggested to analyze shape, dimension and size distribution of the LBL. SAXS is an experimental technique widely used for structural characterization of macromolecules in dilute solutions. SAXS studies have been applied to lignin to characterize lignin molecular architecture, shape, dimensions and intermolecular interactions (Brenelli et al., 2016; Harton et al., 2012).

5.1.9 Molar mass determination

The intrinsic viscosity was graphically obtained by means of the viscosities representation as a function of the LBL concentration. A linear regression corresponding to the obtained points was drawn. Thus, the intrinsic viscosity is the average value of the ordinates. **Figure 5.14** shows the relationship between the intrinsic viscosity and the LBL concentration, observing a linear relationship which indicates that was obtained in a Newton regime and therefore the viscosimetry is valid (Mello et al., 2006; Silva et al., 2013). **Table 5.9** shows the molar mass by viscosimetry of the LBL.

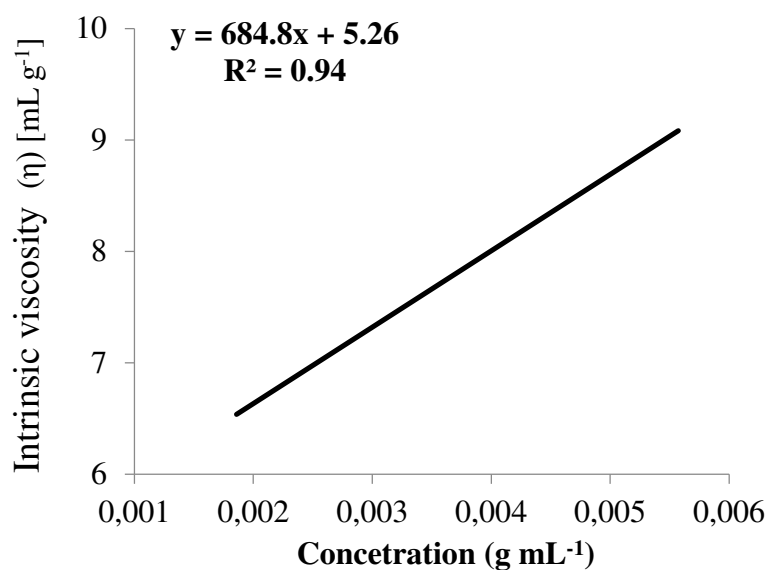


Figure 5.14 – Intrinsic viscosity as a function of the LBL concentration in NaOH 0.5 M solution.

Table 5.9 - Intrinsic viscosity and molar mass of the LBL.

	[η]	Molar mass
Sample	(mL g ⁻¹)	(g mol ⁻¹)
LBL	5.29	106,219

Molar mass values of lignins can depend on lignin source, extraction process, different analysis conditions, such as, system columns, solvents, acetylation, standard type, and others (Constant et al., 2016). Nakanishi (2016) obtained lignins from sugarcane bagasse (SB) submitted to an alkaline pretreatment (1.5% w/v NaOH, S/L 1:15 for 30 min) at 130 °C or 170 °C. Molar mass determination for these lignins was performed using the same methodology that was used for molar mass determination of the LBL. SB lignin from alkaline pretreatment at 130 °C showed a molar mass of 381,130 g mol⁻¹, while for SB lignin from alkaline pretreatment at 170 °C was 280,108 g mol⁻¹. The both lignins from sugarcane bagasse showed higher molar mass than the LBL that it is from *Eucalyptus*.

Molar mass distribution of lignin is one of the main properties to evaluate reactivity and physicochemical characteristics for potential applications (Menezes et al., 2017). Lignin with lower molar mass would be less condensed (Rinaldi et al., 2016), thus it probably has more active-sites for the reaction towards formaldehyde (Ragauskas et al., 2014).

As mentioned in method section, it was not possible to determine the molar mass of the EHR because it was not totally soluble in those solvents. Thus, it is suggested that the alkaline EHR and the acidic-dioxane EHR be submitted to technique of molar mass determination.

5.2 Determination of curing parameters of the phenolic resins with the EHR and LBL

5.2.1 Rheological study

The change in dynamic-mechanical properties of a curing system is directly proportional to the extent of the reaction. The curing processes were carried out for the obtained phenolic resins under isothermal conditions at five different temperatures: 90, 97.5, 105, 112.5 and 120 °C. Gel point values were determined on the crossover between the G' and G'' curves. **Figure 5.15** illustrates an example of how was defined the t_{gel} value. The region of the crossover between G' and G'' was amplified for better visualization of the t_{gel} value.

As pointed out by Knop and Pilato (1985), the temperature acts as catalyst agent in curing process of resole-type phenolic resins, thus, the higher temperature applied in curing system, the lower t_{gel} values. However, isotherms higher than 120 °C were not analyzed on curing process, once deformation of the samples occurred at this condition due to rapid evaporation of the water present in them.

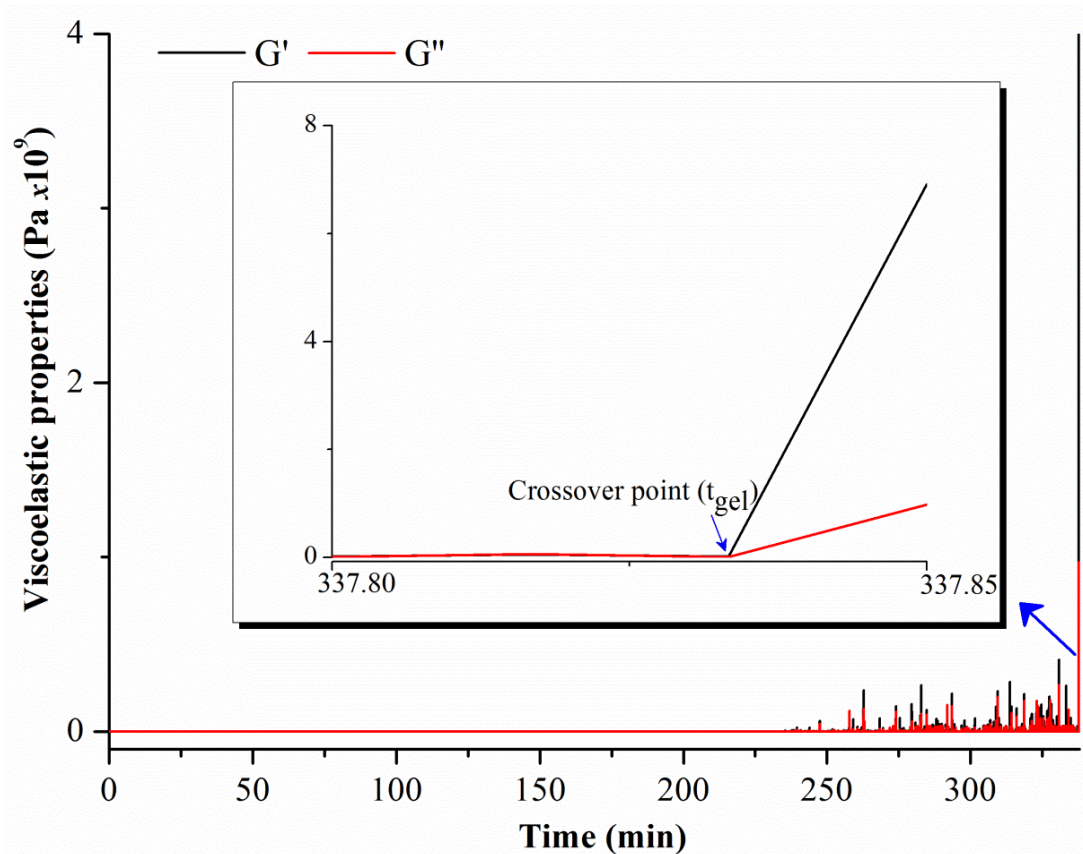


Figure 5.15 - Viscoelastic properties curves of the LBL 60% resin at 105 °C. Crossover region zoom (t_{gel}).

Figure 5.16 depicts t_{gel} values that were determined for all resins at five different isotherms. In general, the LBL and EHR insertion on phenolic resins led to decrease on t_{gel} values, with exception the LBL 60% resin. This resin, as observed on **Table 5.12**, has the highest viscosity value among the phenolic resins with LBL. Thus, it is suggested that this resin be directly used as an adhesive. As it can be observed on **Figure 5.16**, t_{gel} values were lower than 120 min (2 h) at 105 °C for all obtained resins, expect for the LBL 60%. For this reason, the chosen conditions of curing process were 105 °C for 2h to obtain the thermosetting resins (test specimen) for DMTA and DSC analyses. For the LBL 60% resin, the test specimen was not obtained due to the need for a high curing time (almost 6 h). The catalyst addition for curing is suggested.

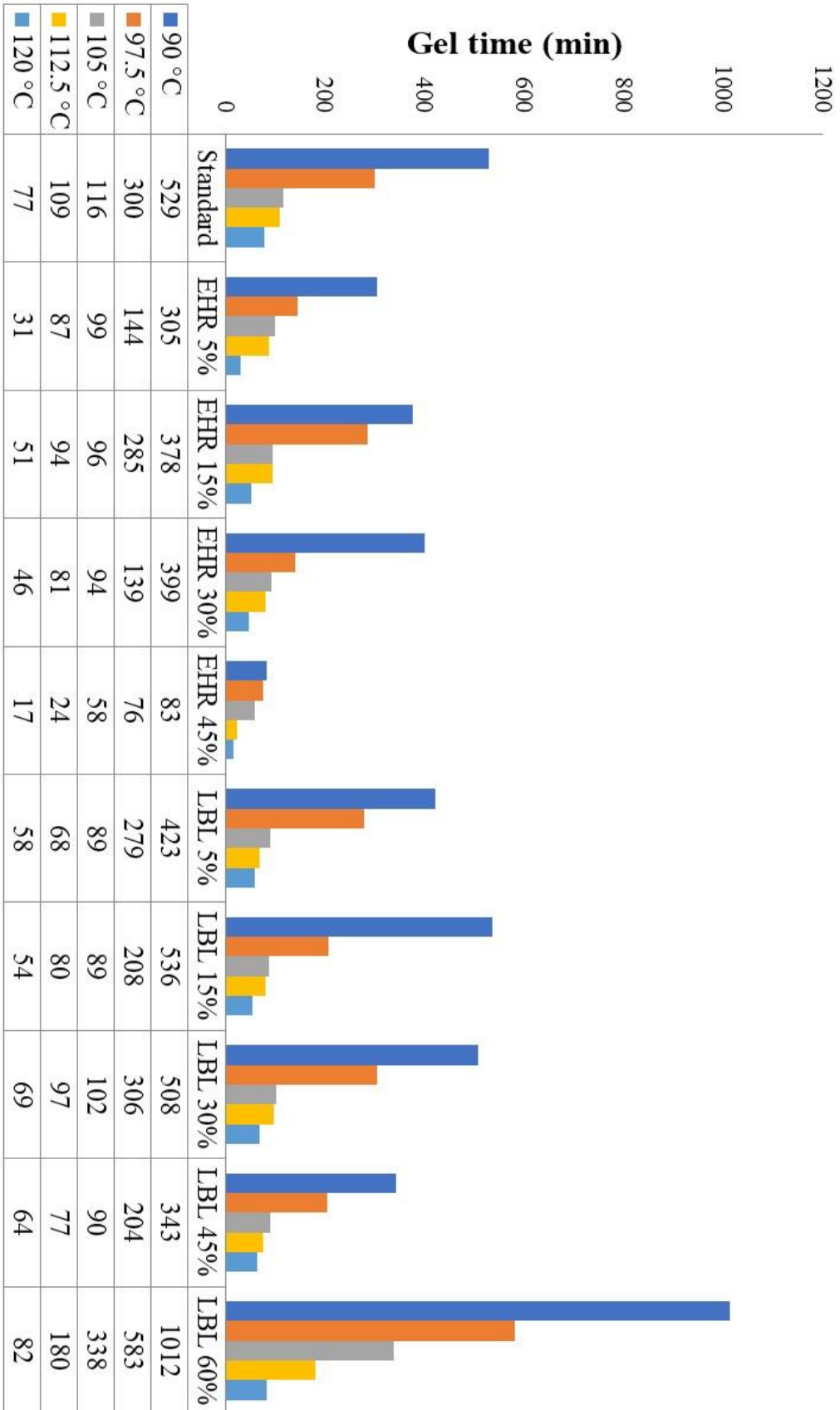


Figure 5.16 - t_{gel} values for all phenolic resins at 90 - 120 °C.

It can be visualized that the higher LBL amount on phenolic resins, the higher t_{gel} values. In general, t_{gel} values diminished as the EHR amount increased (from 15% until 45%). By means of an Arrhenius relationship (**Equation 11**), apparent Activation Energy (E_a) values were determined (**Figure 5.17**) (Laza et al., 2002).

$$\ln t_{gel} = C + \frac{E_a}{R} \frac{1}{T} \quad (11)$$

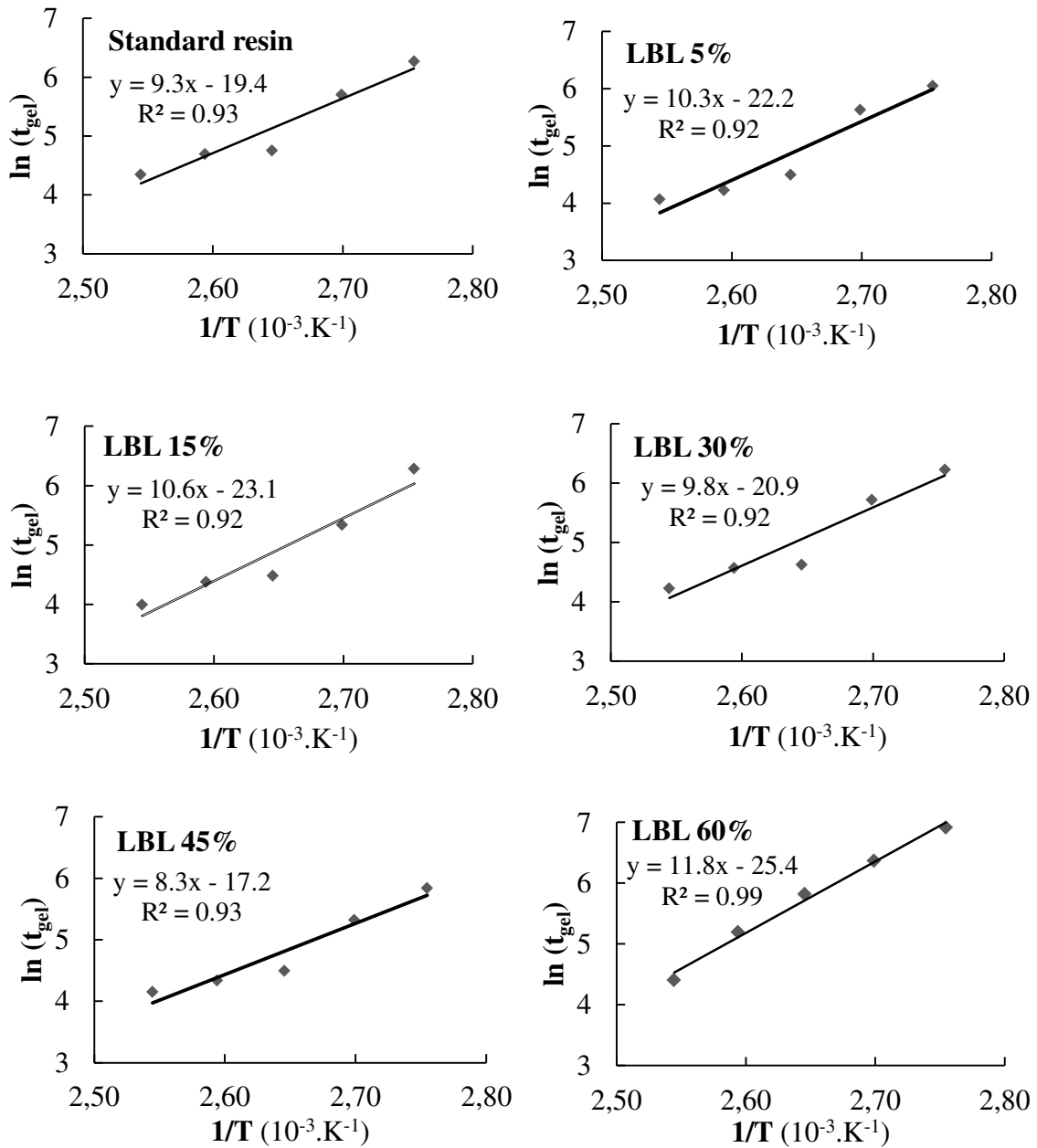


Figure 5.17 - Arrhenius relationship for each phenolic resin.

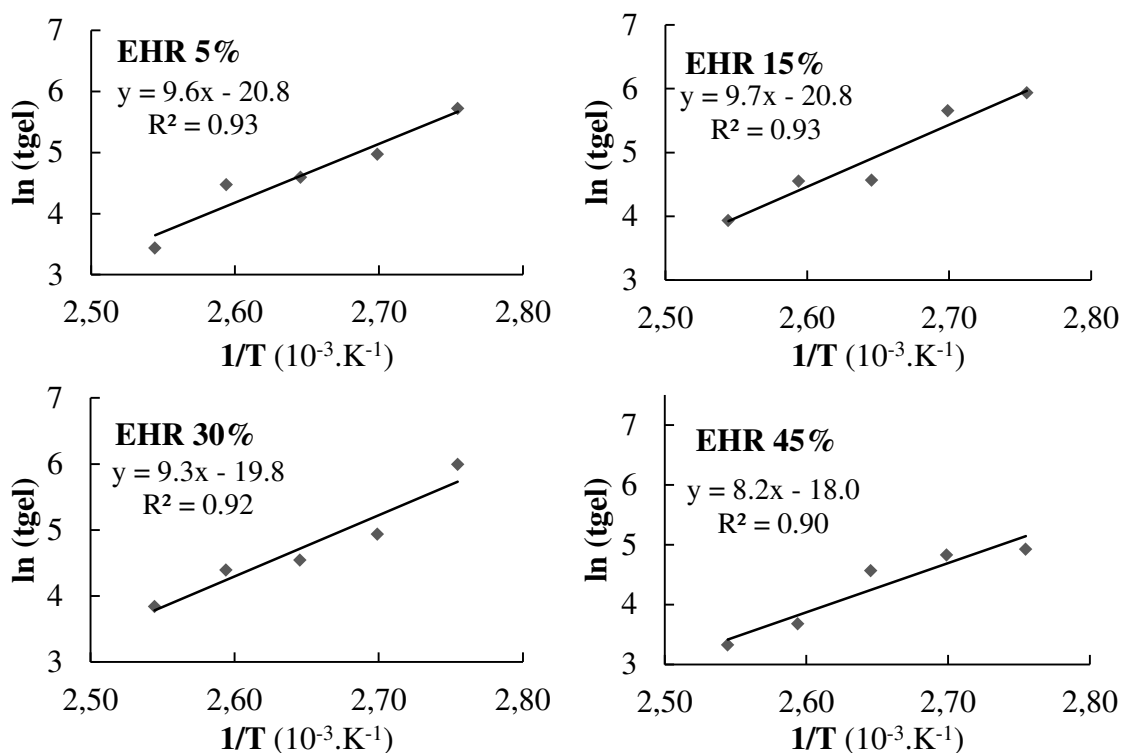


Figure 5.17 (Continuation) - Arrhenius relationship for each phenolic resin.

E_a values for curing reactions were obtained from the slope of equation of ' $\ln(t_{gel})$ ' and the 'inverse of temperature' graphs times the universal gas constant (R). The apparent Activation Energy (E_a) values for each phenolic resin are showed in the **Figure 5.18**.

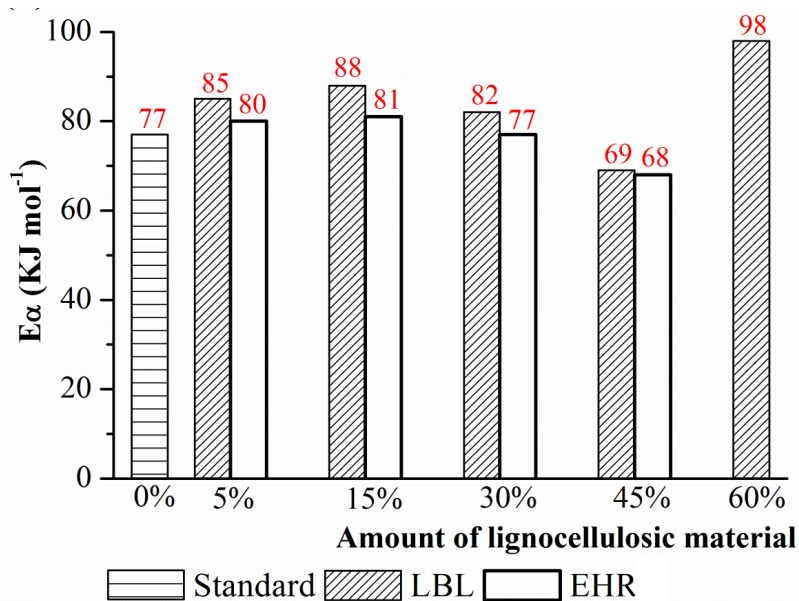


Figure 5.18 - E_a values for each phenolic resin.

The profiles from the EHR and the LBL presented the same downward trend, *i.e.*, the higher biomass amount, the lower E_a values, except the LBL 60% resin. The E_a values for phenolic resins with EHR were lower than using LBL. The results from rheological study indicate that the curing reactions of the phenolic resins with EHR showed lower t_{gel} values, and moreover a lower energy amount (activation energy) (E_a) in comparison to the phenolic resins with LBL.

5.2.2 TG analyses

The curing parameters were also assessed for LBL 5% and EHR 5% by TG analyses. TG curves at 5, 10 and 20 °C min⁻¹ of the LBL 5% and EHR 5% resins are depicted in **Figure 5.19**. The selected region of the loss curves for the curing kinetic analysis was from 50 to 200 °C that correspond to start limit and to stop limit of the loss weight, respectively. The kinetic analysis was carried out using TA Specialty Library package provided by TA instruments.

The TG Kinetics program allows to analyze results from TG data files to calculate the heating rate at each conversion percentage, and then generate plots and tables of kinetic analysis results (TA Instruments, 2003). **Figure 5.20** depicts the conversion percent curves (until 98% of conversion) at different isotherms (90 - 120 °C) for the LBL 5% and EHR 5%. The chosen isotherms were the same applied on rheological study. **Table 5.10** shows the curing time corresponding at 100% of conversion for different isotherms and the E_a values.

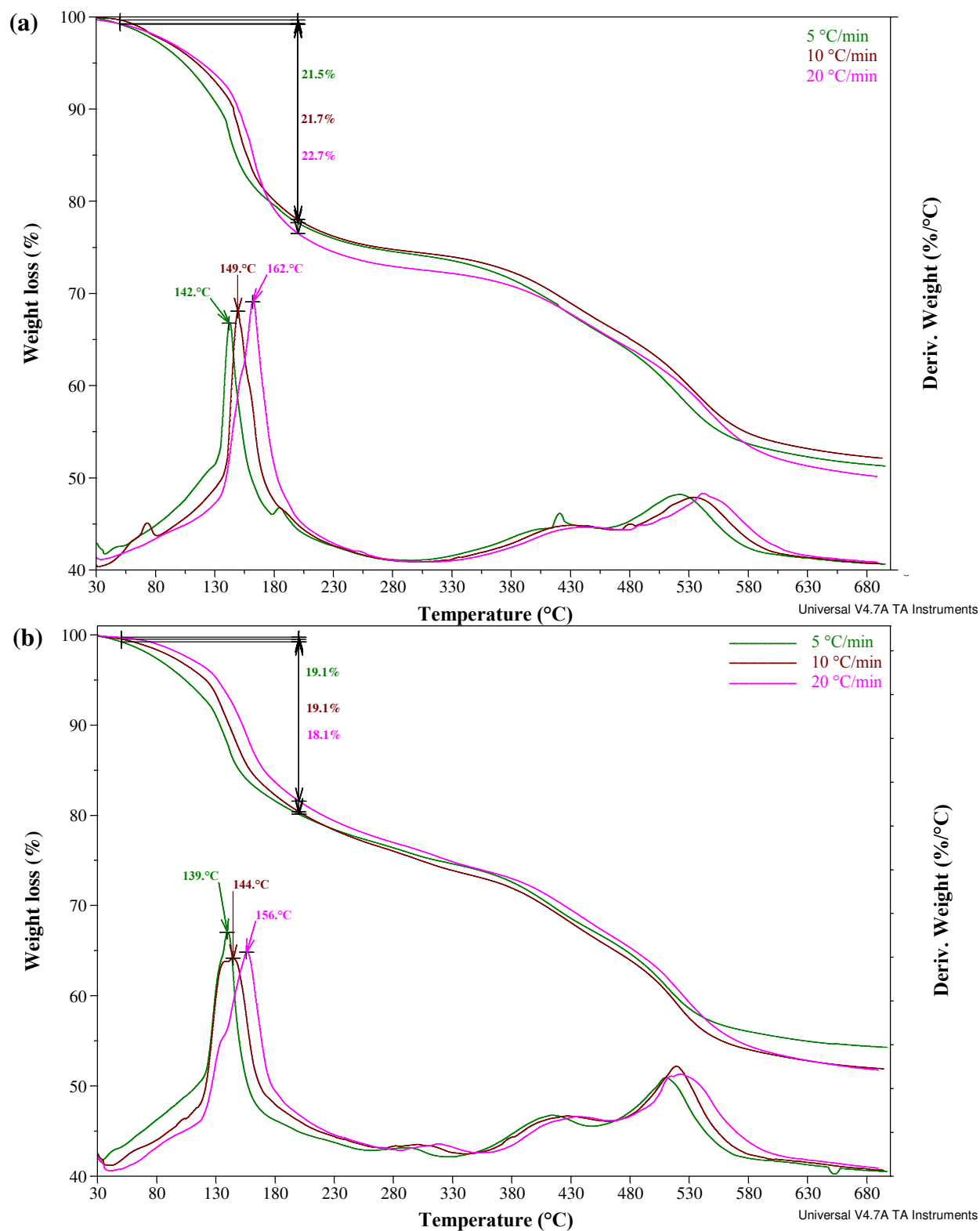


Figure 5.19 - TG and DTG curves at different heating rates of (a) the LBL 5% and (b) EHR 5% resins.

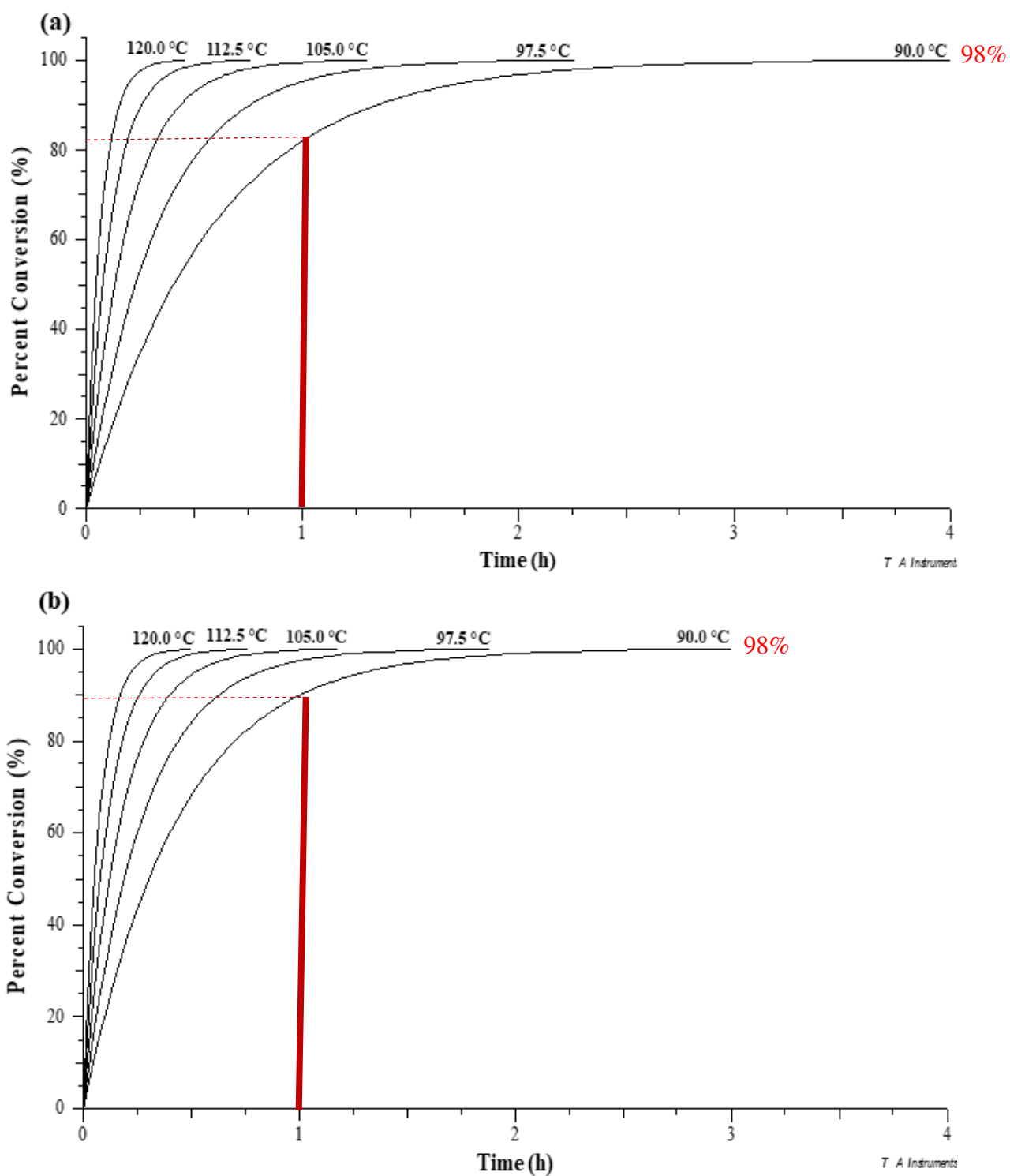


Figure 5.20 - Conversion percent curves for (a) LBL 5% and (b) EHR 5% resins at isotherms from 90 to 120 °C.

Table 5.10 - Curing time for LBL 5% and EHR 5% resins and their E_a values.

	LBL 5%	EHR 5%
	Curing time (min) for 100% conversion	
Isotherms (°C)		
90	348	261
97.5	196	176
105	113	104
112.5	67	67
120	40	45
	E_a (KJ/mol)	
	85.9	70.3

The curves simulated at different temperatures depicted on **Figure 5.20** are interesting to monitor the curing reaction. For example, about 90% of the EHR 5% resin will be cured at 90 °C in 1 h, while the LBL 5% resin (at the same conditions), only about 80% of it will be cured. The curing time values from TG kinetic study (**Table 5.10**) presented the same tendency to the t_{gel} values from rheological study of the EHR 5% and the LBL 5% resins. The curing time values exponentially diminished with temperature increase. In general, EHR 5% resin showed curing time values lower or similar than for LBL 5% resin. EHR 5% resins provided a lower E_a than LBL 5% resin.

Rheological and TG techniques appeared be suitable ways to determine the kinetic parameters of the resins with EHR and LBL. DSC analysis could also be used to assess the curing kinetic of the phenolic resins, however special experimental conditions as high pressure are necessary to suppress the volatilization of the water. The endothermic evaporation of the water by product distorts the exothermic curing, which must be analyzed in its entirety to obtain a valid kinetic model.

5.3 Characterization of the obtained phenolic resins

5.3.1 Solid content, viscosity determination and TG analyses

It was visually observed that the EHR 5% and EHR 15% resins had similar appearances to resins with LBL, appearance of adhesive (before curing), whereas the EHR 30% and EHR 45% had more pasty characteristics, most probably because of the higher amount of cellulose fibers contents. **Table 5.11** gathers solid content and viscosity values for all resins.

Table 5.11 - Solid content, viscosity values (η_0) and TG results.

Samples	^a Solid content - %	^b η_0 - Pa s ⁻¹		TG (weight loss - %)			
		At 25 °C	Until 100 °C	100-200 °C	200-300 °C	300-500 °C	
Standard	86 (1)	1.5 x10 (0.97)	4	19	7	8	
LBL 5%	90 (1)	8.3 x10 (0.90)	2	17	7	10	
LBL 15%	91 (0)	2.6 x10 ² (0.88)	2	17	7	26	
LBL 30%	89 (0)	8.8 x10 (0.99)	3	17	7	16	
LBL 45%	83 (2)	4.1 x10 ³ (0.97)	5	18	8	19	
LBL 60%	90 (0)	1.6 x10 ⁴ (0.99)	2	22	6	24	
EHR 5%	89 (0)	1.1 x10 ² (0.99)	3	16	7	15	
EHR 15%	74 (2)	3.5 x10 ³ (0.99)	13	20	7	18	
EHR 30%	58 (3)	1.7 x10 ⁵ (0.99)	25	27	8	26	
EHR 45%	49 (1)	6.5 x10 ⁶ (0.99)	39	12	8	29	

^aStandard deviation in parenthesis; ^bR value in parenthesis.

The solid contents are inversely proportional to the water and solvent amount leaved after the evaporation process in the rotary evaporator and to the water formation during the curing process inside the oven. The solid contents for the phenolic resins with LBL and EHR are showed on **Table 5.11**. The solids content for the phenolic resins with LBL ranged from 83% to 91% that are close with the solid content of phenolic standard (86%), while the phenolic resins with EHR presented a large decrease from 89% to 49% as higher the EHR amount in phenolic resins. This can be related to the hydrophilic characteristics of cellulose fibers that hindering the solvent/water evaporation in the rotary evaporator. The EHR resins

showed t_{gel} values lower than to the LBL resins. In this way, the EHR seems to benefit the curing process, although the hydrophilic characteristics of cellulose fibers contained it.

Zero-shear rate viscosity of the resins (η_0) at 25 °C increased exponentially as the amount of lignocellulosic material in the resins was increased. The EHR resins had higher viscosity values than those with LBL. This probably indicates that the presence of cellulose fibers influenced on the resins viscosity. All curves of viscosity at low shear rate (0-2 s⁻¹) plotted (η_0 values determination) are showed in **Supplementary Material C**.

The weight loss percent values (**Table 5.11**) were divided on ranges temperature according to main events of the phenolic resins (Lee, 2007; Qiao et al., 2015). Until 100 °C, the weight loss refers, mainly, to the residual water and solvent evaporation. Weight loss values for EHR resins until 100 °C were higher (from 3% to 39%) as the EHR amount was increased on the phenolic resins. TG technique corroborates with the hypothesis of the cellulose fibers from EHR keep within them amounts of water/solvent. The range of 100 - 200 °C refers to evaporation of water formed by resins curing (self-condensation reactions). The range of 200 - 300 °C could be related to a post curing reaction and/or a start of degradation reaction. After 300 °C, weight loss refers to degradation of the phenolic resins and the LBL and EHR, as can be seen in Menezes et al. (2016b). The TG and DTG curves of the phenolic resins with LBL and EHR before a previous curing process in the hydraulic press are gathered in **Supplementary Material D**.

The flow curves (**Figure 5.21**) of shear stress (τ) and viscosity (η) as a function of shear rate ($\dot{\gamma}$) helps to classify a substance according to one of the possible characteristics. **Figure 5.21** presents the viscosity profiles of the phenolic resins at 25 °C. Most of the polymers present behaviour of pseudoplastic, especially for the phenolic resins. Pseudoplastic characteristics in **Figure 5.21** can be observed from the decrease of viscosity (η) with increasing shear rate ($\dot{\gamma}$).

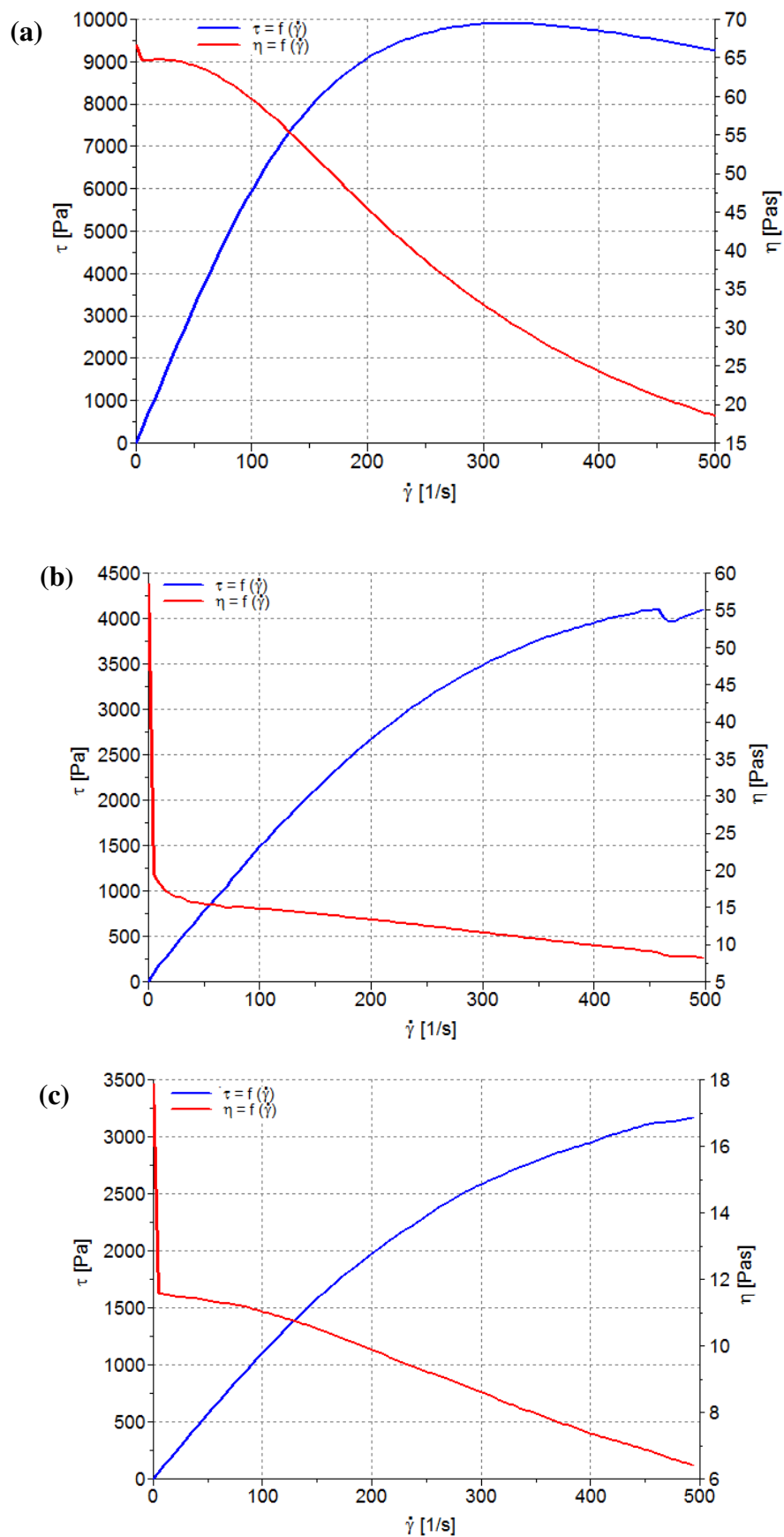


Figure 5.21 - Flow curves of shear stress (τ) and viscosity (η) as a function of shear rate ($\dot{\gamma}$). **(a)** LBL 5% resin, **(b)** EHR 5% resin and **(c)** standard resin.

5.3.2 FTIR spectroscopy

Figure 5.22 depicts the spectra of phenol and formaldehyde reactants that were used in the phenolic resins synthesis, and the spectrum of resole-type phenol-formaldehyde resin obtained as standard. The wavenumber range of interested to synthesis of phenolic resin is between 1750 cm^{-1} and 650 cm^{-1} .

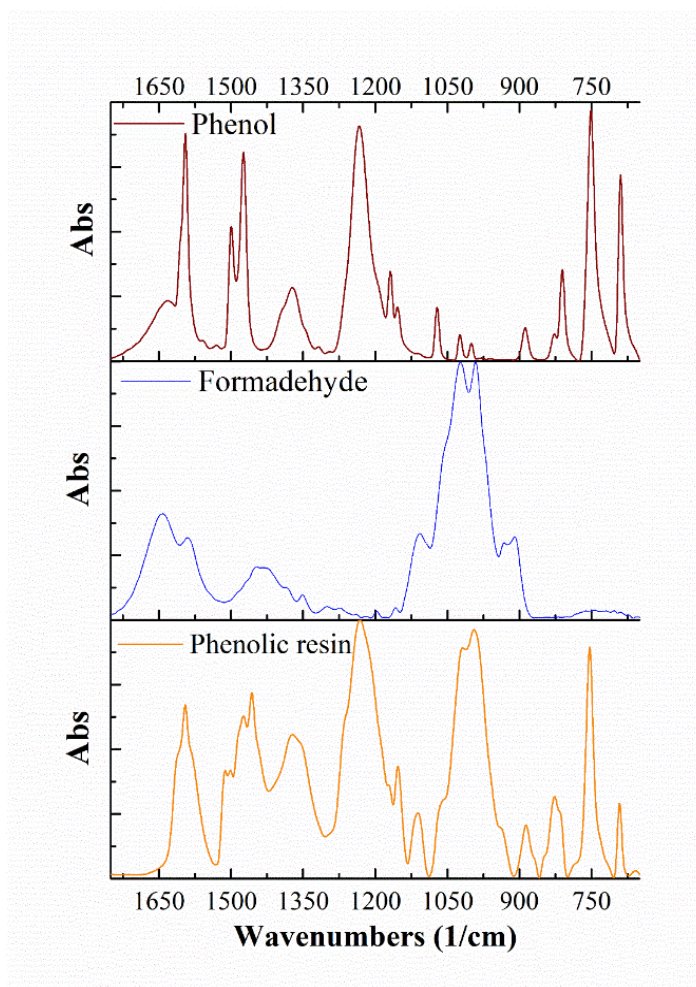


Figure 5.22 - FTIR spectra of the phenol, formaldehyde and Standard phenolic resin.

The characteristic peaks of phenol correspond at wavenumbers of 1596, 1474, 1234, 1168, 1070, 810, 751, 690 cm^{-1} (Poljanšek and Krajnc, 2005). Peaks at 1596 and 1474 cm^{-1} refers to the C=C aromatic ring vibrations. The peaks at 1234 and 1168 cm^{-1} are related to the C-C-O asymmetric stretch and C-H in plane deformations, respectively. The 1070 cm^{-1} correspond to single bond C-O stretching vibrations of -C-OH group. The 810 cm^{-1} peak corresponds to asymmetric stretch of phenolic C-C-OH, and 751 cm^{-1} peak belonged to the C-

H out of plane vibrations. 690 cm^{-1} peak correspond at ring bend (Poljanšek and Krajnc, 2005).

The main characteristic peaks of formaldehyde aqueous solution (methylene glycol) correspond at wavenumbers of 1645 , 1445 , 1107 , 1021 and 994 cm^{-1} . The peak at 1645 cm^{-1} correspond to C=O stretch (overlapped with OH scissors of water). The peak at 1445 cm^{-1} corresponds to C-H band. Peaks at 1107 and 1021 cm^{-1} correspond to C-OH (Poljanšek and Krajnc, 2005).

The observed wavenumbers in phenol-formaldehyde resin spectrum were 1595 and 1512 cm^{-1} correspond to C=C aromatic ring; 1475 cm^{-1} related with C-H aliphatic and =CH₂-deformation; 1456 cm^{-1} corresponding to C=C benzene ring obscured by -CH₂ (methylene bridge); 1373 cm^{-1} correspond to OH in plane; 1232 cm^{-1} correspond to asymmetric stretch of phenolic C-C-OH; 1154 cm^{-1} correspond to C-O stretch; 1112 cm^{-1} correspond to aliphatic hydroxyl; 1020 cm^{-1} correspond to aliphatic hydroxyl; 995 cm^{-1} correspond to C-H from formaldehyde reactant; 888 , 826 and 754 cm^{-1} correspond to CH out-of-plane; 692 cm^{-1} correspond to adjacent 5H.

The resole-type phenolic resins were submitted to FTIR analyses to confirm their reactions. **Figure 5.23 (a)** shows the spectra of the resins before their curing process (adhesives) and **Figure 5.23 (b)** shows the spectra of the resins after their curing process (thermosetting) at the hydraulic press. Comparing the spectrum of the standard resin with the other resins spectra (**Figure 5.23**), it is observed that they are very similar, being a good indication that the reactions of the phenolic resins have occurred.

The main differences between the spectra from **Figure 5.23 (a)** correspond to the following wavenumbers: 1640 , 1595 , 1458 , 1214 , 1111 , 1028 and 812 cm^{-1} . The peaks at 1640 and at 1028 cm^{-1} are more intense in the spectra of the resins with EHR. The assignment at 1640 cm^{-1} can be related to C=O stretch of formaldehyde and OH scissors of water, while the peak at 1028 cm^{-1} can be refers to -C-OH of formaldehyde. This fact could indicate that cellulose fibers from EHR keep within higher amounts of water or formaldehyde. The peak at 1595 cm^{-1} is more intense in standard spectrum than in spectrum of the LBL 60% resin. This peak can be related to C=C aromatic ring of phenol reactant. The intensity of peak at 1458 cm^{-1} is higher for LBL resins than standard resin and is related with C-H deformation. At 1214 cm^{-1} , a peak appears on, mainly, spectra of the LBL 45% and 60% resins. These peaks are related with the S ring + G ring condensed. A peak at 1111 cm^{-1} increased as LBL amount in the phenolic resins was increased. This peak refers to aromatic C-H inplane deformation

(typical for S units). The peak at 812 cm^{-1} , mainly observed on standard resin spectrum, refers to asymmetric stretch of phenolic C-C-OH.

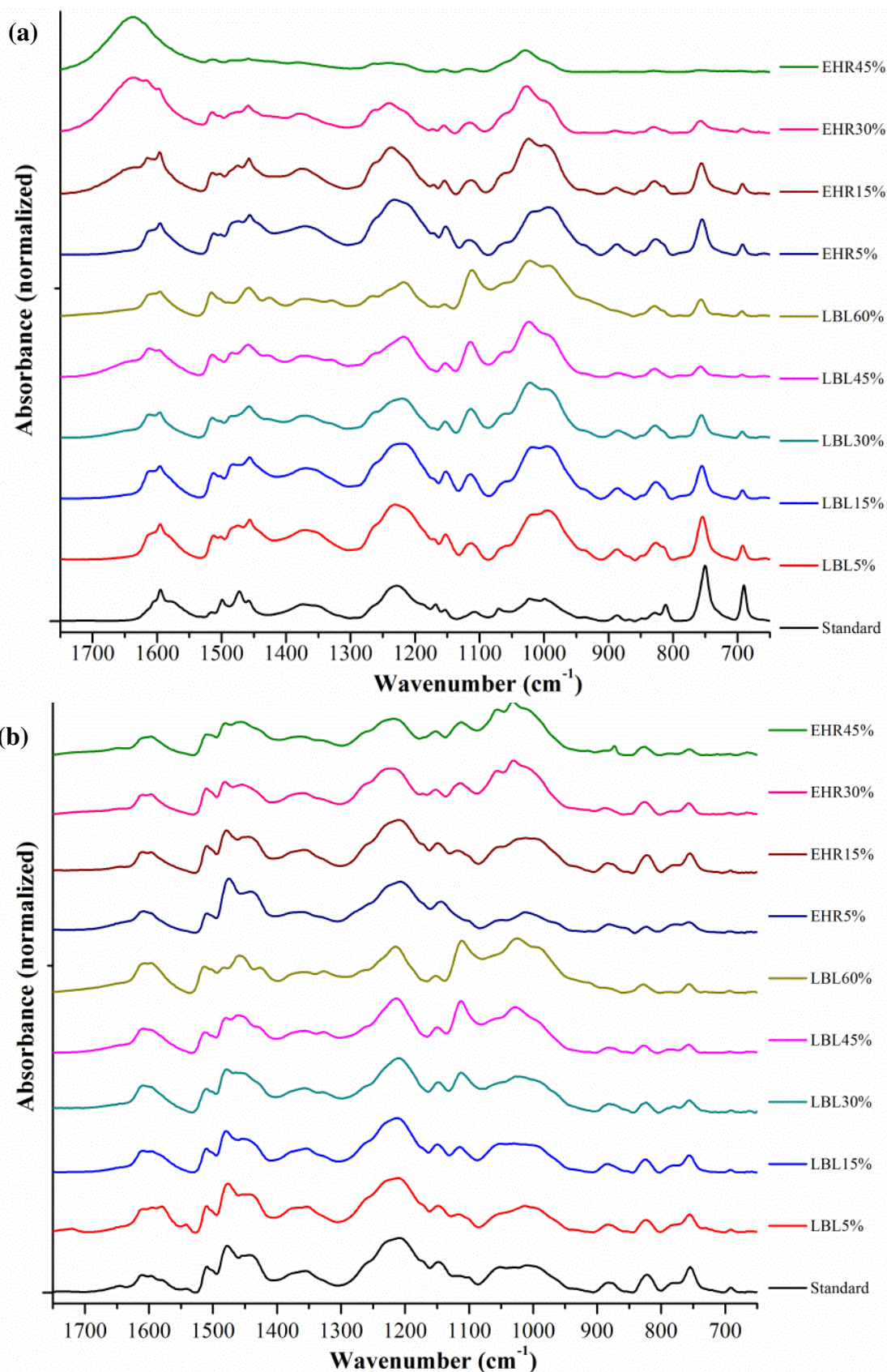


Figure 5.23 - FTIR spectra of (a) phenolic resins before curing reaction; and of (b) phenolic resins after curing reaction.

Figure 5.23 (b) depicts spectra of the thermosetting resins with LBL and EHR. The main differences noted in these spectra are in regions at 1032, 1212 and 1110 cm^{-1} . Peak at 1032 cm^{-1} is more intense in EHR 45% spectrum that refers at aromatic C–H inplane deformation (G>S) and C–O deformation in primary alcohols.

5.3.3 2D NMR spectroscopy (HSQC)

HSQC contour maps of the standard and the LBL 30% resins are displayed in **Figure 5.24**, where their main regions (aliphatic, sidechain and aromatic) are expanded. In the aliphatic region (**Figure 5.24** a and b), the signals from 3.5 to 3.9 ppm (^1H) and from 29 to 41 ppm (^{13}C) is related to methylene bridges formed between the aromatic units in the condensation reaction with formaldehyde. **Figure 5.25** shows the structures of the diarylmethanes where it is possible observe the *ortho-ortho*, *ortho-para* and *para-para* methylene bridges. In the HSQC spectrum of the LBL 30% resin, it is observed the presence of the three-different methylene bridge, while in the standard resin spectrum, it is observed only the *ortho-para* and *para-para* methylene bridges. Yelle and Ralph (2016) also noted the presence of *ortho-ortho* methylene bridge in phenolic resin with wood lignin, while in resin without lignin, it was not observed. The presence of *ortho-ortho* methylene bridge in LBL 30% resin could indicate that lignin free positions (*ortho*) were substituted.

Figure 5.24 (c) and (d) show the sidechain (oxygenated aliphatic) region of the HSQC spectra. The signal at 3.7/57 ppm ($^1\text{H}/^{13}\text{C}$) can be observed in the LBL 30% resin. This signal is typical of methoxyl group and an indication of the presence of lignin. In the both HSQC spectra, *p*-methylol and *o*-methylol were found at 4.4-4.6 ppm (^1H) and 55-60 ppm (^{13}C) region. Methylols are short fractions formed at the reaction beginning, not yet crosslinked as in the thermosetting resin.

In the aromatic region, it is possible visualize the main ^1H - ^{13}C present in the phenol ring inside the phenolic resin structure. In **Figure 5.24** (e), the main linkages were attributed. In the LBL 30% resin, it was also present the syringyl unit once this unit does not participate in the phenolic resin obtainment.

In general, both the standard and the LBL 30% showed HSQC spectrum very similar. Their main differences were the presence in the LBL 30% resin of *o-o* methylene bridge (aliphatic region), of methoxyl group (sidechain region) and of syringyl unit (aromatic

region). It is suggested that both the standard and the LBL 30% resins were again submitted to HSQC NMR analyses after their curing step in order to visualize the substitution in lignin C5 positions, free *ortho* positions, at 6.6/121 ppm (Yelle and Ralph, 2016), indicating that if lignin participate in the phenolic resin reaction. However, a previous milling process would require, as performed by Yelle and Ralph (2016) to analyze thermosetting resins.

It has been experimentally noted that the lignin structure is much more difficult to define its signals in the HSQC spectrum than the standard phenolic resin. A way to mitigate this problem, for example, it would be to couple a triple resonance NMR 'inverse' probe (TCI) that is equipped with cold preamplifiers for ^1H and ^{13}C . TCI design guarantees the highest sensitivity for the lock channel, resulting in excellent stability of the spectrometer (Bruker, 2018). TCI probe is widely applied to NMR structure determination of biological macromolecules and lignin (del Río et al., 2015, 2012; Rencoret et al., 2011; Yelle and Ralph, 2016).

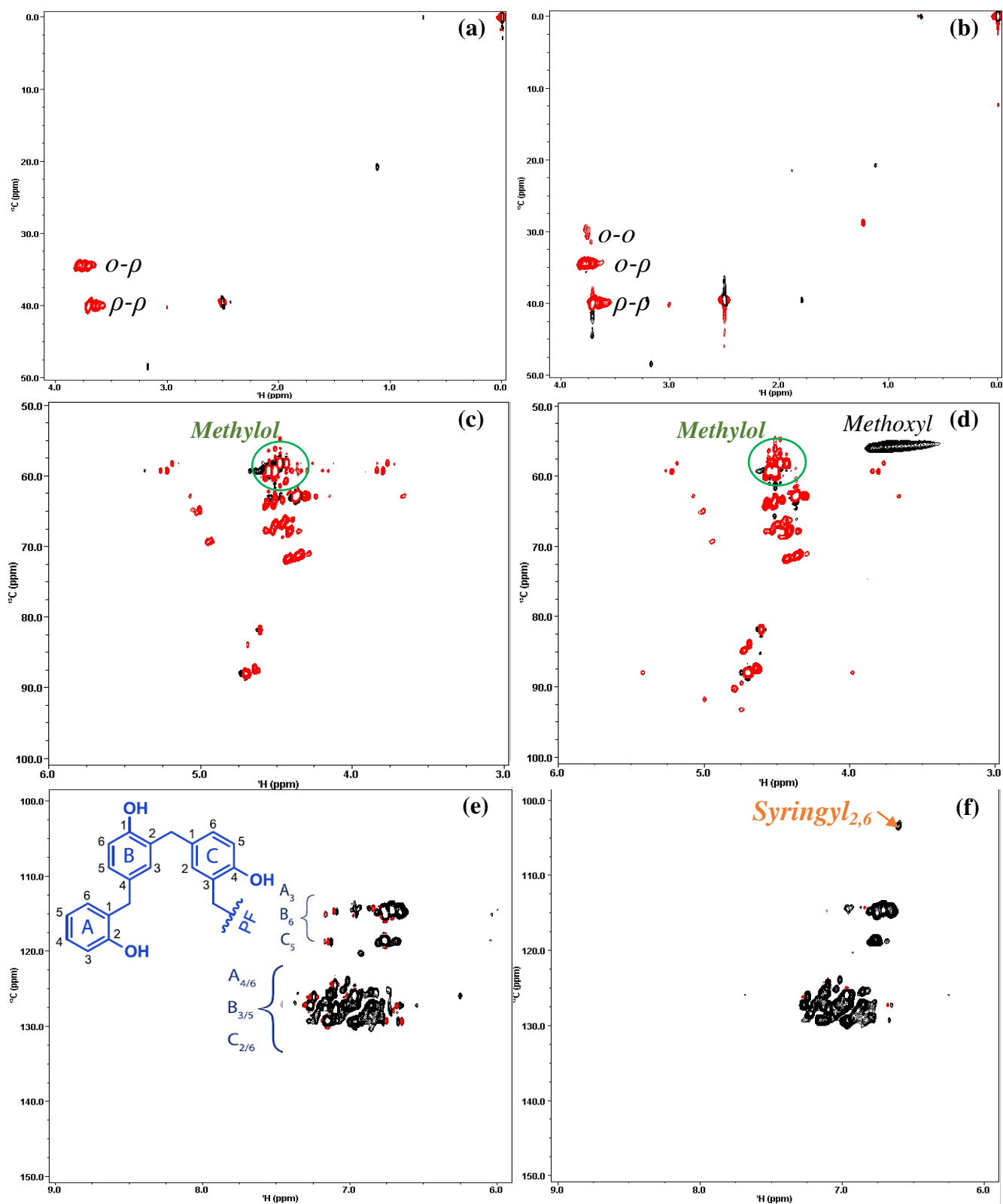


Figure 5.24 - 2D HSQC NMR spectra of the standard and the LBL 30% resins.

Aliphatic region (a) for standard resin and (b) for LBL 30% resin; Oxygenated aliphatic region for (c) for standard resin and (d) for LBL 30% resin; Aromatic region (e) for standard resin and (f) for LBL 30% resin.

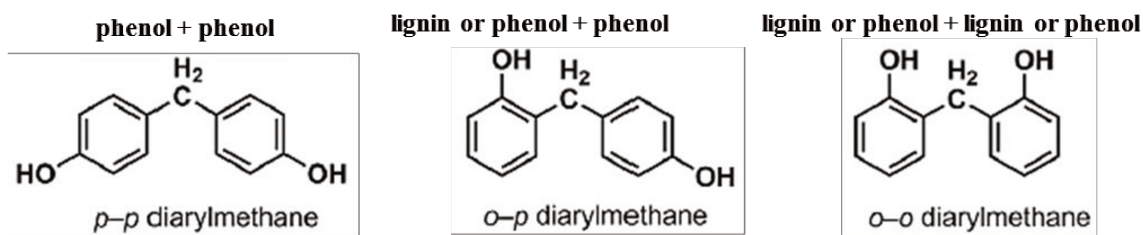


Figure 5.25 - Diarylmethane structures (methylene bridges).

5.3.4 Differential Scanning Calorimetry (DSC)

DSC heat flow curves of the standard, LBL 5%, EHR 5%, LBL 60% and EHR 45% resins before a previous curing process in the hydraulic press are depicted in **Figure 5.26**. The curing process of phenolic resins at dynamic heating rate generally occurs between 100 °C and 200 °C (Alonso et al., 2004). The curing reaction (auto condensation), which forms water, is an exothermic reaction (up direction), while the water evaporation is an endothermic reaction (down direction). As the water formation from curing process occurs above 100 °C, the evaporation of this water occurs almost simultaneously, thus, it is not possible to separate the exothermic and endothermic peaks. It would be possible to delay evaporation of this water if a DSC at high pressure was used.

It can be observed in the DSC heat flow curves (**Figure 5.26**) that the standard, the LBL 5% and the EHR 5% resins presented similar profiles, as well as their solid contents, 86-90% (**Table 5.11**). The exothermic peaks (water formation from curing process) were predominant in DSC curves of the standard, the LBL 5% and the EHR 5% resins. On the other hand, the endothermic peaks (water evaporation) were predominant in DSC heat flow curves of EHR 45% and LBL 60% resins.

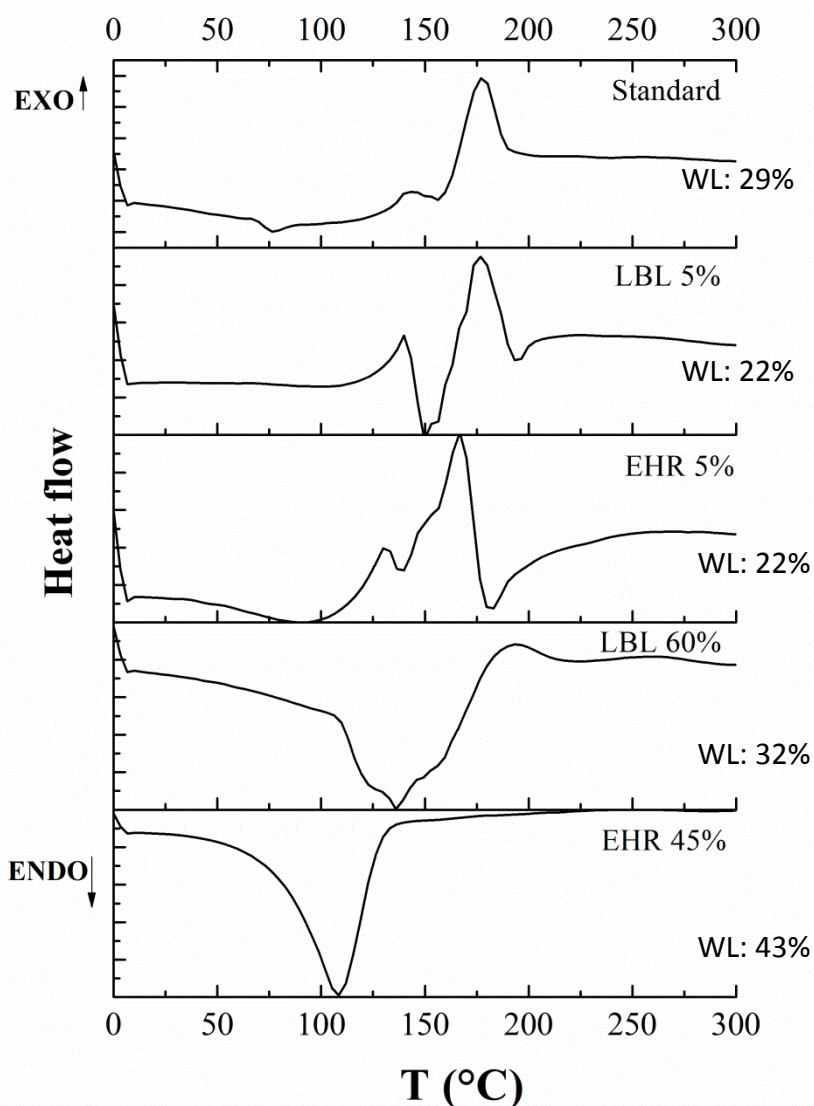


Figure 5.26 - DSC of the phenolic resins without any previous curing process.

*WL: total weight loss (until 300 °C).

In DSC heat flow curve of the EHR 45%, the mainly peak (endothermic) is close to 100 °C, indicating that the evaporation should be of the residual water contained in the cellulose fibers. As previously mentioned, EHR 45% resin presented the lowest solids content and a considerable amount of water, probably, from the cellulose fibers. In relation to the LBL 60% resin, it was possible to observe that the curing process of this resin was the most time consuming among all (see rheological study). Therefore, it was more difficult to observe in DSC heat flow of the LBL 60% resin, the exothermic peak referring to curing of this resin.

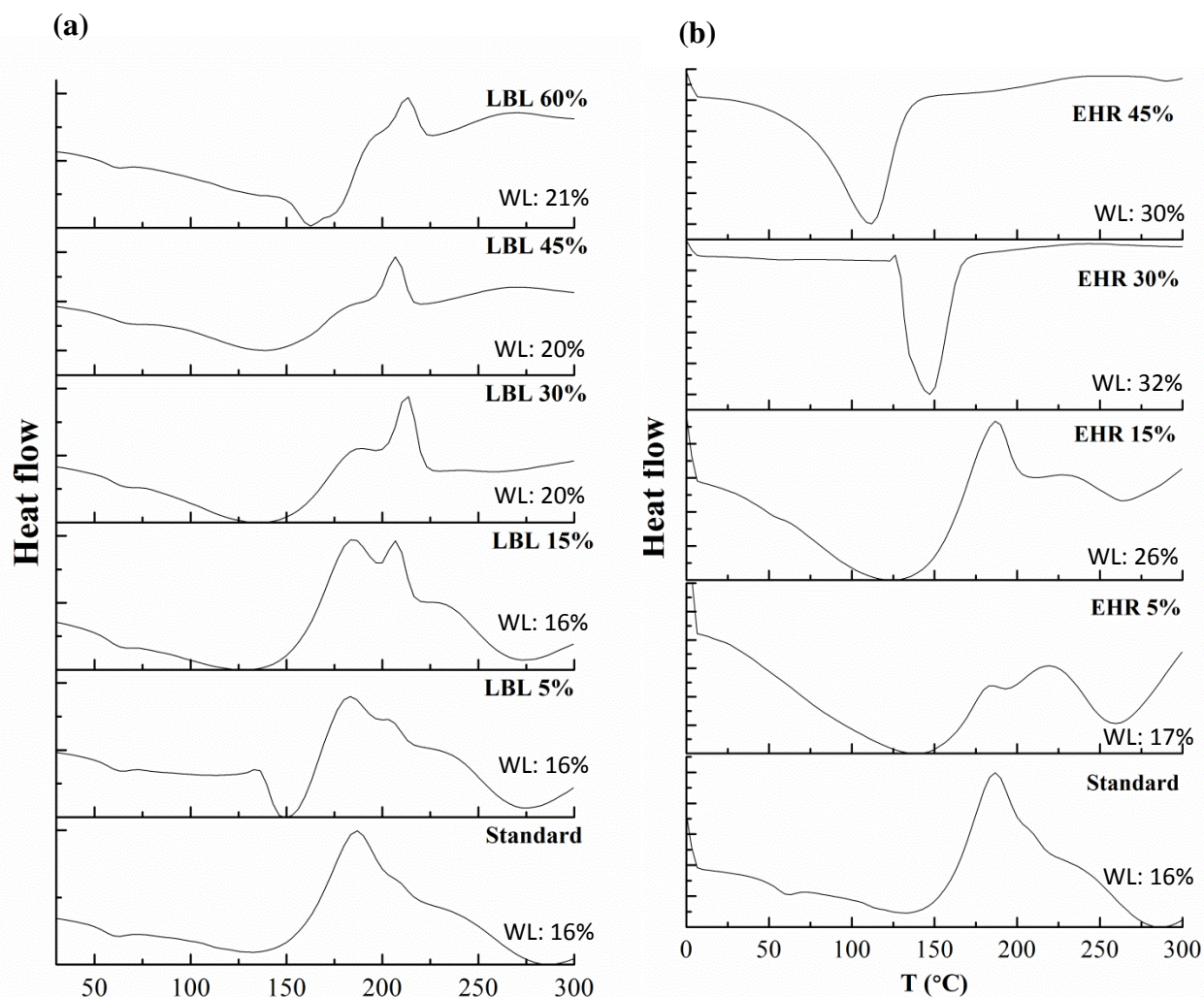


Figure 5.27 - DSC of the thermosetting phenolic resins. (a) Thermosetting resins with LBL; (b) Thermosetting resins with EHR. WL: Total weight loss (until 300 °C).

DSC heat flow curves of the phenolic resins after the curing process in the hydraulic press are depicted in **Figure 5.27**. The initial objective to perform DSC analysis of the thermosetting phenolic resins was to determine their glass transition temperature (T_g). However, it was difficult to determine T_g values for all thermosetting resins. Thus, in **Figure 5.27**, what worth highlighting is that almost all resins presented exothermic peaks (water formation), it may indicate cure reactions even for the thermosetting resins. These events are called as post-cure reaction (Qiao et al., 2015).

5.3.5 Dynamic Mechanical Thermal Analysis (DMTA)

Table 5.12 shows the G' modulus at 35 °C and at 300 °C and the maximum G'' modulus. G' and G'' modulus curves of the resins with LBL and EHR are depicted in **Figure 5.28**.

Table 5.12 - DMTA data for the phenolic resins.

	$G'_{35\text{ °C}}$ (MPa)	$G'_{300\text{ °C}}$ (MPa)	G''_{max} (MPa)
Standard	77 (13)	47 (14)	11 (1)
LBL 5%	159 (24)	96 (4)	13 (2)
LBL 15%	113 (0)	43 (9)	10 (0)
LBL 30%	107 (3)	39 (9)	9 (2)
LBL 45%	140 (1)	79 (24)	13 (1)
EHR 5%	192 (2)	63 (6)	8 (0)
EHR 15%	108 (12)	16 (4)	7 (1)
EHR 30%	125 (9)	21 (2)	12 (1)
EHR 45%	84 (8)	1 (0)	7 (1)

Standard deviation (in parentheses)

For thermosetting resins, G' modulus values can be directly related with their curing degree (Paiva and Frollini, 2001). Phenolic resins with LBL showed G' modulus between (107-159 MPa), while for resins with EHR ranged from 84 to 192 MPa. All phenolic resins exhibited higher G' modulus than the standard resin (77 MPa), indicating that an improvement on curing degree when lignin (LBL or EHR) was inserted on phenolic resins. The EHR 5% resin showed higher G' modulus (about 20% higher) than the LBL 5% resin. This fact indicates that the cellulosic fibers even at lower amount enhance this mechanical property.

A decrease in G' modulus occurred as the temperature increased. Temperature has larger influence on G' modulus for EHR resins than for LBL resins, since the cellulose fibers may begin to degrade from 200 °C (Menezes et al., 2016b; Yang et al., 2007).

G'' modules of the phenolic resins with LBL/EHR ranged of 7 - 13 MPa, while of the Standard resin was 11 MPa. G'' modulus is related to the mobility of the polymer chains in the resin. The higher is the curing degree, the lower is G'' modulus.

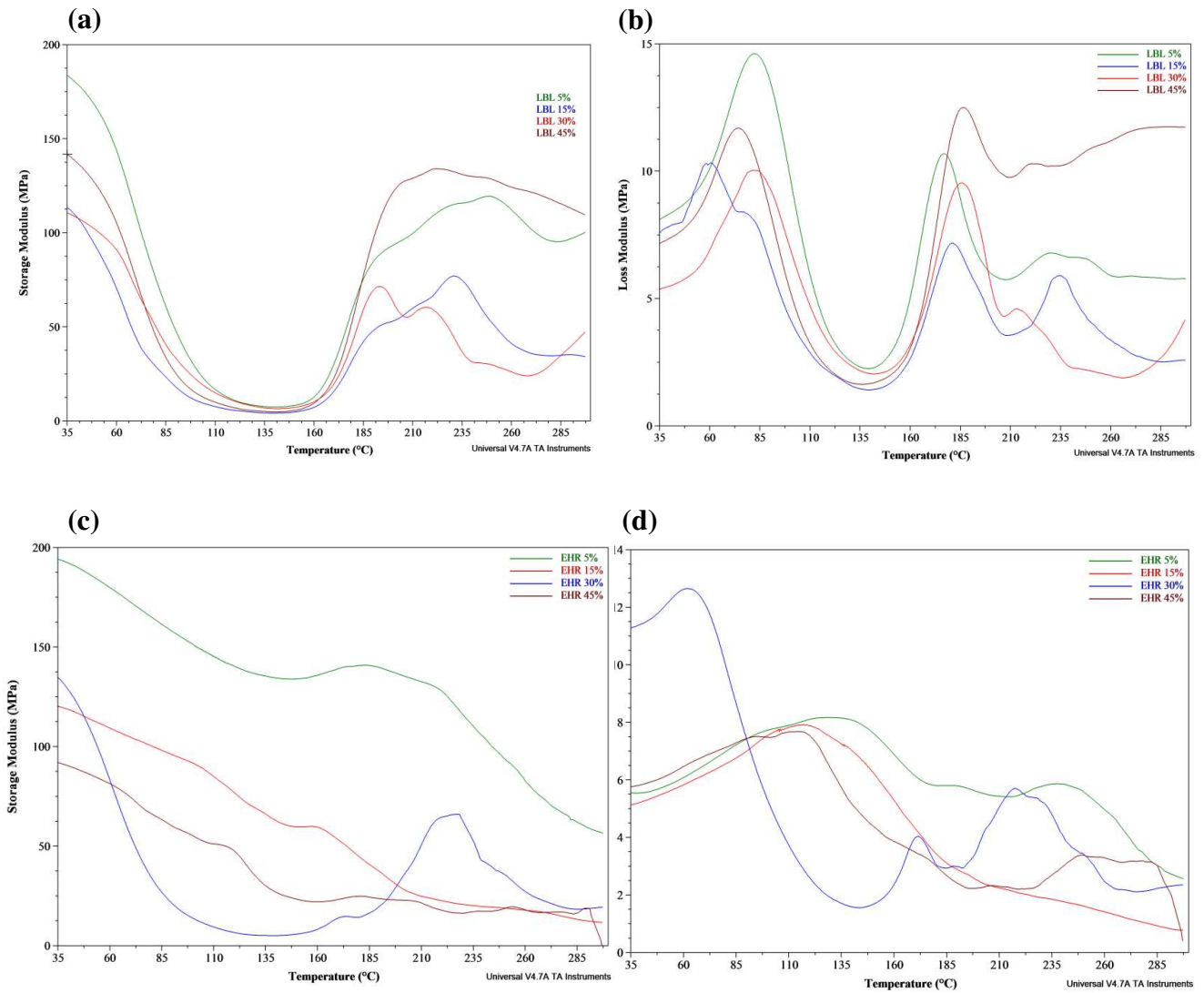


Figure 5.28 - G' and G'' curves of the phenolic resins.

G' modulus curves of the phenolic resins with (a) LBL and (c) EHR. G'' modulus curves of the phenolic resins with (b) LBL and (d) EHR.

Tan delta curves of the resins with LBL and EHR are depicted in **Figure 5.29**. The DMTA curves for the standard resin are depicted in **Supplementary Material E**.

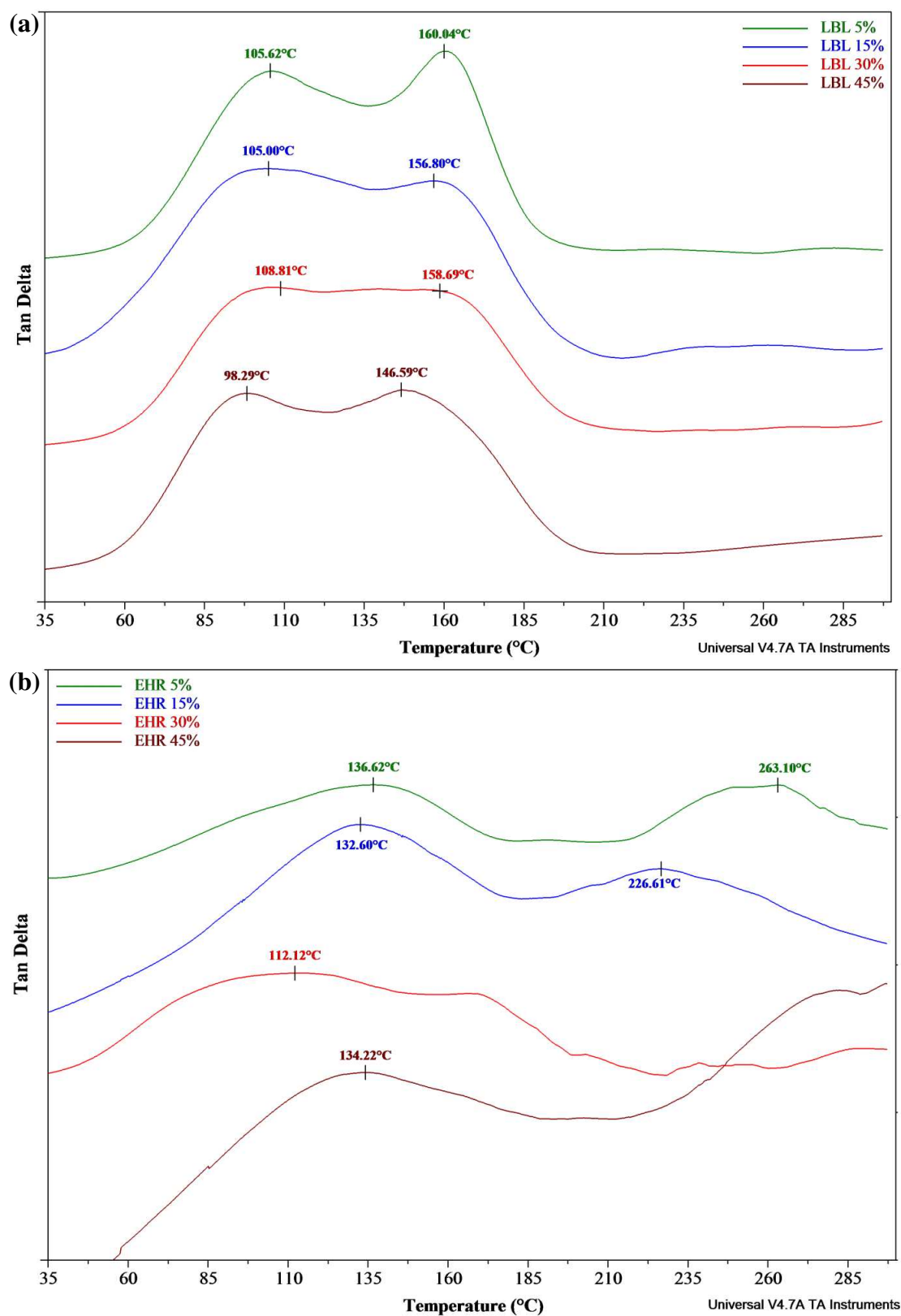


Figure 5.29 - Tan delta curves of the phenolic resins with (a) LBL and (b) EHR.

It was not possible to obtain appropriate samples of thermosetting LBL 60% resin for DMTA analysis. The samples of LBL 60% broke when they were adjusted in the DMTA equipment. A certain fragility in the thermosetting LBL 60% resin was observed. In addition, the LBL 60% needs a much longer curing time than the other resins. Addition of a catalyst as curing agent and/or a reinforcement additive to obtain phenolic thermosetting with more 45% of LBL is suggested.

Chapter 6 CONCLUSIONS AND FUTURE WORK

Enzymatic Hydrolysis Residue (EHR) of the sugarcane bagasse and a LignoBoost Kraft Lignin (LBL) from Eucalyptus were used for the synthesis of the phenolic resins. The EHR and LBL and their phenolic resins were submitted to a full physicochemical and thermomechanical characterization.

The EHR generated in the pilot scale plant is a material mainly composed of lignin (47% w/w) and well dispersed cellulose fibers (40% w/w). The EHR has proven to be more promising for producing phenolic resins than the LBL, since it has a smaller content of the methoxyl group (19%) and showed higher amounts of H-lignin units (22%) than in the LBL (3%). Thermal analysis permitted to observe that the EHR and the LBL are both thermally suitable to be applied in phenolic resin formulations. In this investigation, important characteristics of the EHR and LBL were observed, so that, in the future these 'raw materials' can be applied as feedstock for value-added products.

Phenolic resins using LBL (5 - 60% w/w) and using EHR (5 - 45% w/w) were obtained and compared with the standard resin (without lignin). It was visually observed that the EHR 5% and EHR 15% resins had similar appearances to resins with LBL, appearance of adhesive (before curing), whereas the EHR 30% and EHR 45% had more pasty characteristics, most probably because of the higher amount of cellulose fibers contained in them.

The produced resins were submitted to a complete kinetic study to obtain the curing parameters and to physicochemical and thermomechanical characterization. In general, the EHR or LBL insertion on phenolic resins led to decrease on gel time values, with exception the LBL 60% resin. Phenolic resins with EHR require lower gel time (t_{gel}) and activation energy (E_a) values than phenolic resins with LBL. The curing time values of the EHR 5% and LBL 5% resins from thermal kinetic TG analysis presented the same tendency of rheological study. Rheological study and thermal kinetic TG analysis appeared be suitable to determine the kinetic parameters of the phenolic resins with EHR and LBL.

The solids content and the weight loss values (until before 100 °C) showed that the phenolic resins with EHR exhibited more amounts of water and formaldehyde than usual, which can be due to hydrophilicity of cellulose fibers. Conversely, the rheological study indicated that EHR reduces the gel time of the resins. All phenolic resins with EHR or LBL exhibited higher storage modulus (G') than the standard phenolic resin (77 MPa), indicating

an improvement on curing degree. Phenolic resins with LBL showed G' modulus between (107-159 MPa), while for resins with EHR ranged from 84 to 192 MPa. The EHR 5% resin showed higher G' modulus (about 20% greater) than the LBL 5% resin. This fact indicates that the cellulosic fibers even at lower amount enhance this mechanical property.

Based on this research, it is suggested that thermosetting phenolic resins be formulated with less than 30% of EHR, since above this amount, the high fiber content no longer acts as reinforcement to the phenolic resin matrix. It is also suggested that phenolic resins with more than 45% of LBL be directed to use them as adhesives (before the curing process) and not, as thermosetting, because a certain fragility in the thermosetting LBL 60% resin was observed, beyond its long curing time. Bearing this in mind, the EHR and the LBL can be used to partially replace based-petroleum phenol in phenolic resins production, in general, with appropriate characteristics than the standard resin.

Some suggestions for future work are in following. With respect to characterization of the LBL/EHR, it is suggested to perform Py-GC/MS analysis of the EHR with tetramethylammonium hydroxide (TMAH) addition in order to determine the PCA and FA amounts, once these units can react with formaldehyde; and, to perform SAXS analysis of the LBL to analyze its shape, dimension and size distribution. With respect to determination of curing parameters of phenolic resins, it is suggested to apply the TG kinetics analysis for the remained resins. With regarding to characterization of the phenolic resins, to perform impact tests in order to assess impact resistance of the phenolic resins; and, to submit the phenolic resins (before curing step) to adhesion tests. This test would confirm the potential of the LBL 60% resins on use as adhesive. It is suggested to synthesize and characterize phenolic resins by partially replacing petroleum-based phenol with a mix of the EHR and alkaline EHR. For example, EHR (5-15%) and more alkaline EHR (30%), totaling a substitution of 45% w/w.

REFERENCES

- Alonso, D.M., Wettstein, S.G., Dumesic, J.A., 2012. Bimetallic catalysts for upgrading of biomass to fuels and chemicals. *Chemical Society Reviews* 41, 8075–8098. <https://doi.org/10.1039/C2CS35188A>
- Alonso, M. V, Oliet, M., García, J., Rodríguez, F., Echeverría, J., 2006. Gelation and isoconversional kinetic analysis of lignin-phenol-formaldehyde resol resins cure. *Chemical Engineering Journal* 122, 159–166. <https://doi.org/10.1016/j.cej.2006.06.008>
- Alonso, M. V, Oliet, M., Pérez, J.M., Rodríguez, F., Echeverría, J., 2004. Determination of curing kinetic parameters of lignin-phenol-formaldehyde resol resins by several dynamic differential scanning calorimetry methods. *Thermochimica Acta* 419, 161–167. <https://doi.org/10.1016/j.tca.2004.02.004>
- American Chemical Society National, n.d. Historic Chemical Landmarks. Bakelite: The World's First Synthetic Plastic. [WWW Document]. URL <http://www.acs.org/content/acs/en/education/whatischemistry/landmarks/bakelite.html>
- Balagurumurthy, B., Singh, R., Ohri, P., Prakash, A., 2015. Thermochemical Biorefinery, in: *Recent Advances in Thermo-Chemical Conversion of Biomass*. Elsevier, Boston, pp. 157–174. <https://doi.org/10.1016/B978-0-444-63289-0.00006-5>
- Balakshin, M., Capanema, E., 2015. On the Quantification of Lignin Hydroxyl Groups With ³¹P and ¹³C NMR Spectroscopy. *Journal of Wood Chemistry and Technology* 35, 220–237. <https://doi.org/10.1080/02773813.2014.928328>
- Benali, M., Périn-Levasseur, Z., Savulescu, L., Kouisni, L., Jemaa, N., Kudra, T., Paleologou, M., 2014. Implementation of lignin-based biorefinery into a Canadian softwood kraft pulp mill: Optimal resources integration and economic viability assessment. *Biomass and Bioenergy* 7, 2–11. <https://doi.org/10.1016/j.biombioe.2013.08.022>
- Betts, W.B., Dart, R.K., Ball, A.S., Pedlar, S.L., 1991. Biosynthesis and structure of lignocellulose, in: Betts, W.B. (Ed.), *Biodegradation: Natural and Synthetic Materials*. Springer-Verlag London, pp. 139–155.
- Bezerra, L.T., Ragauskas, A.J., 2016. A review of sugarcane bagasse for second-generation bioethanol and biopower production. *Biofuels, bioproducts & biorefining* 10, 634–647.
- Brandt, A.R., Unnasch, S., 2010. Energy Intensity and Greenhouse Gas Emissions from Thermal Enhanced Oil Recovery. *Energy Fuels* 24, 4581–4589. <https://doi.org/10.1021/ef100410f>
- Brazilian Tree Industry (Ibá), 2017. Statistics of Brazilian Tree Industry. *Cenários Ibá* December, 1–7.
- Brenelli, L.B., Mandelli, F., Mercadante, A.Z., Rocha, G.J. de M., Rocco, S.A., Craievich,

- A.F., Gonçalves, A.R., Centeno, D. da C., de Oliveira Neto, M., Squina, F.M., 2016. Acidification treatment of lignin from sugarcane bagasse results in fractions of reduced polydispersity and high free-radical scavenging capacity. *Industrial Crops and Products* 83, 94–103. <https://doi.org/10.1016/j.indcrop.2015.12.013>
- Bröckel, U., Meier, W., Wagner, G. (Eds.), 2013. Basics of Rheology, in: *Product Design and Engineering: Formulation of Gels and Pastes*. John Wiley & Sons, p. 11.
- Bykov, I., 2008. Characterization of Natural and Technical Lignins using FTIR Spectroscopy. *Construction* 43.
- Calvo-Flores, F.G., Dobado, J.A., 2010. Lignin as Renewable Raw Material. *ChemSusChem* 3, 1227–1235. <https://doi.org/10.1002/cssc.201000157>
- Calvo-Flores, F.G., Dobado, J.A., Isac-García, J., Martín-Martínez, F.J., 2015. *Lignin and Lignans as Renewable Raw Materials: Chemistry, Technology and Applications*. Wiley.
- Campos, A.R., 2014. Deslignificación enzimática de materiales lignocelulósicos de interés industrial. Universidad de Sevilla.
- Cardona, C.A., Quintero, J.A., Paz, I.C., 2010. Production of bioethanol from sugarcane bagasse: Status and perspectives. *Bioresource Technology* 101, 4754–4766. <https://doi.org/10.1016/j.biortech.2009.10.097>
- Carvalho, M. da G.V.S., 1999. Efeito das variáveis de cozimento nas características químicas de pasta Kraft de *Eucalyptus globulus*. Universidade de Coimbra.
- Çetin, N.S., Özmen, N., 2002. Use of organosolv lignin in phenol-formaldehyde resins for particleboard production I. Organosolv lignin modified resins. *International Journal of Adhesion & Adhesives* 22, 477–480.
- Chemicals, G.-P., 2017. Phenolic/Phenol-Formaldehyde (PF) - Resole [WWW Document]. Products. URL http://www.gp-chemicals.com/Phenol-Formaldehyde_Resole_Product_Category (accessed 2.13.17).
- Chen, C.-L., Robert, D., 1988. ^1H and ^{13}C NMR spectroscopy of lignin, in: Wood, W.A., Kellogg, T.S. (Eds.), *Methods in Enzymology*. pp. 154–155.
- Chen, H., 2014. Biotechnology of lignocellulose: Theory and practice, *Biotechnology of Lignocellulose: Theory and Practice*. <https://doi.org/10.1007/978-94-007-6898-7>
- Chung, H., Washburn, N.R., 2012. Chemistry of lignin-based materials. *Green Materials* 1, 137–160. <https://doi.org/10.1680/gmat.12.00009>
- Constant, S., Wienk, H.L.J., Frissen, A.E., Peinder, P. de, Boelens, R., van Es, D.S., Grisel, R.J.H., Weckhuysen, B.M., Huijgen, W.J.J., Gosselink, R.J.A., Bruijninx, P.C.A., 2016. New insights into the structure and composition of technical lignins: a comparative characterisation study. *Green Chem.* 18, 2651–2665. <https://doi.org/10.1039/C5GC03043A>

- Costa, C.N., Teixeira, V.G., Delpech, M.C., Souza, J.V.S., Costa, M.A.S., 2015. Viscometric study of chitosan solutions in acetic acid/sodium acetate and acetic acid/sodium chloride. *Carbohydrate Polymers* 133, 245–250. <https://doi.org/10.1016/j.carbpol.2015.06.094>
- del Río, J.C., Gutiérrez, A., Rodríguez, I.M., Ibarra, D., Martínez, Á.T., 2007. Composition of non-woody plant lignins and cinnamic acids by Py-GC/MS, Py/TMAH and FT-IR. *Journal of Analytical and Applied Pyrolysis* 79, 39–46. <https://doi.org/10.1016/j.jaap.2006.09.003>
- del Río, J.C., Lino, A.G., Colodette, J.L., Lima, C.F., Gutiérrez, A., Martínez, Á.T., Lu, F., Ralph, J., Rencoret, J., 2015. Differences in the chemical structure of the lignins from sugarcane bagasse and straw. *Biomass and Bioenergy* 81, 322–338. <https://doi.org/10.1016/j.biombioe.2015.07.006>
- del Río, J.C., Rencoret, J., Prinsen, P., Martínez, Á.T., Ralph, J., Gutiérrez, A., 2012. Structural characterization of wheat straw lignin as revealed by analytical pyrolysis, 2D-NMR, and reductive cleavage methods. *Journal of Agricultural and Food Chemistry* 60, 5922–5935. <https://doi.org/10.1021/jf301002n>
- Delpech, M.C., Coutinho, F.M.B., Sousa, K.G.M., Cruz, R.C., 2007. Estudo viscosimétrico de prepolímeros uretânicos. *Polímeros* 17, 294–298. <https://doi.org/10.1590/S0104-14282007000400008>
- Demirbas, A., 2010. *Biorefineries: For Biomass Upgrading Facilities*, 1st ed. Springer-Verlag London. <https://doi.org/10.1007/978-1-84882-721-9>
- Demirbas, A., 2004. Combustion characteristics of different biomass fuels. *Progress in Energy and Combustion Science* 30, 219–230. <https://doi.org/10.1016/j.pecs.2003.10.004>
- Demirbaş, A., 2005. Estimating of Structural Composition of Wood and Non-Wood Biomass Samples. *Energy Sources* 27, 761–767. <https://doi.org/10.1080/00908310490450971>
- Demirbas, A., Gullu, D., Çağlar, A., Akdeniz, F., 1997. Estimation of Calorific Values of Fuels from Lignocellulosics. *Energy Sources* 19, 765–770. <https://doi.org/10.1080/00908319708908888>
- Dias, L.M.S., 2014. *Síntese e caracterização de adesivos de lignina kraft de eucalipto*. Universidade Federal de Lavras (UFLA).
- Dong, D., Fricke, A., 1995. Intrinsic viscosity and the molecular weight of kraft lignin. *Polymer* 36, 2075–2078. [https://doi.org/10.1016/0032-3861\(95\)91455-G](https://doi.org/10.1016/0032-3861(95)91455-G)
- Driemeier, C., Oliveira, M.M., Mendes, F.M., Gómez, E.O., 2011. Characterization of sugarcane bagasse powders. *Powder Technology* 214, 111–116. <https://doi.org/10.1016/j.powtec.2011.07.043>
- Ehrman, T., 1996. LAP 004 - Determination of Acid-Soluble Lignin in Biomass. National Renewable Energy Laboratory (NREL).

- Fengel, D., Wegener, G., 1989. *Wood Chemistry, Ultrastructure, Reactions*. Walter de Gruyter, Berlin.
- Fernando, S., Adhikari, S., Chandrapal, C., Murali, N., 2006. Biorefineries: Current Status, Challenges, and Future Direction. *Energy Fuels* 20, 1727–1737. <https://doi.org/10.1021/ef060097w>
- Freeman, B.C., Beattie, G.A., 2008. An Overview of Plant Defenses against Pathogens and Herbivores. *The Plant Health Instructor* 1–8. <https://doi.org/10.1094/PHI-I-2008-0226-01>
- Fukushima, R.S., Hatfield, R.D., 2001. Extraction and isolation of lignin for utilization as a standard to determine lignin concentration using the acetyl bromide spectrophotometric method. *Journal of Agricultural and Food Chemistry* 49, 3133–3139. <https://doi.org/10.1021/jf010449r>
- Galbe, M., Zacchi, G., 2010. Produção de etanol a partir de materiais lignocelulósicos, in: *Bioetanol de Cana-de-Açúcar: P&D Para a Produtividade E Sustentabilidade*. Blusher, São Paulo, pp. 697–712.
- García-Pérez, M., Chaala, A., Roy, C., 2002. Vacuum pyrolysis of sugarcane bagasse. *Journal of Analytical and Applied Pyrolysis* 65, 111–136. [https://doi.org/10.1016/S0165-2370\(01\)00184-X](https://doi.org/10.1016/S0165-2370(01)00184-X)
- Georgia-Pacific Chemicals, 2017. Phenolic Novolac Resins [WWW Document]. URL http://www.gp-chemicals.com/Phenol-Formaldehyde_Novolac_Product_Category (accessed 2.13.17).
- Geyer, R., Jambeck, J.R., Law, K.L., 2017. Production, use, and fate of all plastics ever made. *Science Advances* 3, e1700782. <https://doi.org/10.1126/sciadv.1700782>
- Gonçalves, A.R., Schuchardt, U., Bianchi, M.L., Curvelo, A.A.S., 2000. Piassava Fibers (*Attalea funifera*): NMR Spectroscopy of their Lignin. *Journal of the Brazilian Chemical Society* 11, 491–494. <https://doi.org/10.1590/S0103-50532000000500010>
- Gosselink, R.J.A., Jong, E. de, Guran, B., Abächerli, A., 2004. Co-ordination network for lignin-standardisation, production and applications adapted to market requirements (EUROLIGNIN). *Industrial Crops and Products* 20, 121–129. <https://doi.org/10.1016/j.indcrop.2004.04.015>
- Gouveia, E.R., Nascimento, R.T. do, Souto-Maior, A.M., Rocha, G.J. de M., 2009. Validación de metodologia para caracterização química de bagazo de cana-de-açúcar. *Química Nova* 32, 1500–1503. <https://doi.org/10.1590/S0100-40422009000600026>
- Granata, A., Argyropoulos, D.S., 1995. 2-Chloro-4,4,5,5-tetramethyl-1,3,2-dioxaphospholane, a Reagent for the Accurate Determination of the Uncondensed and Condensed Phenolic Moieties in Lignins. *Journal of Agricultural and Food Chemistry* 43, 1538–1544. <https://doi.org/10.1021/jf00054a023>

- Hames, B.R., 2009. Biomass compositional analysis for energy applications, in: *Biofuels: Methods and Protocols*. pp. 145–167.
- Harton, S.E., Pingali, S.V., Nunnery, G.A., Baker, D.A., Walker, S.H., Muddiman, D.C., Koga, T., Rials, T.G., Urban, V.S., Langan, P., 2012. Evidence for complex molecular architectures for solvent-extracted lignins. *ACS Macro Letters* 1, 568–573. <https://doi.org/10.1021/mz300045e>
- Hemminger, W., Sarge, S.M., 1998. Definitions, nomenclature, terms and literature, in: Brown, M.E. (Ed.), *Handbook of Thermal Analysis and Calorimetry*. Elsevier Science, pp. 1–73.
- Hitachi, 1981. DSC Measurements of Thermosetting Resins - application brief 1–3.
- Hu, J., Zhang, Q., Lee, D.J., 2018. Kraft lignin biorefinery: A perspective. *Bioresource Technology*. <https://doi.org/10.1016/j.biortech.2017.08.169>
- Huggins, M.L., 1942. The Viscosity of Dilute Solutions of Long-Chain Molecules. IV. Dependence on Concentration. *Journal of the American Chemical Society* 64, 2716–2718. <https://doi.org/10.1021/ja01263a056>
- Hussein, A.S., Ibrahim, K.I., Abdulla, K.M., 2011. Tannin-phenol Formaldehyde Resins as Binders for Cellulosic Fibers: Mechanical Properties. *Natural Resources* 2, 98–101. <https://doi.org/10.4236/nr.2011.22013>
- Ibarra, D., Chávez, M.I., Rencoret, J., Del Río, J.C., Gutiérrez, A., Romero, J., Camarero, S., Martínez, M.J., Jiménez-Barbero, J., Martínez, A.T., 2007. Lignin modification during *Eucalyptus globulus* kraft pulping followed by totally chlorine-free bleaching: A two-dimensional nuclear magnetic resonance, Fourier transform infrared, and pyrolysis-gas chromatography/mass spectrometry study. *Journal of Agricultural and Food Chemistry* 55, 3477–3490. <https://doi.org/10.1021/jf063728t>
- Ibeh, C.C., 1998. Phenol-Formaldehyde Resins, in: Goodman, S.H. (Ed.), *Handbook of Thermoset Plastics*. p. 49.
- Intelligence, M., 2017. Sample - Global Lignin Products Market (2017 - 2022). Bengaluru - India.
- Isikgor, F.H., Becer, C.R., 2015. Lignocellulosic Biomass: a sustainable platform for production of bio-based chemicals and polymers. *Polymer Chemistry* 6, 4497–4559. <https://doi.org/10.1039/c3py00085k>
- Jiang, Z.-H., Argyropoulos, D.S., 1998. Coupling P-31 NMR with the Mannich reaction for the quantitative analysis of lignin. *Canadian Journal of Chemistry* 76, 612–622. <https://doi.org/10.1139/cjc-76-5-612>
- Jin, Y., Cheng, X., Zheng, Z., 2010. Preparation and characterization of phenol-formaldehyde adhesives modified with enzymatic hydrolysis lignin. *Bioresource Technology* 101, 2046–2048. <https://doi.org/10.1016/j.biortech.2009.09.085>

- Kamm, B., Kamm, M., 2004. Principles of biorefineries. *Applied Microbiology and Biotechnology* 64, 137–145. <https://doi.org/10.1007/s00253-003-1537-7>
- Kasaai, M.R., 2007. Calculation of Mark-Houwink-Sakurada (MHS) equation viscometric constants for chitosan in any solvent-temperature system using experimental reported viscometric constants data. *Carbohydrate Polymers* 68, 477–488. <https://doi.org/10.1016/j.carbpol.2006.11.006>
- Kenney, K.L., Smith, W.A., Gresham, G.L., Westover, T.L., 2014. Understanding biomass feedstock variability. *Biofuels* 4, 111–127.
- Khan, M.A., Ashraf, S.M., Malhotra, V.P., 2004. Development and characterization of a wood adhesive using bagasse lignin. *International Journal of Adhesion and Adhesives* 24, 485–493. <https://doi.org/10.1016/j.ijadhadh.2004.01.003>
- Kim, J.-Y., Hwang, H., Oh, S., Kim, Y.-S., Kim, U.-J., Choi, J.W., 2014. Investigation of structural modification and thermal characteristics of lignin after heat treatment. *International journal of biological macromolecules* 66, 57–65. <https://doi.org/10.1016/j.ijbiomac.2014.02.013>
- Kim, M., Day, D.F., 2011. Composition of sugar cane, energy cane, and sweet sorghum suitable for ethanol production at Louisiana sugar mills. *Journal of Industrial Microbiology and Biotechnology* 38, 803–807. <https://doi.org/10.1007/s10295-010-0812-8>
- Kraemer, E.O., 1938. Molecular Weights of Celluloses and Cellulose Derivates. *Industrial & Engineering Chemistry* 30, 1200–1203. <https://doi.org/10.1021/ie50346a023>
- Larkin, P., 2011. Introduction: Infrared and Raman Spectroscopy, in: *Infrared and Raman Spectroscopy*. pp. 1–5. <https://doi.org/10.1016/B978-0-12-386984-5.10001-1>
- Laza, J.M., Vilas, J.L., Rodríguez, M., Garay, M.T., Mijangos, F., León, L.M., 2002. Analysis of the crosslinking process of a Phenolic Resin by thermal scanning rheometry. *Journal of Applied Polymer Science* 83, 57–65. <https://doi.org/10.1002/app.22106>
- Lee, R., 2007. Phenolic Resin chemistry and proposed mechanism for thermal decomposition. Washington: NASA Marshall Space Flight Center 7–13.
- Liitiä, T., Tamminen, T., 2016. Value from lignin - promises, challenges and breakthroughs [WWW Document]. VTT Technical research centre of Finland LTD. URL <http://www.vttresearch.com/media/events/webinar-value-from-lignin-promises-challenges-and-breakthroughs> (accessed 2.15.18).
- Lima, M. A, Gomez, L.D., Steele-King, C.G., Simister, R., Bernardinelli, O.D., Carvalho, M. A, Rezende, C. A, Labate, C. A, Deazevedo, E.R., McQueen-Mason, S.J., Polikarpov, I., 2014. Evaluating the composition and processing potential of novel sources of Brazilian biomass for sustainable biorenewables production. *Biotechnology for biofuels* 7, 10. <https://doi.org/10.1186/1754-6834-7-10>

- Loh, Y.R., Sujan, D., Rahman, M.E., das, C.A., 2013. Sugarcane bagasse - The future composite material: A literature review. *Resources, Conservation and Recycling* 75, 14–22. <https://doi.org/10.1016/j.resconrec.2013.03.002>
- Lora, J.H., Glasser, W.G., 2002. Recent Industrial Applications of Lignin: A Sustainable Alternative to Nonrenewable MMaterial. *Journal of Polymers and the Environment* 10, 39–48.
- Lu, F., Ralph, J., 1997. Derivatization Followed by Reductive Cleavage (DFRC Method), a New Method for Lignin Analysis: Protocol for Analysis of DFRC Monomers. *Journal of Agricultural and Food Chemistry* 45, 2590–2592. <https://doi.org/10.1021/jf970258h>
- Mansouri, N.-E. El, Salvadó, J., 2006. Structural characterization of technical lignins for the production of adhesives: Application to lignosulfonate, kraft, soda-anthraquinone, organosolv and ethanol process lignins. *Industrial Crops and Products* 24, 8–16. <https://doi.org/10.1016/j.indcrop.2005.10.002>
- Mello, I.L., Delpech, M.C., Coutinho, F.M.B., Albino, F.F.M., 2006. Viscometric Study of high-cis polybutadiene in toluene solution. *Journal of the Brazilian Chemical Society* 17, 194–199. <https://doi.org/10.1590/S0103-50532006000100028>
- Menezes, F.F. de, Maciel Filho, R., Rocha, G.J. de M., 2016a. Obtainment and characterization of lignin from enzymatic hydrolysis of sugarcane bagasse of 2G ethanol process in pilot scale. *Chemical Engineering Transactions* 50.
- Menezes, F.F. de, Silva, R.H.F. da, Rocha, G.J. de M., Maciel Filho, R., 2016b. Physicochemical characterization of residue from the enzymatic hydrolysis of sugarcane bagasse in a cellulosic ethanol process at pilot scale. *Industrial Crops and Products* 94, 463–470. <https://doi.org/10.1016/j.indcrop.2016.09.014>
- Menezes, F.F. de, Rencoret, J., Nakanishi, S.C., Nascimento, V.M., Silva, V.F.N., Gutiérrez, A., Del Río, J.C., Rocha, G.J. de M., 2017. Alkaline Pretreatment Severity Leads to Different Lignin Applications in Sugar Cane Biorefineries. *ACS Sustainable Chemistry and Engineering* 5. <https://doi.org/10.1021/acssuschemeng.7b00265>
- Menon, V., Rao, M., 2012. Trends in bioconversion of lignocellulose: Biofuels, platform chemicals & biorefinery concept. *Progress in Energy and Combustion Science* 38, 522–550. <https://doi.org/10.1016/j.peccs.2012.02.002>
- Mesa, L., López, N., Cara, C., Castro, E., González, E., Mussatto, S.I., 2016. Techno-economic evaluation of strategies based on two steps organosolv pretreatment and enzymatic hydrolysis of sugarcane bagasse for ethanol production. *Renewable Energy* 86, 270–279. <https://doi.org/10.1016/j.renene.2015.07.105>
- Michel, D., Bachelier, B., Drean, J.-Y., Harzallah, O., 2013. Preparation of Cellulosic Fibers from Sugarcane for Textile Use. *Conference Papers in Engineering* 2013, 1–6. <https://doi.org/10.1155/2013/651787>

- Mobley, C.D., 1994. Light and water: radiative transfer in natural waters. Academic Press, Michigan.
- Moghaddam, L., Zhang, Z., Wellard, R.M., Bartley, J.P., O'Hara, I.M., Doherty, W.O.S., 2014. Characterisation of lignins isolated from sugarcane bagasse pretreated with acidified ethylene glycol and ionic liquids. *Biomass and Bioenergy* 70, 498–512. <https://doi.org/10.1016/j.biombioe.2014.07.030>
- Mohamad Ibrahim, M.N., Zakaria, N., Sipaut, C.S., Sulaiman, O., Hashim, R., 2011. Chemical and thermal properties of lignins from oil palm biomass as a substitute for phenol in a phenol formaldehyde resin production. *Carbohydrate Polymers* 86, 112–119. <https://doi.org/10.1016/j.carbpol.2011.04.018>
- Mousavioun, P., Doherty, W.O.S., 2010. Chemical and thermal properties of fractionated bagasse soda lignin. *Industrial Crops and Products* 31, 52–58. <https://doi.org/10.1016/j.indcrop.2009.09.001>
- Murciano Martínez, P., Punt, A.M., Kabel, M.A., Gruppen, H., 2016. Deconstruction of lignin linked p-coumarates, ferulates and xylan by NaOH enhances the enzymatic conversion of glucan. *Bioresource Technology* 216, 44–51. <https://doi.org/10.1016/j.biortech.2016.05.040>
- Nadji, H., Diouf, P.N., Benaboura, A., Bedard, Y., Riedl, B., Stevanovic, T., 2009. Comparative study of lignins isolated from Alfa grass (*Stipa tenacissima* L.). *Bioresource technology* 100, 3585–92. <https://doi.org/10.1016/j.biortech.2009.01.074>
- Nakanishi, S.C., 2016. Estudo da ampliação de escala do processo de pré-tratamento alcalino do bagaço de cana-de-açúcar para obtenção de etanol de segunda geração. University of São Paulo State (USP).
- Neiva, D., Fernandes, L., Araújo, S., Lourenço, A., Gominho, J., Simões, R., Pereira, H., 2015. Chemical composition and kraft pulping potential of 12 eucalypt species. *Industrial Crops and Products* 66, 89–95. <https://doi.org/10.1016/j.indcrop.2014.12.016>
- Nongthombam, G.D., Labala, R.K., das, S., Handique, P.J., Talukdar, N.C., 2017. Evaluation and Selection of Potential Biomass Sources of North-East India towards Sustainable Bioethanol Production. *Frontiers in Energy Research* 5. <https://doi.org/10.3389/fenrg.2017.00016>
- Ohara, H., 2003. Biorefinery. *Applied Microbiology and Biotechnology* 62, 474–477. <https://doi.org/10.1007/s00253-003-1383-7>
- Oliveira, F.B. de, 2008. Utilização de matéria-prima obtida de fonte renovável na preparação de compósitos de matriz do tipo fenólica. University of São Paulo State (USP).
- Paiva, J.M.F., Frollini, E., 2001. Sugarcane bagasse reinforced phenolic and lignophenolic composites. *Journal of Applied Polymer Science* 83, 880–888. <https://doi.org/10.1002/app.10085>

- Pandey, M.P., Kim, C.S., 2011. Lignin Depolymerization and Conversion: A Review of Thermochemical Methods. *Chemical Engineering and Technology* 34, 29–41. <https://doi.org/10.1002/ceat.201000270>
- Pardini, L.C., Levy Neto, F., 2006. *Compósitos estruturais: ciência e tecnologia*. Edição. Ed. Edgard Blucher. São Paulo.
- Pasch, H., Schrod, M., 2004. Preparation and Analysis of Phenol-Formaldehyde Resins by High-Throughput Techniques. *Macromolecular Rapid Communications* 25, 224–230. <https://doi.org/10.1002/marc.200300145>
- Pepper, J.M., Baylis, P.E.T., Adler, E., 1959. The isolation and properties of lignins obtained by the Acidolysis of Spruce and Aspen Woods in Dioxane-water medium. *The Canadian Journal of chemical Engineering* 37.
- Piccolo, R.S.J., Santos, F., Frollini, E., 1997. Sugar Cane Bagasse Lignin in Resol-Type Resin: Alternative Application for Ligninphenol-Formaldehyde Resins. *Journal of Macromolecular Science, Part A* 34, 153–164. <https://doi.org/10.1080/10601329708014943>
- Plaza, G.A., Wandzich, D., 2016. Biorefineries - new green strategy for development of smart and innovative industry. *Management Systems in Production Engineering* 3, 150–155. <https://doi.org/10.12914/MSPE>
- Poljanšek, I., Krajnc, M., 2005. Characterization of phenol-formaldehyde prepolymer resins by in line FT-IR spectroscopy. *Acta Chimica Slovenica* 52, 238–244.
- Popescu, C.M., Popescu, M.C., Singurel, G., Vasile, C., Argyropoulos, D.S., Willfor, S., 2007. Spectral characterization of eucalyptus wood. *Applied Spectroscopy* 61, 1168–1177. <https://doi.org/10.1366/000370207782597076>
- Pu, Y., Cao, S., Ragauskas, A.J., 2011. Application of quantitative ³¹P NMR in biomass lignin and biofuel precursors characterization. *Energy & Environmental Science* 4, 3154. <https://doi.org/10.1039/c1ee01201k>
- Qiao, W., Li, S., Guo, G., Han, S., Ren, S., Ma, Y., 2015. Synthesis and characterization of phenol-formaldehyde resin using enzymatic hydrolysis lignin. *Journal of Industrial and Engineering Chemistry* 21, 1417–1422. <https://doi.org/10.1016/j.jiec.2014.06.016>
- Rabemanolontsoa, H., Kuninori, Y., Saka, S., 2015. High conversion efficiency of Japanese cedar hydrolyzates into acetic acid by co-culture of *Clostridium thermoaceticum* and *Clostridium thermocellum*. *Journal of Chemical Technology & Biotechnology* n/a-n/a. <https://doi.org/10.1002/jctb.4679>
- Ragauskas, A.J., Beckham, G.T., Bidddy, M.J., Chandra, R., Chen, F., Davis, M.F., Davison, B.H., Dixon, R.A., Gilna, P., Keller, M., Langan, P., Naskar, A.K., Saddler, J.N., Tschaplinski, T.J., Tuskan, G.A., Wyman, C.E., 2014. Lignin Valorization: Improving Lignin Processing in the Biorefinery. *Science* 344.

<https://doi.org/10.1126/science.1246843>

- Ralph, J., Brunow, G., Boerjan, W., 2007. Lignins. *Encyclopedia of Life Sciences* 1–10. <https://doi.org/10.1002/9780470015902.a0020104>
- Ralph, J., Hatfield, R.D., 1991. Pyrolysis-GC-MS characterization of forage materials. *Journal of Agricultural and Food Chemistry* 39, 1426–1437. <https://doi.org/10.1021/jf00008a014>
- Ralph, J., Landucci, L.L., 2010. NMR of Lignins, in: Heitner, C., Dimmel, D.R., Schmidt, J.A. (Eds.), *Lignin and Lignans: Advances in Chemistry*. Taylor and Francis, Boca Raton, pp. 137–244.
- Ralph, S.A., Ralph, J., Landucci, L.L., 2004. NMR database of lignin and cell wall model compounds. [WWW Document].
- Rencoret, J., Gutiérrez, A., Nieto, L., Jiménez-Barbero, J., Faulds, C.B., Kim, H., Ralph, J., Martínez, A.T., Del Río, J.C., 2011. Lignin composition and structure in young versus adult *Eucalyptus globulus* plants. *Plant physiology* 155, 667–82. <https://doi.org/10.1104/pp.110.167254>
- Rencoret, J., Marques, G., Gutiérrez, A., Nieto, L., Santos, J.I., Martínez, J.J.-B.Á.T., Río, J.C. del, 2009. HSQC-NMR analysis of lignin in woody (*Eucalyptus globulus* and *Picea abies*) and non-woody (*Agave sisalana*) ball-milled plant materials at the gel state 10th EWLP. *Holzforschung* 63, 691–698.
- Rennè, D.S., Wilcox, S., Marion, W., Maxwell, G.L., Rymes, M., Phillips, J., Berg, D.E., Franklin, M.A., Brown, R.C., 2007. Availability of Renewable Resources, in: Kreith, F., Goswami, D.Y. (Eds.), *Energy, Handbook of Energy Efficiency and Renewable*. Taylor and Francis, p. 69.
- Rinaldi, R., Jastrzebski, R., Clough, M.T., Ralph, J., Kennema, M., Bruijninx, P.C.A., Weckhuysen, B.M., 2016. Paving the Way for Lignin Valorisation: Recent Advances in Bioengineering, Biorefining and Catalysis. *Angewandte Chemie - International Edition* 55, 8164–8215. <https://doi.org/10.1002/anie.201510351>
- RISI, 2013. World Pulp Annual Historical Data - Excerpt [WWW Document]. URL www.risinfo.com/Marketing/ahd/Excerpts/world_pulp.pdf%0A (accessed 2.1.15).
- Rocha, G.J. de M., Nascimento, V.M., Gonçalves, A.R., Silva, V.F.N., Martín, C., 2015. Influence of mixed sugarcane bagasse samples evaluated by elemental and physical–chemical composition. *Industrial Crops and Products* 64, 52–58. <https://doi.org/10.1016/j.indcrop.2014.11.003>
- Rocha, G.J. de M., Silva, F.T., Araújo, G.T., Curvelo, A.A., 1997. A fast and accurate method for determination of cellulose and polyoses by HPLC., in: *Proceedings of the V Brazilian Symposium on the Chemistry of Lignin and Other Wood Components*. Curitiba, pp. 113–115.

- Salmén, L., Olsson, A., 1998. Interaction between hemicelluloses, lignin and cellulose: structure-property relationships. *Journal of pulp and paper science* 24, 99–103.
- Samuel, R., Foston, M., Jaing, N., Cao, S., Allison, L., Studer, M., Wyman, C., Ragauskas, A.J., 2011. HSQC (heteronuclear single quantum coherence) ¹³C-¹H correlation spectra of whole biomass in perdeuterated pyridinium chloride-DMSO system: An effective tool for evaluating pretreatment. *Fuel* 90, 2836–2842. <https://doi.org/10.1016/j.fuel.2011.04.021>
- Samuel, R., Pu, Y., Raman, B., Ragauskas, A.J., 2010. Structural characterization and comparison of switchgrass ball-milled lignin before and after dilute acid pretreatment. *Applied Biochemistry and Biotechnology* 162, 62–74. <https://doi.org/10.1007/s12010-009-8749-y>
- Santos, R.B., Capanema, E.A., Balakshin, M.Y., Chang, H.M., Jameel, H., 2011. Effect of hardwoods characteristics on kraft pulping process: Emphasis on lignin structure. *BioResources* 6, 3623–3637.
- Shen, Q., Mu, D., Yu, L.W., Chen, L., 2004. A simplified approach for evaluation of the polarity parameters for polymer using the K coefficient of the Mark-Houwink-Sakurada equation. *Journal of Colloid and Interface Science* 275, 30–34. <https://doi.org/10.1016/j.jcis.2004.01.041>
- Showa Denko Group, 2017. Industrial Phenolic Resin [WWW Document]. Products. URL <http://www.sds.com.sg/products/functional-polymers/industrial-phenolic-resin/> (accessed 2.13.17).
- Silva, G.M., Ferreira, I.L.M., Delpech, M.C., Costa, M.A.S., 2013. Estudo viscosimétrico de copolímeros à base de 1,3-butadieno e 1-octeno em tolueno e hexano. *Polimeros* 23, 758–763. <https://doi.org/10.4322/polimeros.2013.064>
- Singh, R., Shukla, A., Tiwari, S., Srivastava, M., 2014. A review on delignification of lignocellulosic biomass for enhancement of ethanol production potential. *Renewable and Sustainable Energy Reviews* 32, 713–728. <https://doi.org/10.1016/j.rser.2014.01.051>
- Singh, R., Singh, S., Trimukhe, K.D., Pandare, K. V., Bastawade, K.B., Gokhale, D. V., Varma, a. J., 2005. Lignin-carbohydrate complexes from sugarcane bagasse: Preparation, purification, and characterization. *Carbohydrate Polymers* 62, 57–66. <https://doi.org/10.1016/j.carbpol.2005.07.011>
- Sjöström, E., 1993. *Wood Chemistry: Fundamentals and applications*, 2nd ed. ed. San Diego: Academic press.
- Sluiter, A., Hames, B., Ruiz, R., Scarlata, C., Sluiter, J., Templeton, D., 2008a. Determination of ash in biomass. National Renewable Energy Laboratory (NREL) Analytical Procedures 5. <https://doi.org/NREL/TP-510-42619>
- Sluiter, A., Ruiz, R., Scarlata, C., Sluiter, J., Templeton, D., 2008b. Determination of

- Extractives in Biomass. National Renewable Energy Laboratory (NREL) Analytical Procedures 1–9. <https://doi.org/NREL/TP-510-42621>
- Sluiter, J.B., Ruiz, R.O., Scarlata, C.J., Sluiter, A.D., Templeton, D.W., 2010. Compositional analysis of lignocellulosic feedstocks. 1. Review and description of methods. *Journal of Agricultural and Food Chemistry* 58, 9043–9053. <https://doi.org/10.1021/jf1008023>
- Suzano (Papel e Celulose), 2018. Negocios e produtos - Lignina [WWW Document]. URL <http://www.suzano.com.br/negocios-e-produtos/lignina/>
- TA Instruments, 2004. Understanding Rheology of Thermosets [WWW Document]. URL http://tainstruments.com/pdf/literature/AAN015_V1_U_Thermoset.pdf (accessed 2.13.17).
- TA Instruments, 2003. Thermal Specialty Library - Chapter 3 - Analyzing data.
- Tana, T., Zhang, Z., Moghaddam, L., Rackemann, D.W., Rencoret, J., Gutiérrez, A., del Río, J.C., Doherty, W.O.S., 2016. Structural Changes of Sugar Cane Bagasse Lignin during Cellulosic Ethanol Production Process. *ACS Sustainable Chemistry & Engineering* 4, 5483–5494. <https://doi.org/10.1021/acssuschemeng.6b01093>
- Tejado, A., Peña, C., Labidi, J., Echeverria, J.M., Mondragon, I., 2007. Physico-chemical characterization of lignins from different sources for use in phenol-formaldehyde resin synthesis. *Bioresource Technology* 98, 1655–1663. <https://doi.org/10.1016/j.biortech.2006.05.042>
- Templeton, D.W., Wolfrum, E.J., Yen, J.H., Sharpless, K.E., 2016. Compositional Analysis of Biomass Reference Materials: Results from an Interlaboratory Study. *Bioenergy Research* 9, 303–314. <https://doi.org/10.1007/s12155-015-9675-1>
- Thermo Nicolet, 2002. FT-IR vs. Dispersive Infrared: Theory of Infrared Spectroscopy Instrumentation. A Thermo Electron business 2.
- Thyrel, M., 2014. Spectroscopic Characterization of Lignocellulosic Biomass. Swedish University of Agricultural Sciences.
- Tomani, P., 2010. The LignoBoost process. *Cellulose Chemistry and Technology* 44, 53–58.
- Traoré, M., Kaal, J., Martínez Cortizas, A., 2016. Application of FTIR spectroscopy to the characterization of archeological wood. *Spectrochimica Acta - Part A: Molecular and Biomolecular Spectroscopy* 153, 63–70. <https://doi.org/10.1016/j.saa.2015.07.108>
- Tucker, M.P., Nguyen, Q.A., Eddy, F.P., Kadam, K.L., Gedvilas, L.M., Webb, J.D., 2001. Fourier transform infrared quantitative analysis of sugars and lignin in pretreated softwood solid residues. *Applied biochemistry and biotechnology* 91–93, 51–61. <https://doi.org/10.1385/ABAB:91-93:1-9:51>
- Tye, Y.Y., Lee, K.T., Wan Abdullah, W.N., Leh, C.P., 2016. The world availability of non-wood lignocellulosic biomass for the production of cellulosic ethanol and potential

- pretreatments for the enhancement of enzymatic saccharification. *Renewable and Sustainable Energy Reviews* 60, 155–172. <https://doi.org/10.1016/j.rser.2016.01.072>
- Vassilev, S. V., Baxter, D., Andersen, L.K., Vassileva, C.G., 2010. An overview of the chemical composition of biomass. *Fuel* 89, 913–933. <https://doi.org/10.1016/j.fuel.2009.10.022>
- Vázquez, G., Antorrena, G., González, J., Mayor, J., 1995. Lignin-phenol-formaldehyde adhesives for exterior grade plywoods. *Bioresource Technology* 51, 187–192. [https://doi.org/10.1016/0960-8524\(94\)00120-P](https://doi.org/10.1016/0960-8524(94)00120-P)
- Verbruggen, A., Marchohi, M. Al, 2010. Views on peak oil and its relation to climate change policy. *Energy Policy* 38, 5572–5581. <https://doi.org/http://dx.doi.org/10.1016/j.enpol.2010.05.002>
- Verma, D., Gope, P.C., Maheshwari, M.K., Sharma, R.K., 2012. Bagasse Fiber Composites-A Review. *Journal of Material and Environmental Sciences* 3, 1079–1092.
- Waliszewska, B., Prączyński, W., Zborowska, M., Stachowiak-Wencek, A., Waliszewska, H., Spek-Dźwigala, A., 2015. The diversification of chemical composition of pine wood depending on the tree age. *Forestry and Wood Technology* 91, 182–187.
- Wang, M., Leitch, M., (Charles) Xu, C., 2009. Synthesis of phenol-formaldehyde resol resins using organosolv pine lignins. *European Polymer Journal* 45, 3380–3388. <https://doi.org/10.1016/j.eurpolymj.2009.10.003>
- White, J.E., Catallo, W.J., Legendre, B.L., 2011. Biomass pyrolysis kinetics: A comparative critical review with relevant agricultural residue case studies. *Journal of Analytical and Applied Pyrolysis* 91, 1–33. <https://doi.org/10.1016/j.jaap.2011.01.004>
- Winandy, J.E., Rowell, R.M., 2005. *Chemistry of Wood Strength, Handbook of Wood Chemistry and Wood Composites*. <https://doi.org/doi:10.1201/b12487-15>
- Yang, H., Yan, R., Chen, H., Lee, D.H., Zheng, C., 2007. Characteristics of hemicellulose, cellulose and lignin pyrolysis. *Fuel* 86, 1781–1788. <https://doi.org/10.1016/j.fuel.2006.12.013>
- Yang, S., Wen, J.-L., Yuan, T.-Q., Sun, R.-C., 2014. Characterization and phenolation of biorefinery technical lignins for lignin-phenol-formaldehyde resin adhesive synthesis. *RSC Adv.* 4, 57996–58004. <https://doi.org/10.1039/C4RA09595B>
- Yelle, D.J., Ralph, J., 2016. Characterizing phenol-formaldehyde adhesive cure chemistry within the wood cell wall. *International Journal of Adhesion and Adhesives* 70, 26–36. <https://doi.org/10.1016/j.ijadhadh.2016.05.002>
- Zhang, W., Ma, Y., Wang, C., Li, S., Zhang, M., Chu, F., 2013a. Preparation and properties of lignin-phenol-formaldehyde resins based on different biorefinery residues of agricultural biomass. *Industrial Crops and Products* 43, 326–333. <https://doi.org/10.1016/j.indcrop.2012.07.037>

- Zhang, W., Ma, Y., Xu, Y., Wang, C., Chu, F., 2013b. Lignocellulosic ethanol residue-based lignin-phenol-formaldehyde resin adhesive. *International Journal of Adhesion and Adhesives* 40, 11–18. <https://doi.org/10.1016/j.ijadhadh.2012.08.004>
- Zhang, Y.-H.P., Lynd, L.R., 2004. Toward an aggregated understanding of enzymatic hydrolysis of cellulose: Noncomplexed cellulase systems. *Biotechnology and Bioengineering* 88, 797–824. <https://doi.org/10.1002/bit.20282>
- Zhu, Y., Lee, Y.Y., Elander, R.T., 2005. Optimization of dilute-acid pretreatment of corn stover using a high-solids percolation reactor. *Applied biochemistry and biotechnology* 121–124, 1045–1054. <https://doi.org/10.1385/ABAB:124:1-3:1045>
- Zuniga Linan, L., Nascimento Lima, N.M., Filho, R.M., Sabino, M.A., Kozlowski, M.T., Manenti, F., 2015. Pilot-scale synthesis and rheological assessment of poly(methyl methacrylate) polymers: Perspectives for medical application. *Materials Science and Engineering C* 51, 107–116. <https://doi.org/10.1016/j.msec.2015.02.038>

SUPPLEMENTARY MATERIAL

Supplementary Material A: Research dissemination

Supplementary Material B: Gel time determination

Supplementary Material C: Zero shear rate viscosity (η_0) determination

Supplementary Material D: TG and DTG curves of the phenolic resins

Supplementary Material E: DMTA curves of the Standard phenolic resin

Supplementary Material A: Research dissemination

Papers

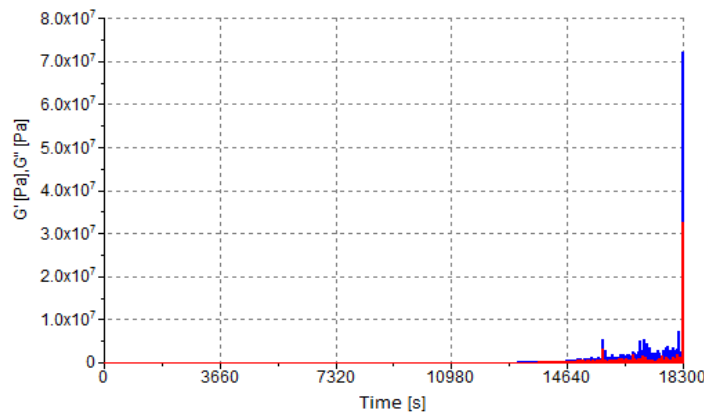
- a. Menezes, F. F.; Rocha, G. J. M.; Maciel Filho, R. Obtainment and Characterization of Lignin from Enzymatic Hydrolysis of Sugarcane Bagasse of 2G Ethanol Process in Pilot Scale. *Chemical Engineering Transactions*, v. 50, p. 397-402, 2016.
- b. Menezes, F. F.; Fernandes, R. H. da S.; Rocha, G. J. de M.; Maciel Filho, R. Physicochemical characterization of residue from the enzymatic hydrolysis of sugarcane bagasse in a cellulosic ethanol process at pilot scale. *Industrial Crops and Products (Print)*, v. 94, p. 463-470, 2016.

Poster/Abstract

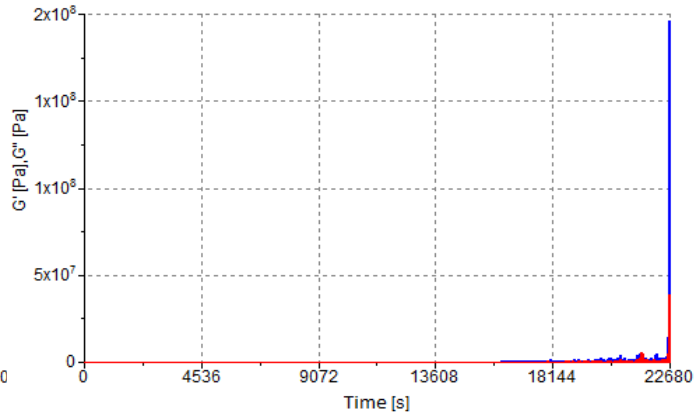
1. Menezes, F. F.; Nakanishi, S. C.; Rocha, G. J. M.; Maciel Filho, R. Different lignins from sugarcane bagasse in cellulosic ethanol pilot plant to phenolic resin production In: 39th Symposium on Biotechnology for Fuels and Chemicals, 2017, San Francisco.
2. Menezes, F. F.; Rocha, G. J. M.; Maciel Filho, R. Obtainment and Characterization of Lignin from Enzymatic Hydrolysis of Sugarcane Bagasse of 2G Ethanol Process in Pilot Scale. In: International Conference on Biomass (ICONBM), 2016, Giardini Naxos, Taormina (Italy).
3. Menezes, F. F.; Linan, L. Z.; Rocha, G. J. M.; Maciel Filho, R. Potencial da lignina proveniente da hidrólise enzimática do bagaço de cana-de-açúcar e da lignina Kraft proveniente do processo LignoBoost para a produção de resinas lignofenólicas. In Workshop em Engenharia de Materiais, 2016, Instituto Federal do Maranhão – IFMA, São Luís, Maranhão.

Supplementary Material B: Gel time determination

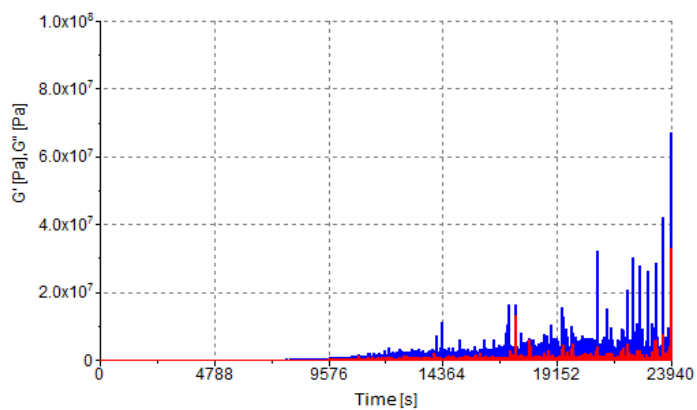
EHR 5% - 90 °C



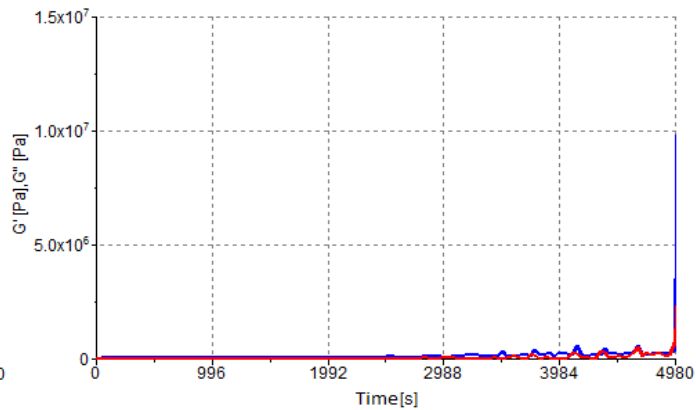
EHR 15% - 90 °C



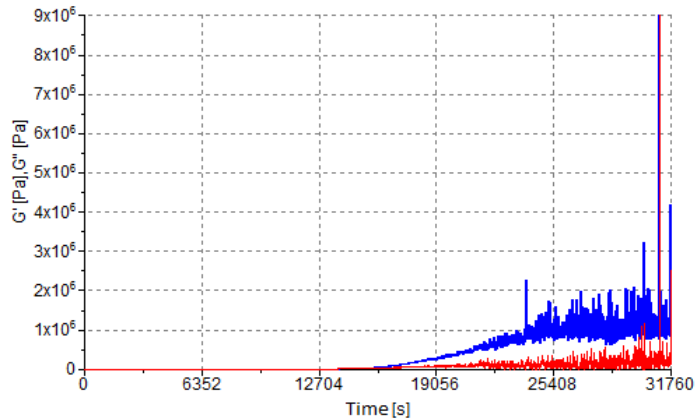
EHR 30% - 90 °C



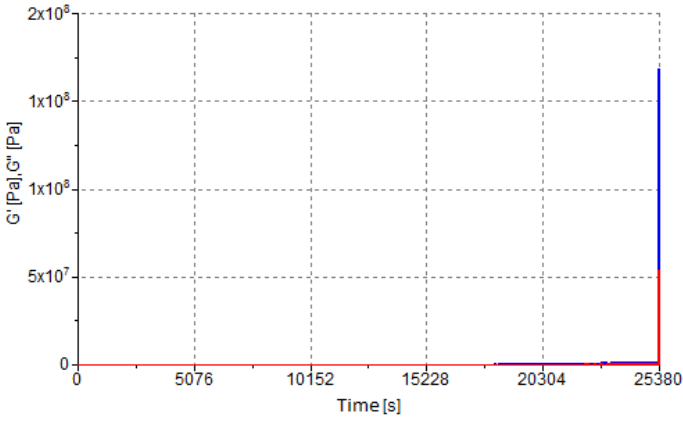
EHR 45% - 90 °C



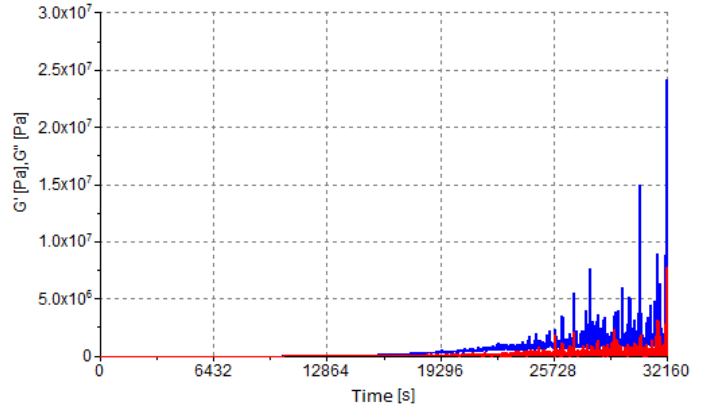
Standard - 90 °C



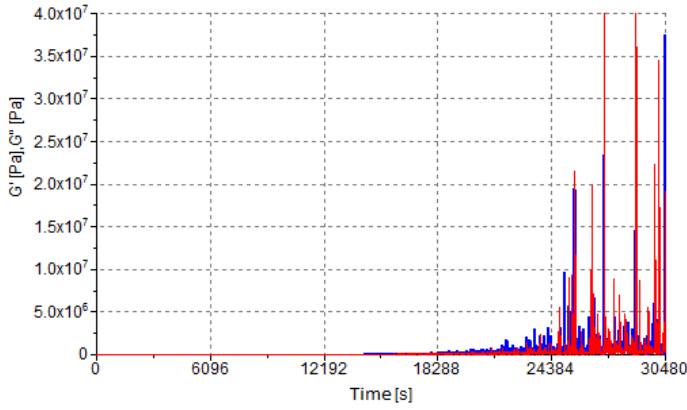
LBL 5% - 90 °C



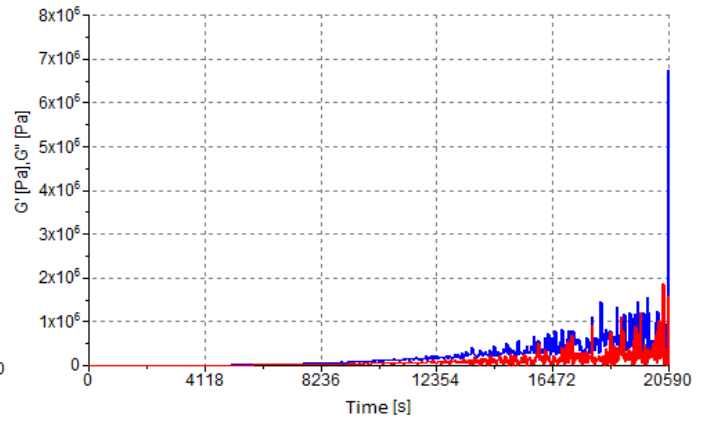
LBL 15% - 90 °C



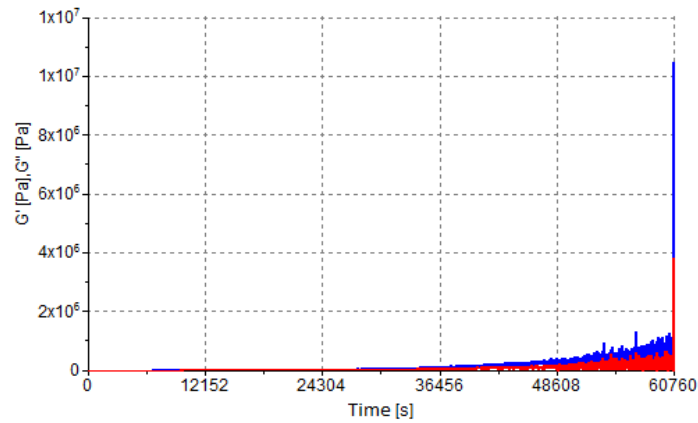
LBL 30% - 90 °C



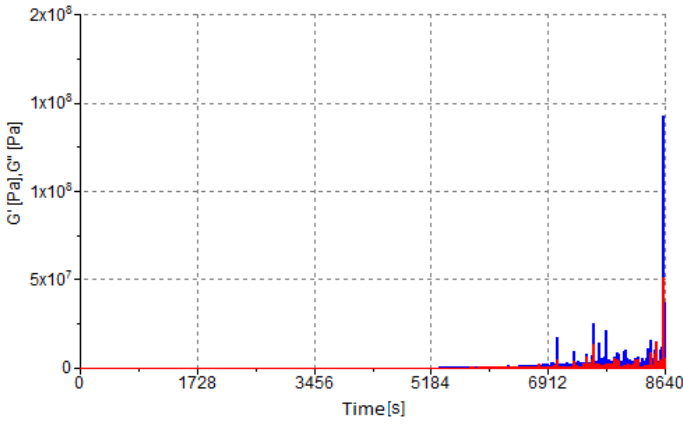
LBL 45% - 90 °C



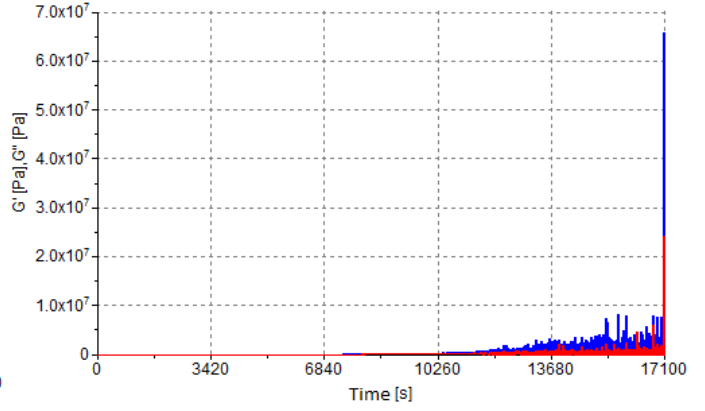
LBL 60% - 90 °C



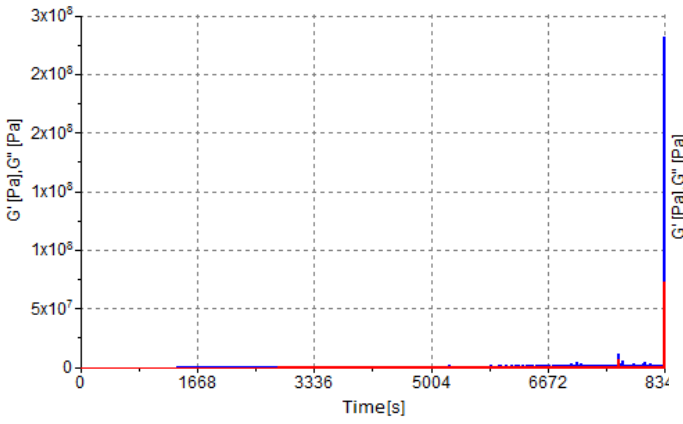
EHL 5% - 97.5 °C



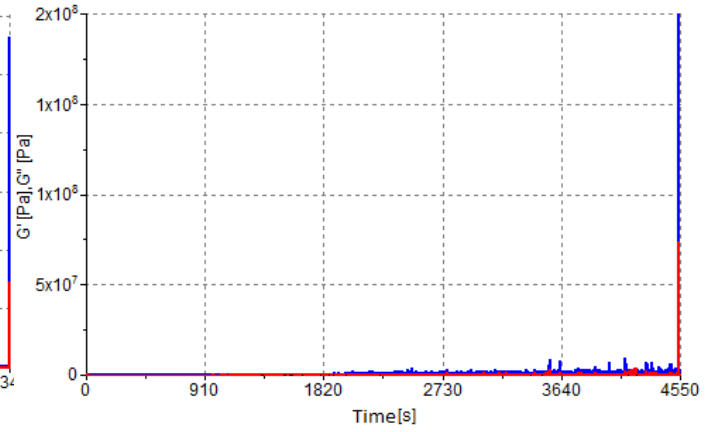
EHL 15% - 97.5 °C



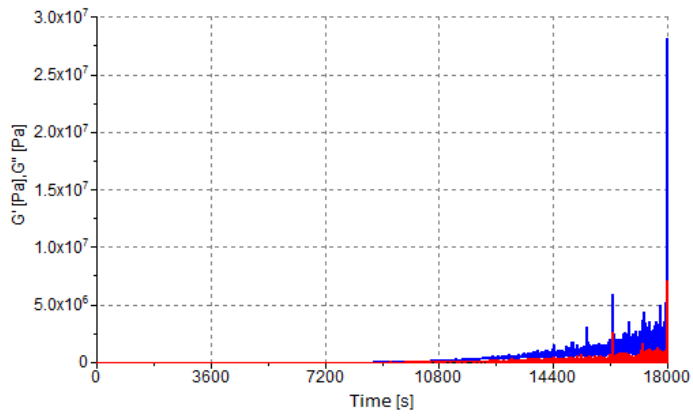
EHL 30% - 97.5 °C



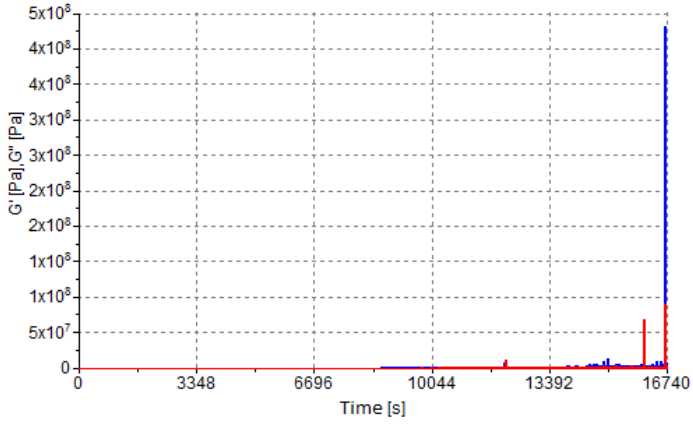
EHL 45% - 97.5 °C



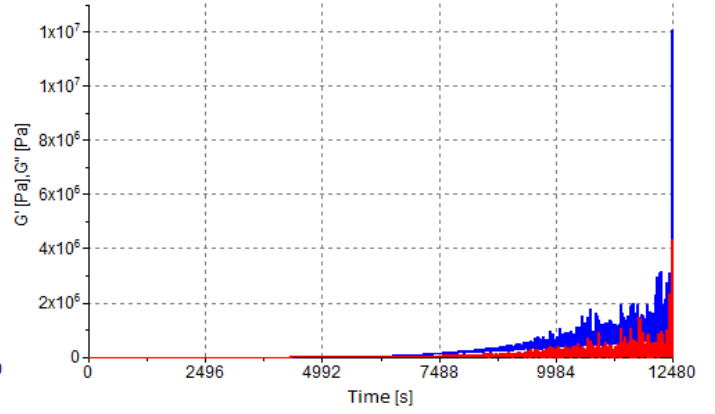
Standard - 97.5 °C



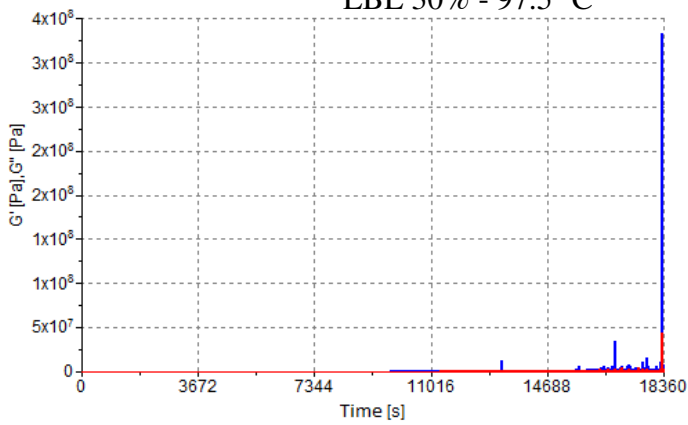
LBL 5% - 97.5 °C



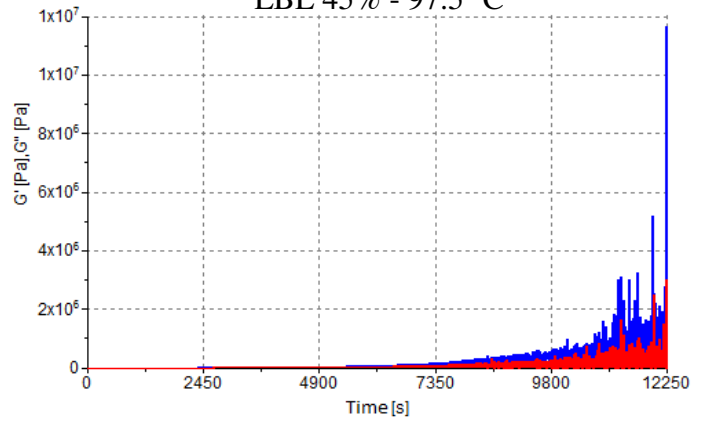
LBL 15% - 97.5 °C



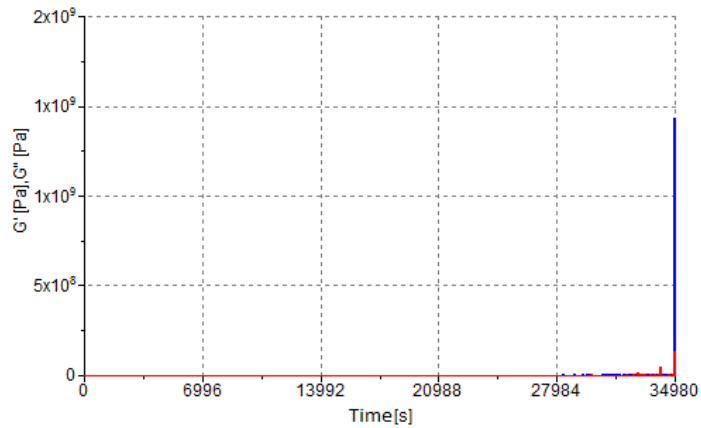
LBL 30% - 97.5 °C



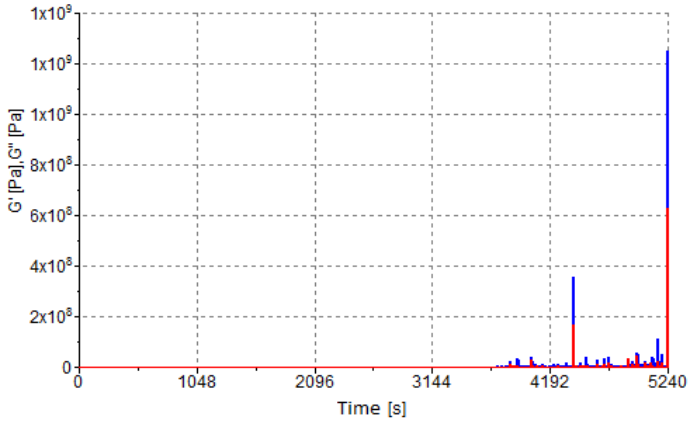
LBL 45% - 97.5 °C



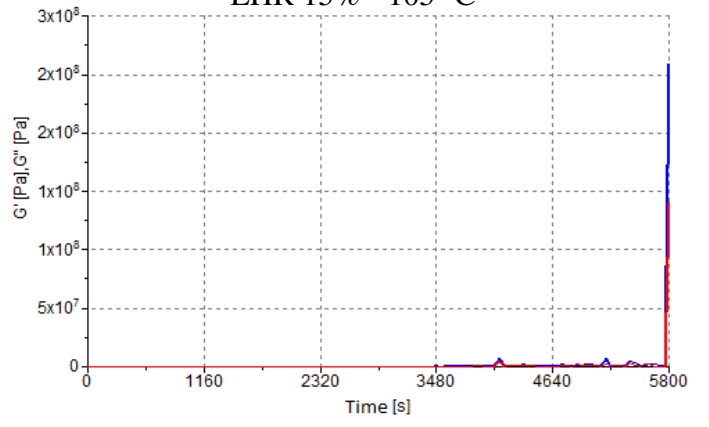
LBL 60% - 97.5 °C



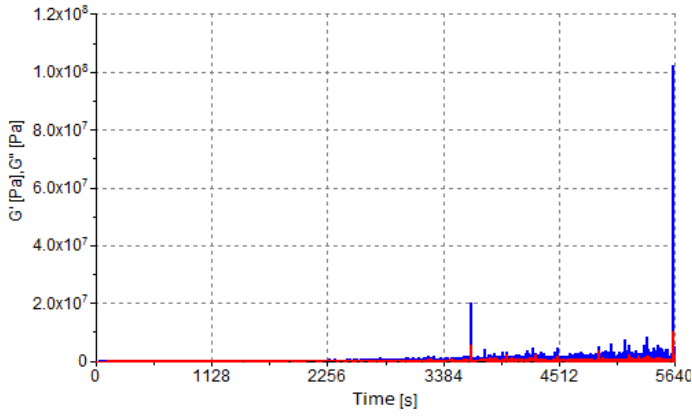
EHR 5% - 105 °C



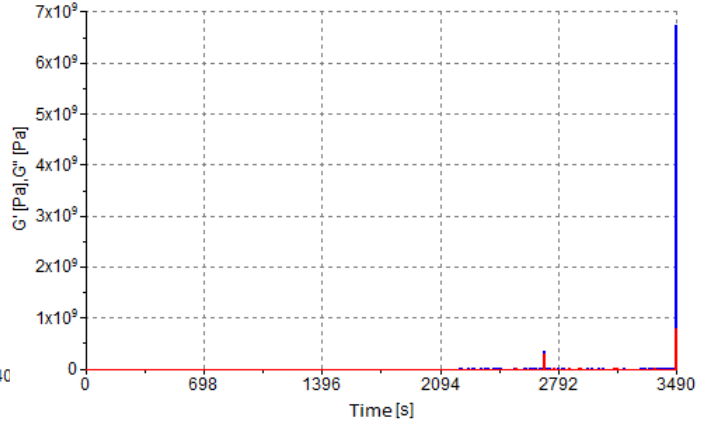
EHR 15% - 105 °C



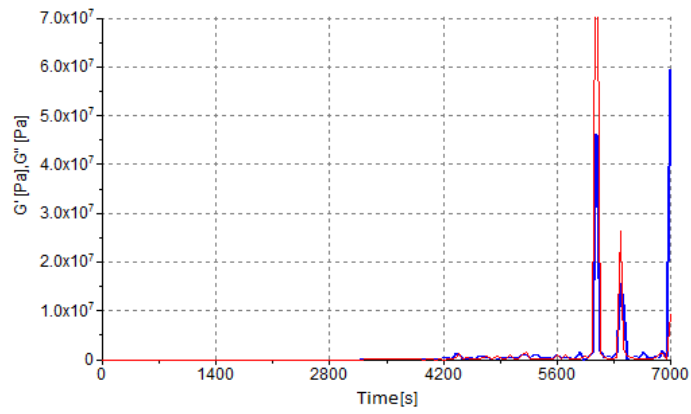
EHR 30% - 105 °C



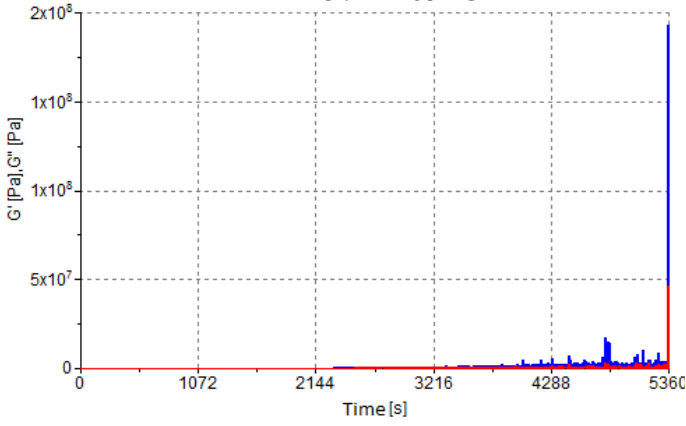
EHR 45% - 105 °C



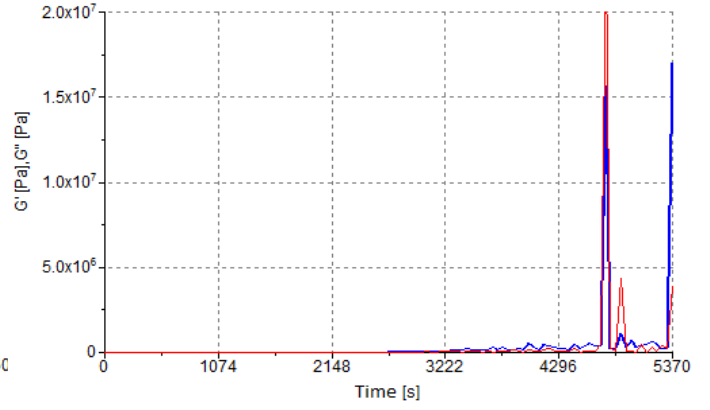
Standard - 105 °C



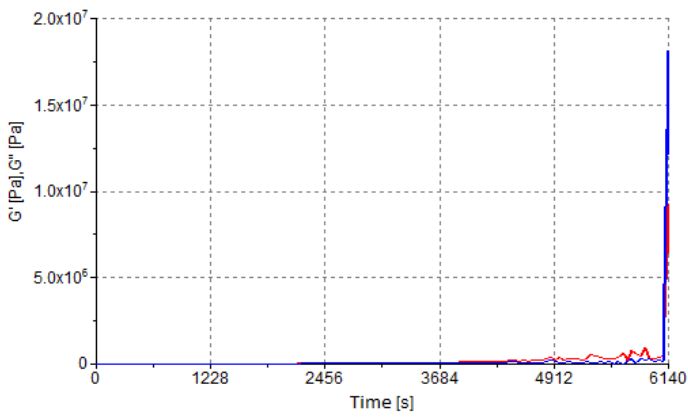
LBL 5% - 105 °C



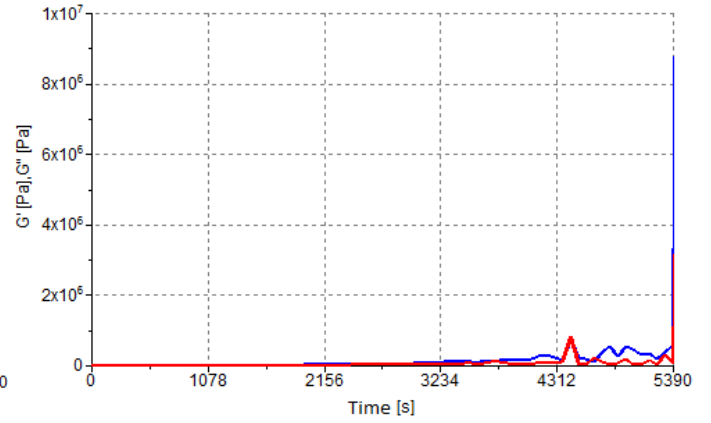
LBL 15% - 105 °C



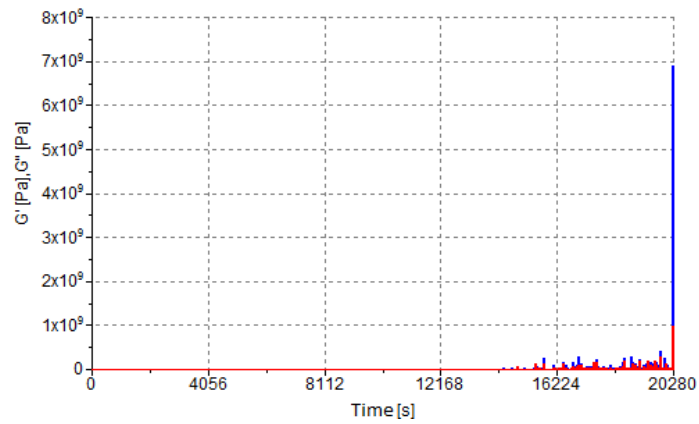
LBL 30% - 105 °C



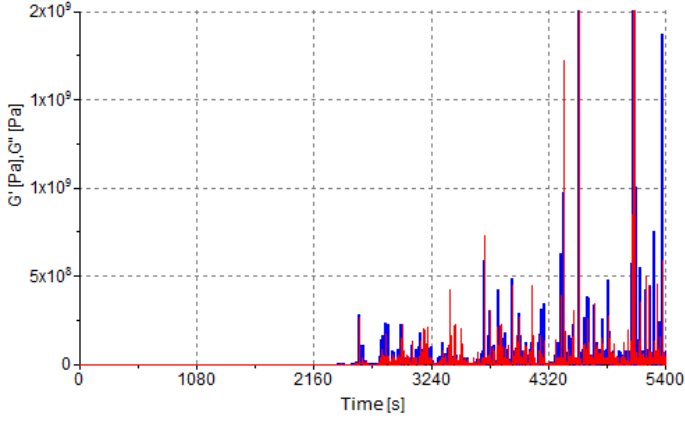
LBL 45% - 105 °C



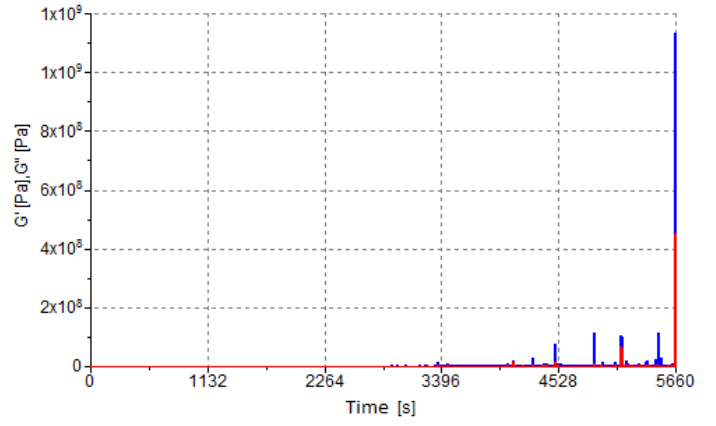
LBL 60% - 105 °C



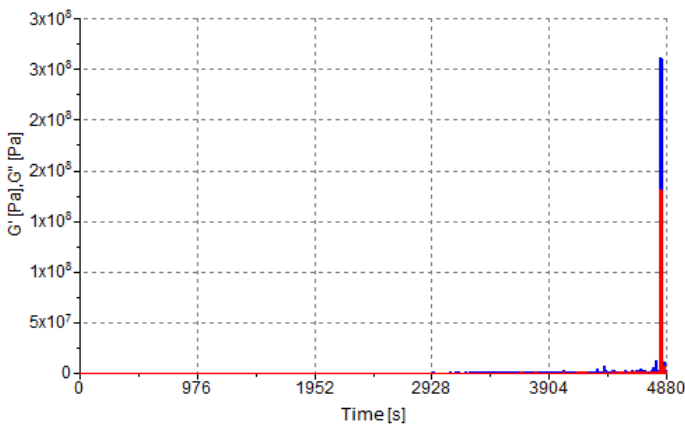
EHR 5% - 112.5 °C



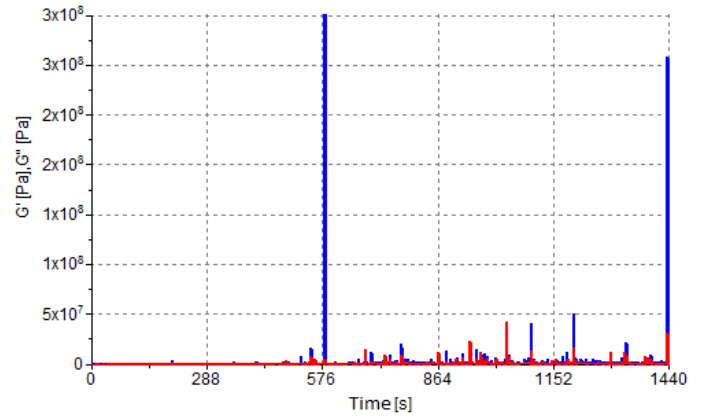
EHR 15% - 112.5 °C



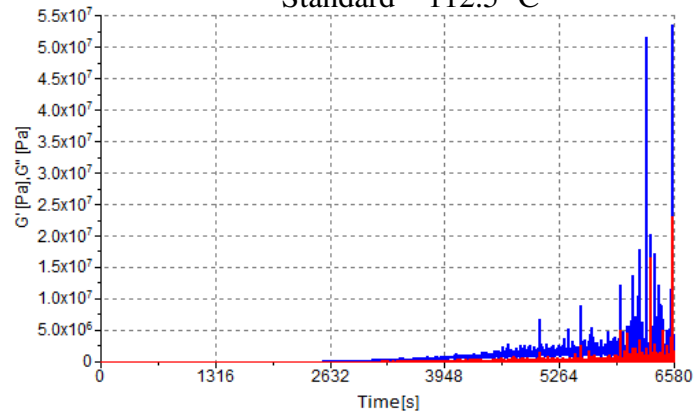
EHR 30% - 112.5 °C



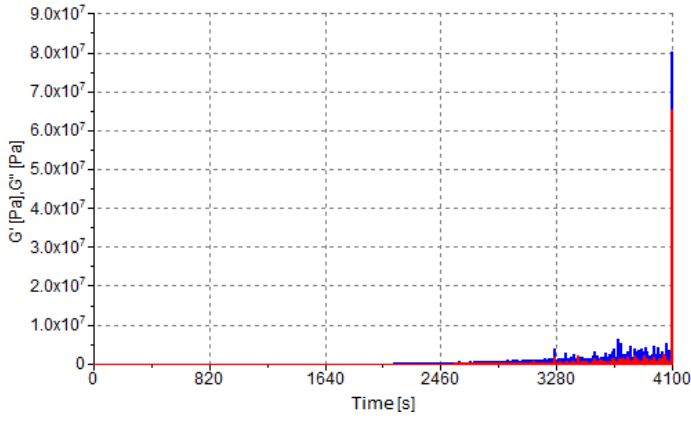
EHR 45% - 112.5 °C



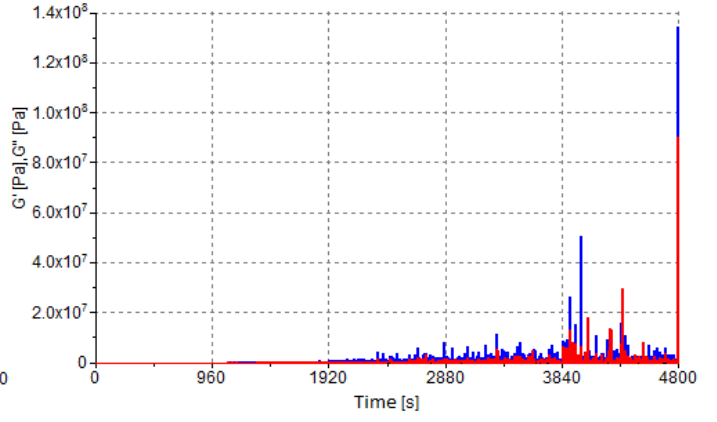
Standard - 112.5 °C



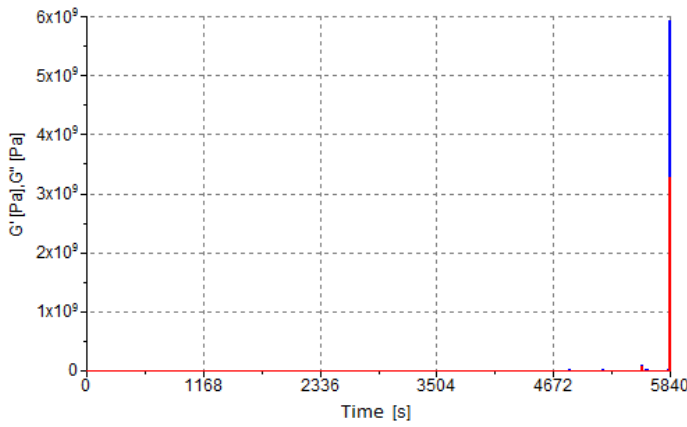
LBL 5% - 112.5 °C



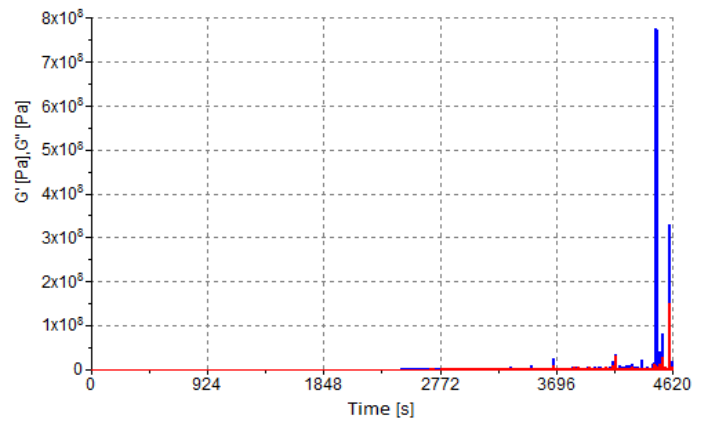
LBL 15% - 112.5 °C



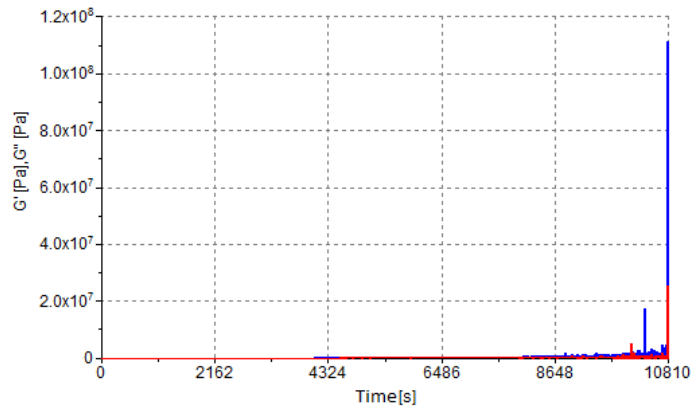
LBL 30% - 112.5 °C



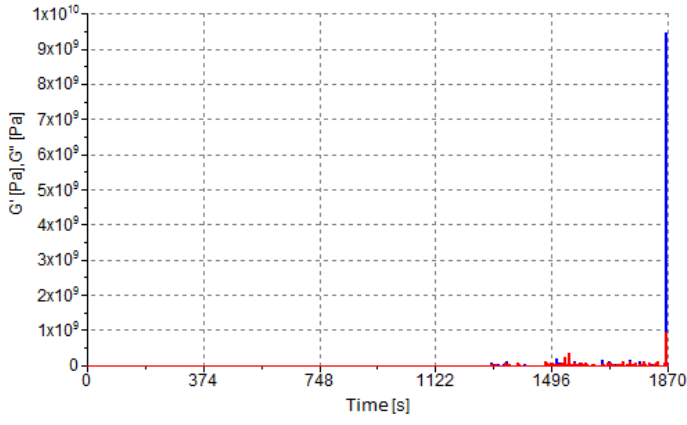
LBL 45% - 112.5 °C



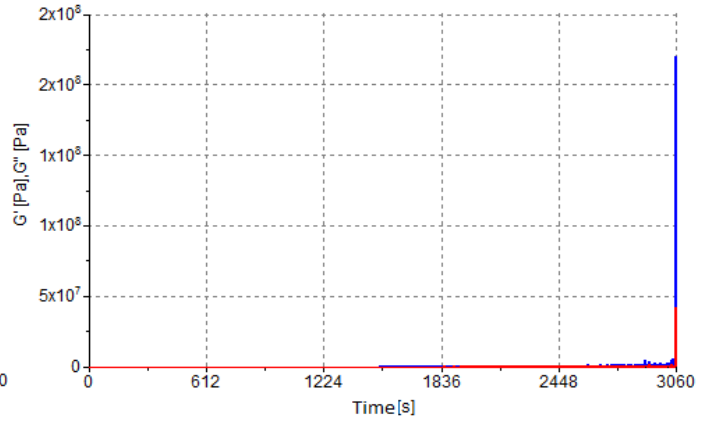
LBL 60% - 112.5 °C



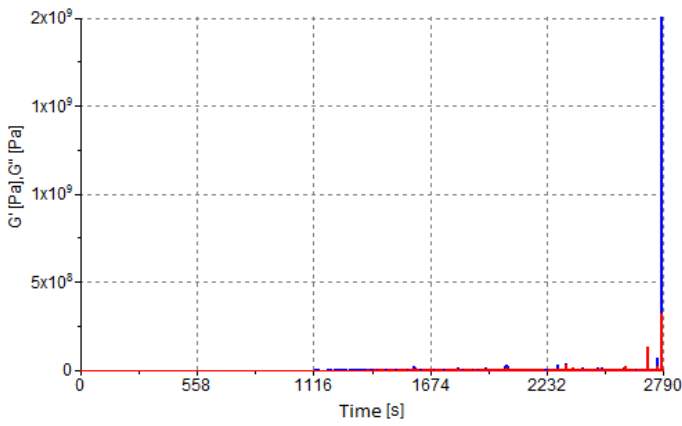
EHR 5% - 120 °C



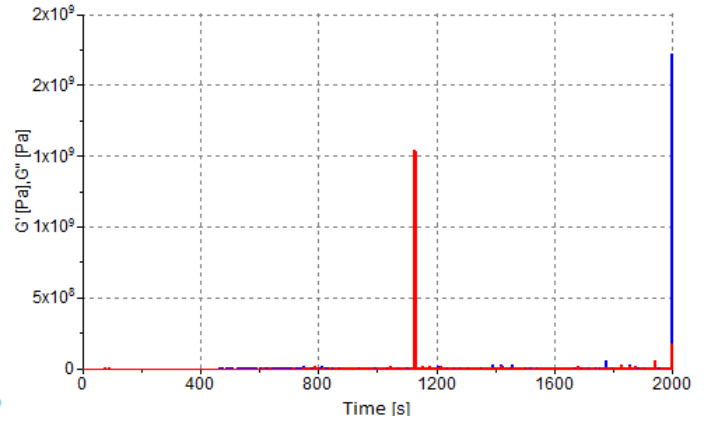
EHR 15% - 120 °C



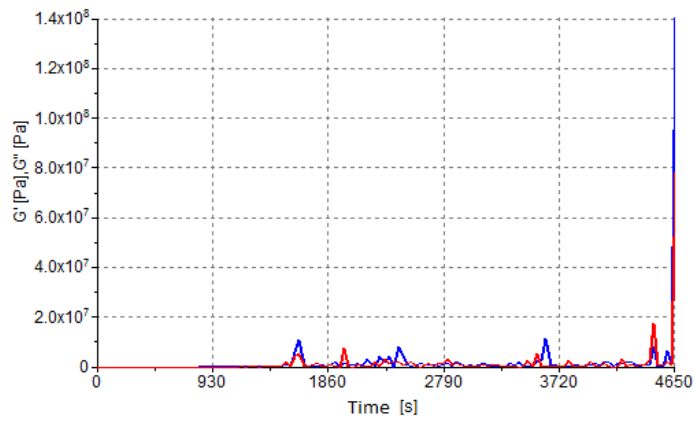
EHR 30% - 120 °C



EHR 45% - 120 °C



Standard - 120 °C



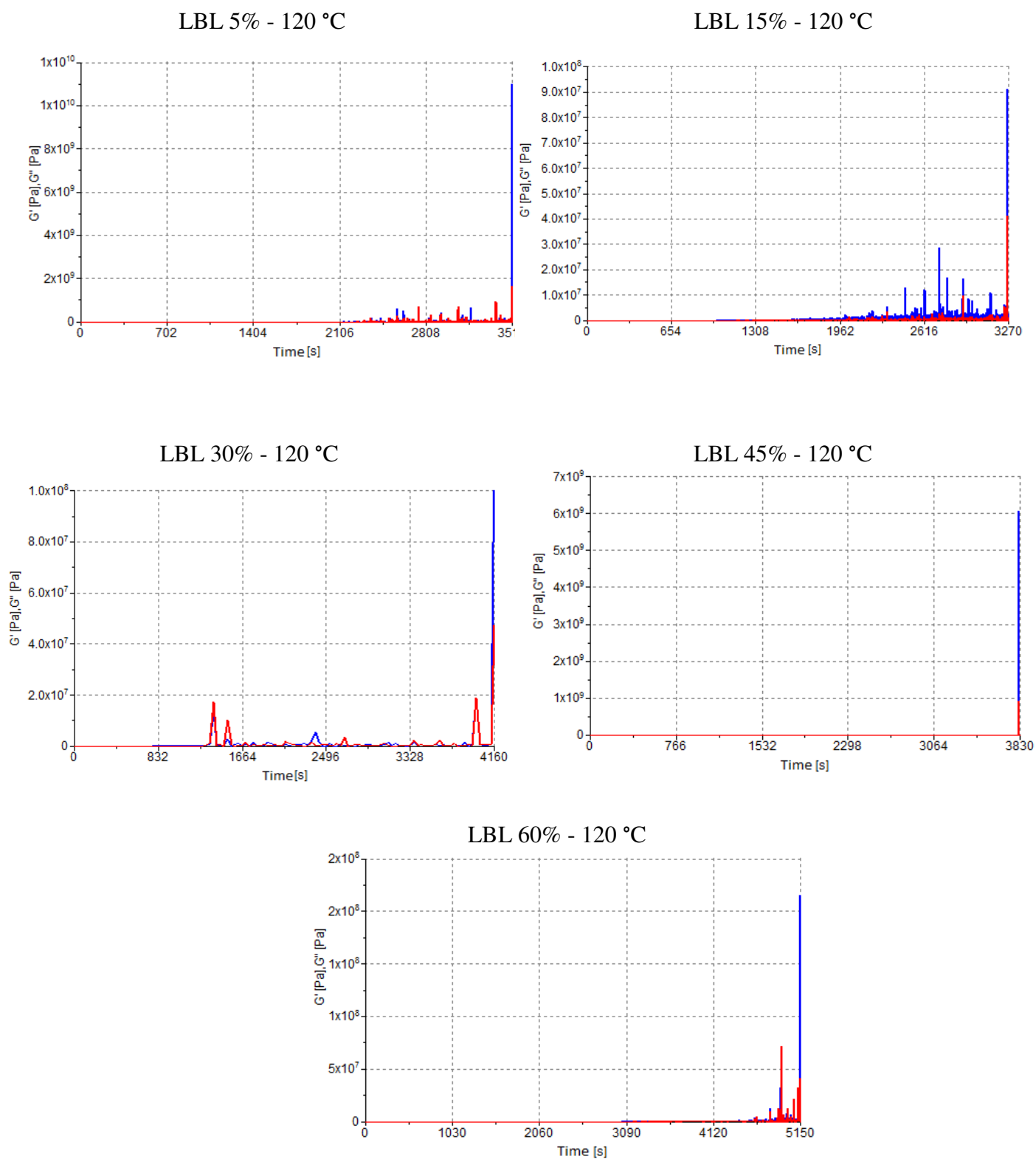
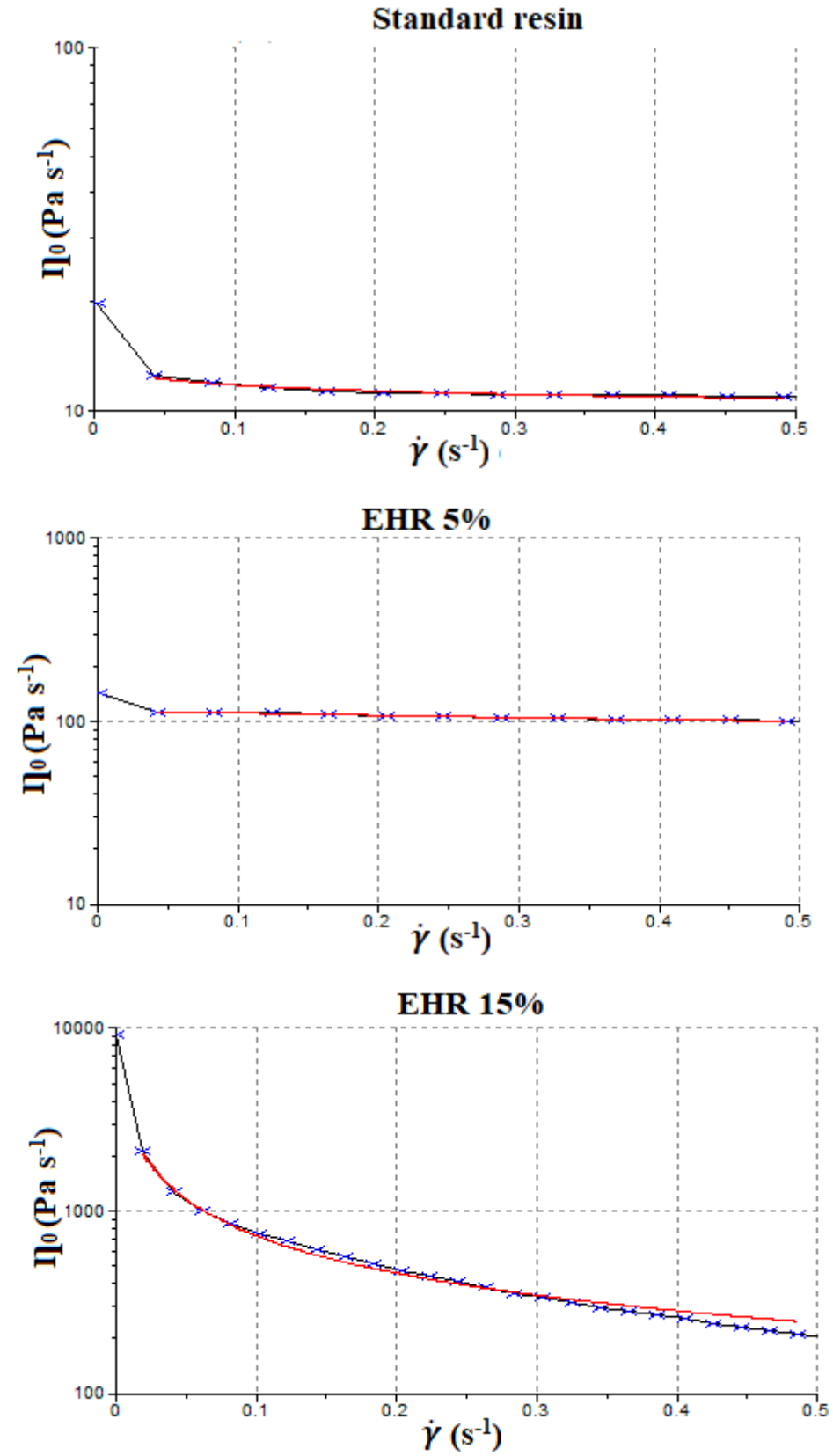
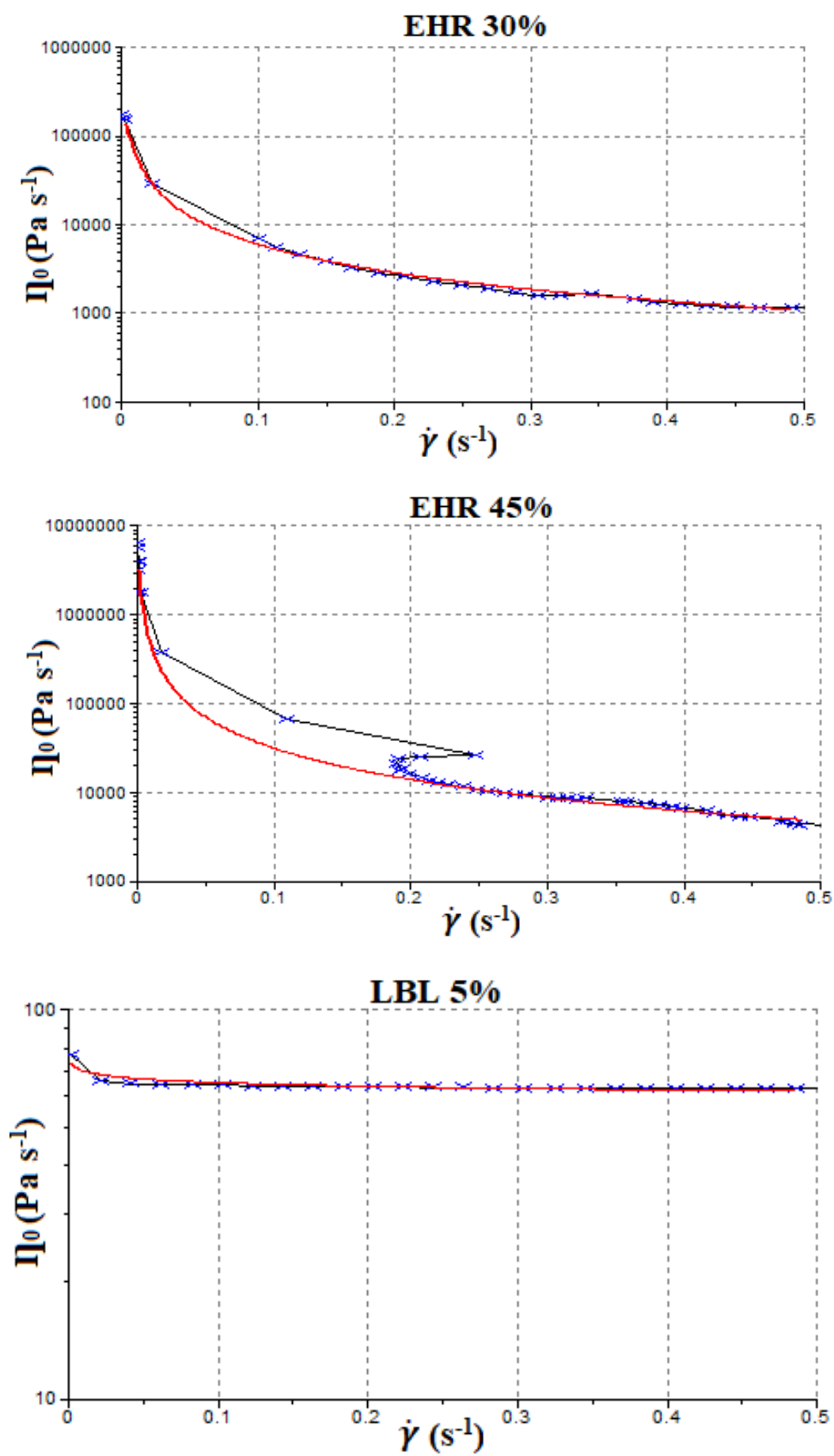
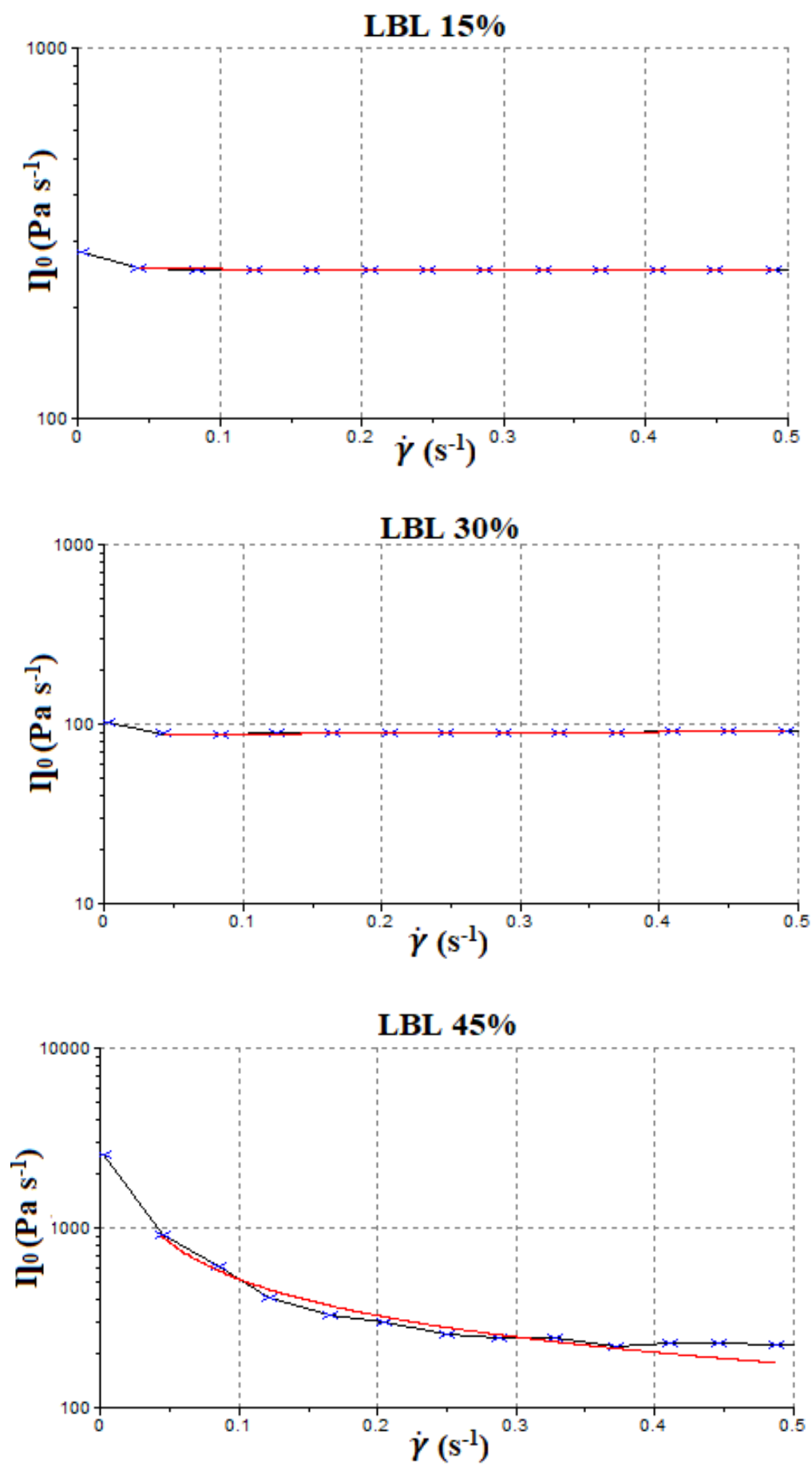


Figure S1 - Curves of viscoelastic properties as a function of time. Blue curve: G' ; Red curve: G'' .

Supplementary Material C: Zero shear rate viscosity (η_0) determination





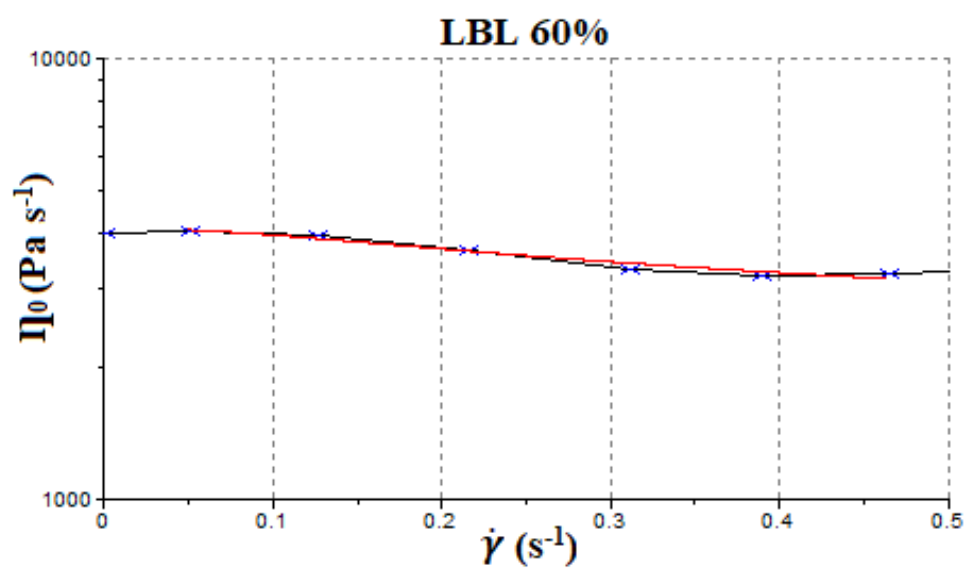


Figure S2- Viscosity curves for determination of zero shear rate viscosity (η_0).

—*— $\eta = f(\dot{\gamma})$
— Carreau-Yasuda (Visc)

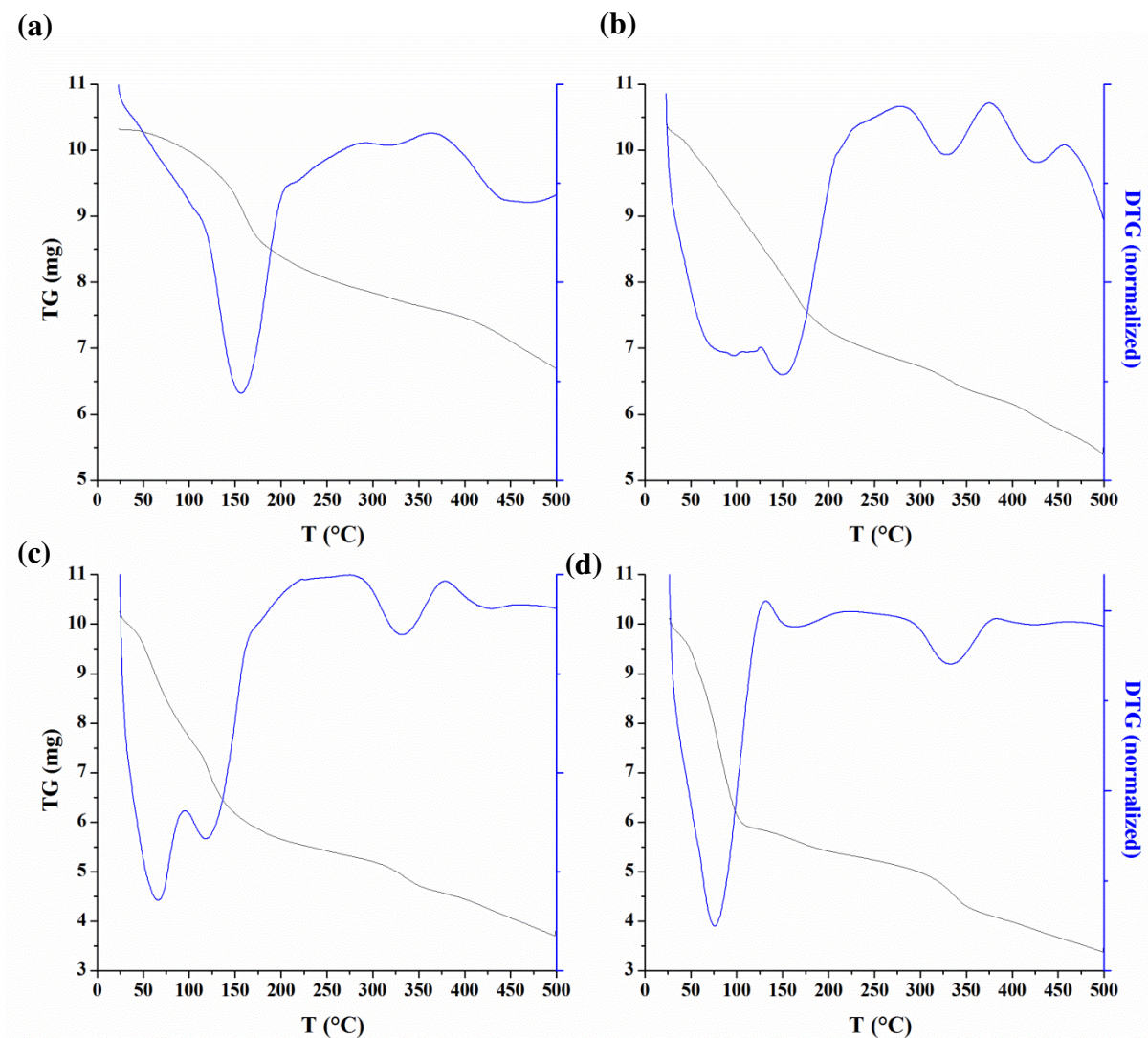
Supplementary Material D: TG and DTG curves of the phenolic resins

Figure S3 - TG and DTG curves for EHR resins.
(a) EHR 5%, (b) EHR 15%, (c) EHR 30% and (d) EHR 45% resins.

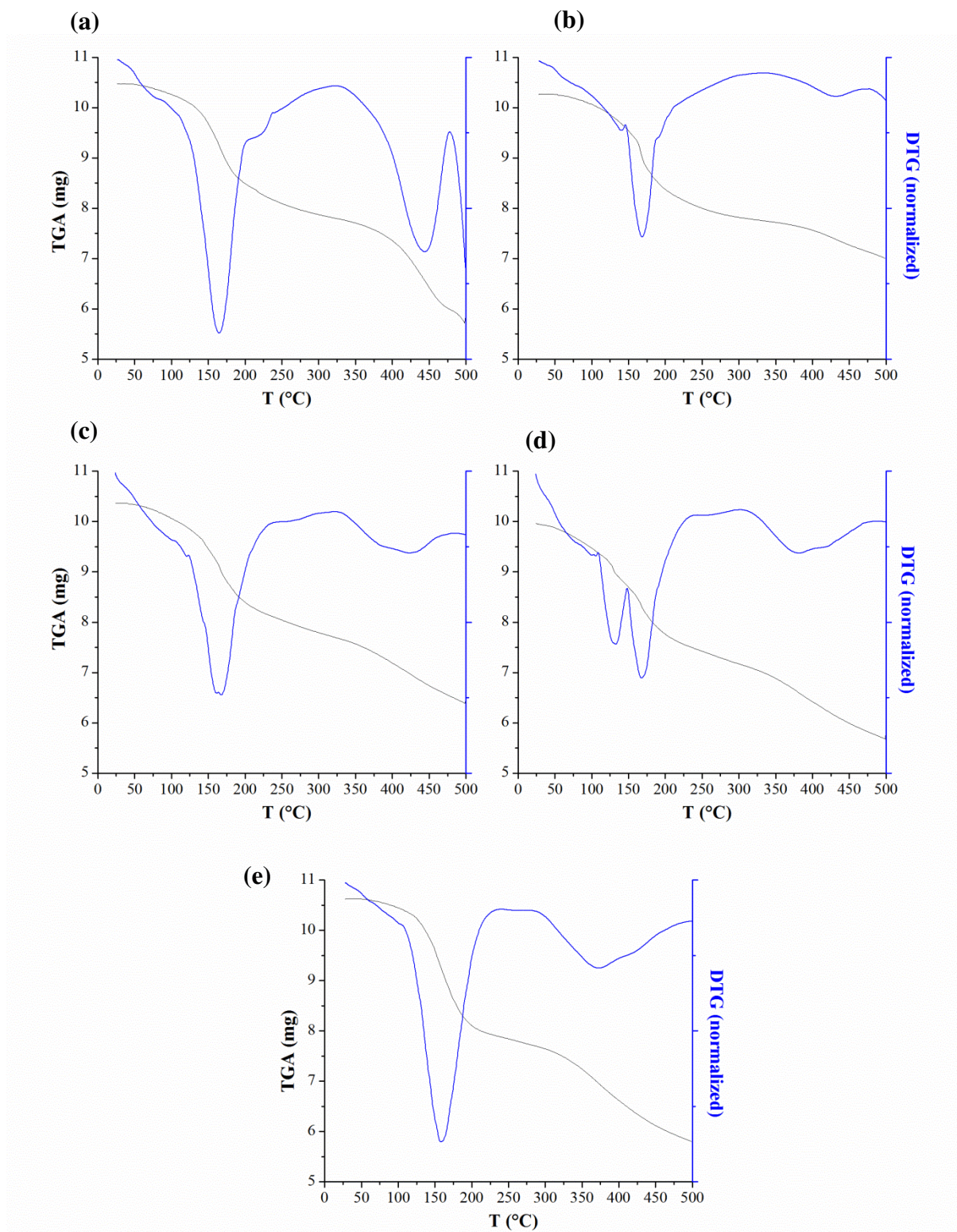


Figure S4 - TG and DTG curves for LBL resins.

(a) LBL 5%, (b) LBL 15%, (c) LBL 30%, (d) LBL 45% and (e) LBL 60% resins.

Supplementary Material E: DMTA curves of the Standard phenolic resin

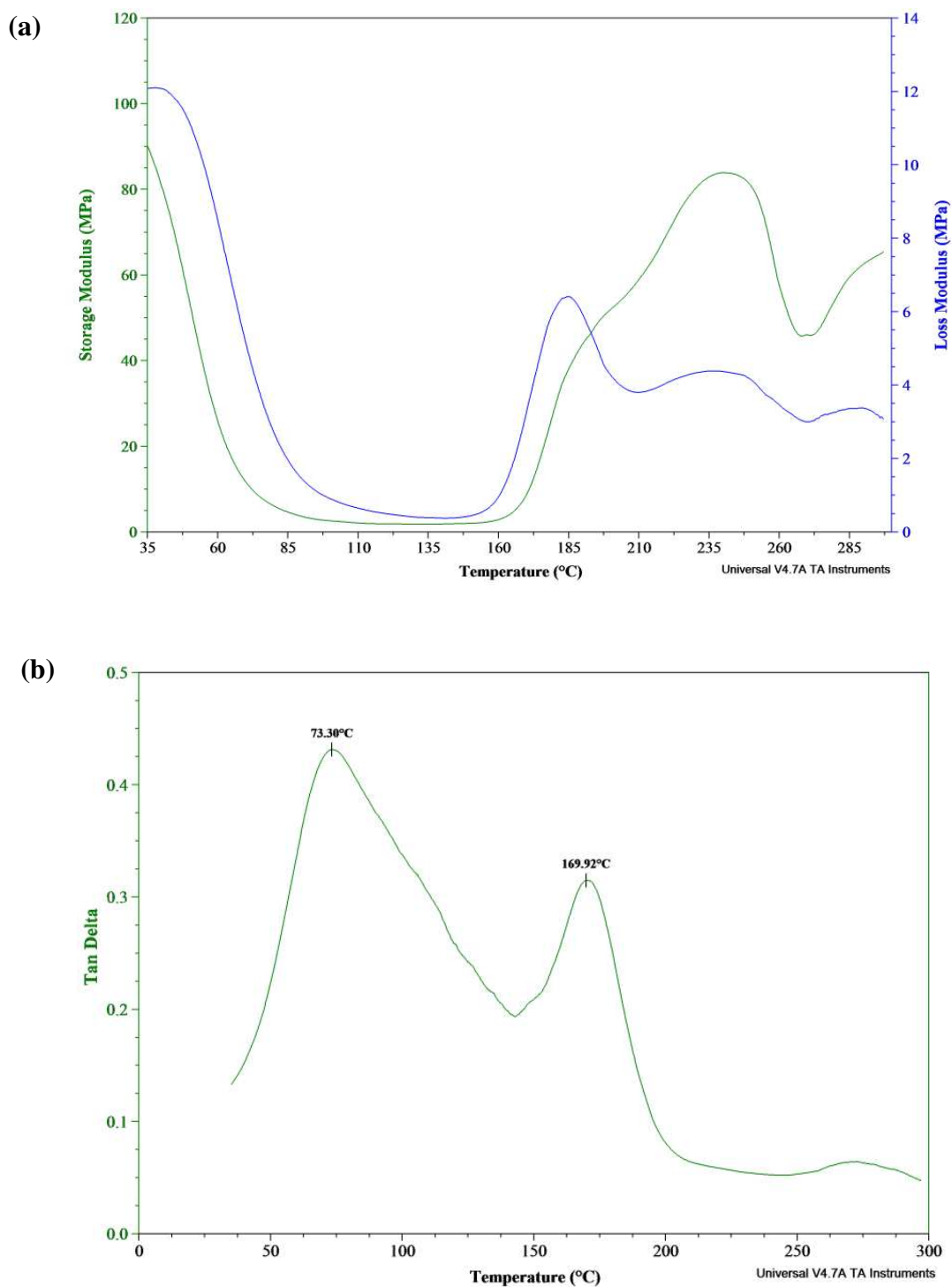


Figure S5 - DMTA curves of the standard phenolic resin.
(a) G' and G'' curves; (b) $\tan \delta$ curve.